The Effect of Temperature on the SWCC and Estimation of the SWCC from Moisture Profile under a Controlled Thermal Gradient

by

Pedram Roshani

Thesis submitted to the
Faculty of Graduate and Postdoctoral Studies
Under Supervision of Dr. Julio Á. Infante Sedano, P.Eng.

In partial fulfillment of the requirements
For the M.A.Sc. degree in
Civil Engineering

School of Civil Engineering
Faculty of Engineering
University of Ottawa

The Masters of Applied Science in Civil Engineering is a joint program between Carleton University and University of Ottawa, which is administered by the Ottawa-Carleton Institute for Civil Engineering

Abstract

In many situations, the upper layers of soil above the ground water table are in a state of unsaturated condition. Although unsaturated soils are found throughout the world, they are predominant in arid or semi-arid regions. In these areas, the soil water characteristic curve (SWCC) which relates the water content to the matric suction could be used as key tool to implement the mechanics of unsaturated soils into the designs of geotechnical structures such as dams, embankments, pavements, canals, and foundations. Several experimental techniques are available for determining the SWCC in a laboratory environment. However, these experimental techniques are expensive, time consuming typically requiring days or weeks, depending on the soil type, and demanding intricate testing equipment. Due to these reasons, there has been a growing interest to find other means for estimating SWCC and encourage the adoption of unsaturated soils mechanics in geotechnical engineering practice.

Several methods exist to indirectly estimate the SWCC from basic soil properties. Some may include statistical estimation of the water content at selected matric suction values, correlation of soil properties with the fitting parameters of an analytical equation that represents the SWCC, estimation of the SWCC using a physics-based conceptual model, and artificial intelligence methods such as neural networks or genetic programming. However, many studies have shown that environmental effects such as temperature, soil structure, initial water content, void ratio, stress history, compaction method, etc. can also affect the SWCC. This means that the estimation SWCC from set of conditions may not reliably predict the SWCC in other conditions. Due to this reason, it is crucial for engineers involved with unsaturated soils to take into account all the factors that influence the SWCC.

The two key objectives of the present thesis are the development of a method based on first principles, using the capillary rise theory, to predict the variation of the SWCC as a function of temperature, as well as developing a technique for the prediction of the fixed parameters of a well known function representing the SWCC based on basic soil properties together with the moisture profile of a soil column subjected to a known temperature gradient.

A rational approach using capillary rise theory and the effect of temperature on surface tension and liquid density is developed to study the relation between temperature and

the parameters of the Fredlund and Xing (1994) equation. Several tests, using a Tempe cell submerged in a controlled temperature bath, were performed to determine the SWCC of two coarse-grained soils at different temperatures. A good comparison between the predicted SWCC at different temperatures using the proposed model and the measured values from the Tempe cell test results is achieved.

Within the scope of this thesis, a separate testing program was undertaken to indirectly estimate the SWCC of the same two coarse-grained soils from the measurement of their steady state soil-moisture profile while subjected to a fixed temperature differences. The water potential equation in the liquid and vapor phases is used to analyse the steady state flow conditions in the unsaturated soil. A good comparison is obtained for the SWCC estimated using this technique with the SWCC measured used a Tempe cell submerged in a controlled temperature bath.

The results of this study indicate that knowledge of the moisture content of a soil specimen under a constant thermal gradient and basic soil properties can be used to estimate the SWCC of the soil at the desired temperature.

Acknowledgements

I would like to express my sincere appreciation to my supervisor, Dr. Julio Ángel infante sedano, for his solid assistance, support, and encouragement throughout my research.

I would like to thank Dr. Sai Vanapalli who has given me so many ideas during teaching the course on unsaturated soil mechanics. Thanks also to all the technical and administrative staff in department of Civil Engineering specially Jean Claude Celestin.

I am grateful to Mr. Javad Sheikhtaheri as a good friend for his supporter and mentor for this work. I am also indebted to my colleagues and friends Niloufar, Fathi, Afshin, Ali, Aida, Morvarid, and Farzad for their unceasing help and good company.

Thanks also goes to the financial supports from the Natural Sciences and Engineering Research Council (NSERC).

I would like to express my gratitude to my uncles, Masoud Naderi and Afshin Naderi, for their supports and generous care.Finally, special appreciations go to my lovely parents, Fahmieh Naderi, Reza Roshani and my dear sister,Pardis Roshani whom I dedicate this thesis. I cannot complete this thesis without their love, support, and encouragements.

Contents

List of Tables

List of Figures

Chapter 1

INTRODUCTION

1.1 General Statement

In many parts of the world, which constitute approximately one third of the earth surface, soils are located above the natural ground water levelare typically in state of unsaturated condition. In these arid and semi-arid areas, a vast majority of infrastructures such as shallow or deep foundations, road and railway embankments, and slopes are founded on unsaturated soils. To describe and mathematically simulate the behavior of the unsaturated soils many researchers agree that the soil-water characteristic curve (SWCC) is perhaps the most important tool available. The SWCC is defined as the relationship between the capillary forces above the ground water table and the amount of water held within the soil. Many unsaturated soil properties such as the coefficient of permeability (Marshall 1958; Mualem 1976; van Genuchten 1980), shear strength (Vanapalli et al. 1996), and coefficient of water volume change (Fredlund and Rahardjo 1993) are highly correlated to the SWCC behavior.

Several factors such as the soil structure, initial water content, void ratio, stress history, compaction method, hysteresis, and temperature can affect the SWCC (Vanapalli et al. 1999; Zhou and Yu 2005). Therefore, assuming a unique relationship of for the SWCC of a soil in all practical scenarios may not be reasonable. While much attention has been given to the factors such as effect of the void ratio and fabric on the SWCC, relatively less has been written regarding the effect of temperature. Experimental evidence indicates that the temperature effect in unsaturated soils has an important role in analysing water movement under non isothermal condition and cannot be ignored (Philip and De Vries 1957; Liu et al 2006). Consequently, it is desirable to develop a model for

estimating the temperature dependence of the SWCC which can accurately describe this effect.

1.2 Objectives of the Thesis

The purpose of the present study is to present a method for predicting the changes of the SWCC of a soil subjected to different temperatures. This method should also enable the user to predict the moisture profile of a soil subjected to a temperature gradient. In addition, a method for indirectly estimating the SWCC of a coarse-grained soils using the change of water content, or degree of saturation, induced by a controlled thermal gradient on a soil with a known grain-size distribution and void ratio is proposed.

To develop a method for estimating the SWCC at different temperatures, knowledge of the SWCC at room temperature is necessary. First principles and the theoretical relationship between capillary rise and temperature can then be applied to estimate the effect of temperature on the parameters of the Fredlund and Xing (1994) equation (i.e., a, n, and, m) which is commonly used in the literature as a mathematical representation of the SWCC.

To achieve this goal, a test program is conducted to measure the SWCC of two coarse-grained soils at low suction range (i.e. 0 to 30 kPa) and at three different temperatures. A sensitivity analysis is then performed on the measured data to find how well the suggested approach can predict the SWCC with respect to temperature.

A related objective of this study is estimating the SWCC of a coarse-grained soil based on its grain size distribution and the water content distribution at equilibrium within a soil column subjected to a fixed temperature gradient. For this purpose, a comprehensive column test program is carried out on selected soils to determine the movement of water through the investigated soil sample under a constant thermal gradient. To investigate the limitations of the proposed approach, the redistribution of soil water in response to a fixed temperature gradient is examined at three different initial water contents.

1.3 Scope of the Thesis

In order to achieve the objectives of this thesis, an experimental program was carried out in the geotechnical laboratory at the University of Ottawa using two different sandy soils namely; Unimin Silica Sand 7030 and Industrial sand. A rational approach for estimating

the parameters used in the Fredlund and Xing equation (1994) as a function of temperature is presented. This approach estimates the effects of temperature on the air-entry value of the model by applying first principles and the theoretical relationship between capillary rise and temperature. The SWCC of the studied soils is measured in accordance with ASTM D-6836 (2002) using a Tempe Cell apparatus. The applicability of the proposed approach is investigated by measuring the SWCC at three different temperatures, namely; ($4\,^{\circ}\mathrm{C}, 20\,^{\circ}\mathrm{C}$,and $49\,^{\circ}\mathrm{C}$). For the $20\,^{\circ}\mathrm{C}, 49\,^{\circ}\mathrm{C}$, the Tempe cell is submerged into thermal bath that provides a constant temperature within $\pm 0.6\,^{\circ}\mathrm{C}(\pm 1^{\circ}F)$. For the cold end of the temperature range, the ($4\,^{\circ}\mathrm{C}$) temperature was maintained taking advantage of the latent heat of melting ice.

To estimate the SWCC of these coarse-grained soils based on their grain size distribution and moisture profile at equilibrium under a fixed thermal gradient, the vapor and liquid movement formulations for unsaturated soils under non isothermal condition given by Thomas (1992), is used. The proposed model relies on solving simultaneously the water potential equation in the liquid and vapor phases which can be used for analyzing steady flow conditions in unsaturated soils and the proposed equation for describing the relationship between the SWCC and temperature. To verify this new approach, an experimental setup inspired by the work of Evgin and Svec (1988) was designed and conducted on the same soils studied in the first part of the investigation. The fixed temperature gradient was generated by circulating water, at two different temperatures, in two containers that are placed at the extremities of the soil specimen. During the experiment, the temperature profile along the soil specimen is measured regularly via an infrared thermal emissivity thermometer and the gravimetric moisture content is measured at steady state by extracting soil specimens from ports placed along the specimen length. The method is validated using these experimental results and data extracted from the literature.

The results of this research program can potentially be valuable for geotechnical engineers who deal with the unsaturated soil mechanics. The outcome may lead to methods reduce the time and resources required to establish the SWCC and encourage broader use of unsaturated soil mechanics in conventional geotechnical and geoenvironmental engineering practice.

1.4 Organization of the Thesis

The thesis is divided into five chapters. Chapter One contains the introduction, while Chapter Two provides the literature review.

Eight sections are included in Chapter Two; Section One discusses the effective stress concepts and stress state variable in unsaturated soils; Section Two introduces the concept of matric suction and the capillary model; Sections Three and Four provide an overview of the SWCC and its implementation for geotechnical engineering purposes; Section Five presents the conventional experimental methods for measuring the SWCC; Section Six provides the suggested mathematical equations for describing the SWCC; Section Seven discusses the effect of different environmental factors on the SWCC; and finally, Section Eight gives the background information on the Thermo-Hydraulic relationships

Chapter Three investigates the effect of temperature on the SWCC. The chapter contains a description of the principles used to predict the changes in SWCC related to a change in temperature. An experimental program aiming to provide data to validate the method is also presented.

Chapter Four introduces a new method to estimate the SWCC using the moisture profile in an unsaturated soil column subjected to a constant temperature gradient, as well as the grain size distribution and void ratio. An experimental program to subject two soils with known SWCC to a thermal gradient to test the methods applicability is also presented.

Chapter Five contains a summary of the observations and conclusions that have been developed throughout this thesis.

Chapter 2

THEORETICAL AND TECHNICAL BACKGROUND

2.1 Introduction

The aim of the research presented in this thesis is to understand the influence of temperature on the SWCC and develop a new technique for indirectly predicting the SWCC of coarse-grained soils using the water movement in unsaturated soils under a fixed temperature gradient. To achieve this objective, background information related to heat and moisture migration in unsaturated soils is required. This chapter briefly provides background about the concept of soil-water characteristic curve (SWCC) and its use in engineering problems. In addition, the effects of the initial environmental conditions such as temperature, compaction, stress history, and texture of the soil on the SWCC are also discussed succinctly. Common numerical approaches for simulating coupled heat and moisture transport in unsaturated soils are also discussed.

2.2 Effective stress concept and stress state variable in unsaturated soils

In many regions of the world, soil condition is neither fully saturated and nor fully dried. Due to a higher annual rate of evaporation in comparison with the rate of infiltration, these types of soils are in a state of unsaturated condition (Vanapalli et al. 1996). Unlike the saturated soils, which are comprised of two phases: solid (soil particles) and liquid

(water), the unsaturated soils represent a multi-phase system which consists of air, solid, and water. Davies and Rideal (1963) stated that air-water interface can be considered as an independent property and definite bounding surface (i.e., contractile skin) and therefore should be categorized as a fourth phase in unsaturated soils. Figure 2.1 illustrates unsaturated soil elements which are seen as the combination of four independent phases.

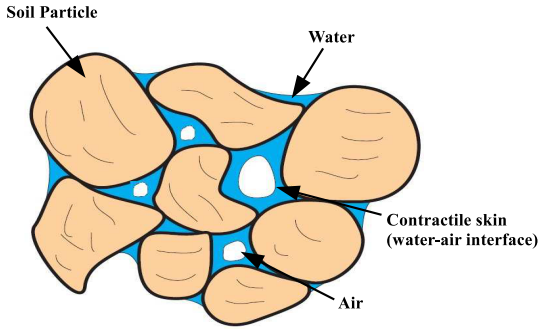

Figure 2.1: Typical structure in an unsaturated soil

The pore-air, u_a and pore-water, u_w pressures in the soil structure of unsaturated soils affect their engineering behavior such as flow, shear strength and volume change behavior. Considerable experimental and theoretical efforts have been undertaken to understand stress state variables in unsaturated soils beginning with Bishops work (1959). The first model was derived by extending the approach of the single stress state variable $(\sigma - u_w)$ that Terzaghi (1936) proposed for interpreting the mechanics of saturated soils and was given as (Bishops 1959):

$$\sigma' = (\sigma - u_a) + \chi(u_a - u_w) \tag{2.1}$$

where, σ' = effective stress,σ = total stress, u_a = air pressure in the pore space, u_w =pore-water pressure, $(\sigma - u_a)$= net normal stress, and $(u_a - u_w)$ = matric suction. In Bishops model, a factor χ was defined as an effective stress parameter which depends on the degree of saturation. It can be seen that there is a smooth transition from Terzaghi's effective stress equation to the Bishop's equation.

In 1961, The validity of this approach was examined by performing triaxial tests on an unsaturated silty soil in which the values of the stress state $(\sigma - u_a)$ or $(u_a - u_w)$ was keeping constant while values of σ, u_a, and u_w were varied. The results indicated that

the measured stress-stain curve had a monotonic behaviour which indirectly supported by Bishop's equation (Bishop and Donland 1961).

However, further studies in this field by Jennings and Burland (1962), Burland (1964), and Fredlund and Morgenstern (1977) indicated that the parameter χ is also function of other soil properties such as soil structure, wetting and drying cycle and etc. which, in turn, affect the existence of a unique relationship between the parameter χ and degree of saturation (Figure 2.2).

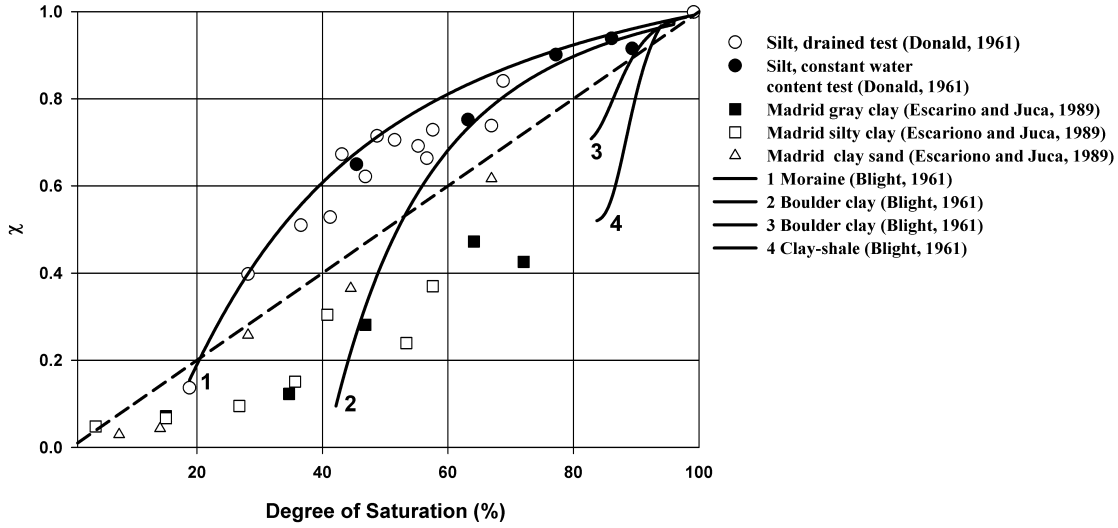

Figure 2.2: Experimental results showing the relationship between χ parameter and the degree of saturation (Lu and Likos 2004)

Fredlund and Morgenstern (1977) introduced the conventional concept of using two independent stress-state variables instead of a single stress state variable for describing the unsaturated soil properties. Fredlund et al. (1978) indicated that this approach eliminates the limitation of using single stress state variable in Bishop's equation and may overcome the difficulty in the interpretation of some soil properties in partially saturated soils such as the shear strength behaviour. According to this approach, the unsaturated soil is influenced independently by two stresses namely; net normal stress $(\sigma - u_a)$, the difference between the total normal stress and the pore-air pressure, and matric suction $(u_a - u_w)$, the difference between the pore-air and pore-water pressures. However, additional experimental evidence has shown that the magnitude of the matric suction is often considerably higher than the magnitude of the net normal stress (Fredlund and Rahardjo

1993). For this reason, more attention has recently been directed towards providing a relation between the matric suction and the basic soil properties such as the degree of saturation that can help measure its value in a practical way.

2.3 Concept of matric suction and capillary model

Soil suction or total suction can be defined as the free energy state of soil water which is expressed in terms of pressure. Conceptually soil suction is the ability of an unsaturated soil to retain water (Edlefsen and Anderson 1943). If gravity, temperature, and inertial effects are ignored, the main physical and physiochemical mechanisms which are responsible for this attraction can be divided into two key components: matric suction and osmotic suction (Aitchison, 1965). Therefore, the total suction can be expressed as:

$$\psi = (u_a - u_w) + \pi \tag{2.2}$$

where π is the osmotic pressure and $(u_a - u_w)$ is the matric suction which was introduced previously as an independent stress state variable (Fredlund and Rahardjo 1993). The osmotic suction stems from chemical interaction effects such as dissolved solutes and can occur in either saturated or unsaturated soils. However, the matric suction stems from the physical interaction effects or capillary forces and can happen only in unsaturated soils.

If the pores of an unsaturated soil are assumed to be a series of cylinders, the movement of water in the liquid phase due to matric suction can be formulated by using capillary theory. In this theory, the term of wettability is defined as the attraction of one fluid for solid particles in the presence of air. Assuming a small glass which is placed into water under atmospheric conditions(Figure 2.3), the rise of water within this tube is the result of surface tension (T_s) and the tendency of water, referred to as the wetting fluid, to wet the glass (Duncan and Wright 2005). The difference between the wetting and non-wetting fluid can be expressed by the contact angle (α). If this angle is less than 90 °, water can wet the surface of the solid particles. The relation between the pore size geometry, surface tension, and matric suction can be obtained from simple analysis in equilibrium condition and calculated as:

$$(u_a - u_w) = \frac{2T_s}{R_s} \tag{2.3}$$

where R_s =the radius of curvature of the meniscus (i.e. $\frac{r}{cos\alpha}$), (T_s) is the surface tension of water, and ($u_a - u_w$) is the matric suction or the difference between the non-wetting, and wetting fluid pressure.

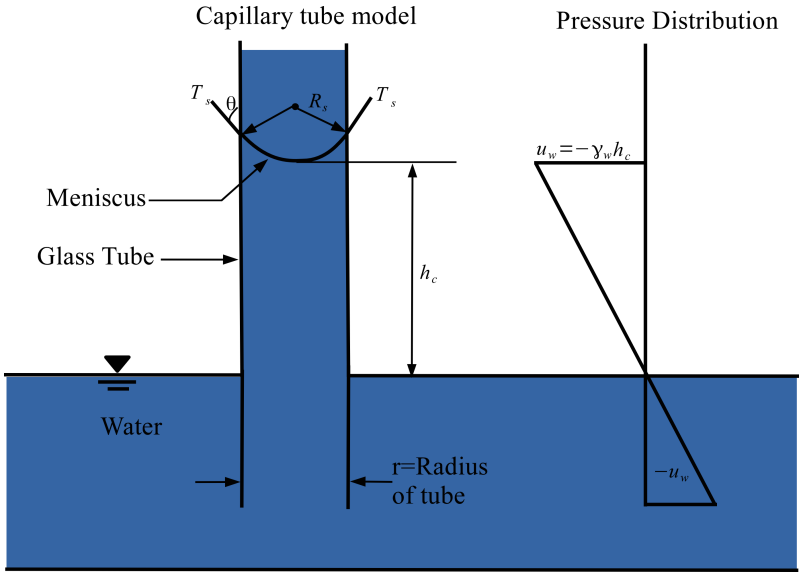

Figure 2.3: Physical model and phenomenon related to capillary theory

2.4 Soil Water-Characteristic Curve (SWCC)

The soil water-characteristic curves (SWCC) is broadly defined as the relationship between soil matric suction ($u_a - u_w$) and gravimetric water content w or the volumetric water content θ, or the degree of saturation S (Buckingham 1907; Williams 1982). Indeed, the SWCC is used as a conceptual tool for understanding the relationship between the capillary model and the distribution of water within voids. A comprehensive summary of the early understanding of the SWCC can be found in Barbour (1998). According to Barbour (1998), the key transition points in SWCC are:

(i) Air-entry value or the air-entry pressure.

(ii) Residual volumetric water content.

The air entry value or bubbling pressure is defined as the matric suction where the air begins to enter (assuming a drying path) the largest pores or represents the difference

between the air pressure and water pressure in the largest pores (Vanapalli et al. 1996). It should be noted that the process of desaturation only occurs at suction values greater than the air entry value. Therefore, at suction values lower than air entry value, the soil remains almost saturated. The residual volumetric water content represents the condition of soil at which the liquid phase becomes discontinuous and it is increasingly difficult to remove water from the soil sample.

Soil scientists traditionally assume that the residual state of soils is around $1500kPa$ where the plants cannot imbibe any more moisture from the soil. This point corresponds to the wilting point for many plants (Vanapalli et al. 1996). However, more experimental results on a number of different soils by Croney and Coleman (1961), Koorevaar et al. (1983), and Vanapalli (1994) indicated that the volumetric water content approaches zero as the suction approaches $1000000kPa$. This value is also supported by thermodynamic considerations (Richards 1965).

The SWCC is normally plotted on semi-logarithmic scales to cover the full range of suction from zero to $1000000kPa$. In order to describe the SWCC, Vanapalli et al. (1999) divided the SWCC into three different segments, which are: boundary effect, transition, and residual zones, as shown in Figure 2.4.

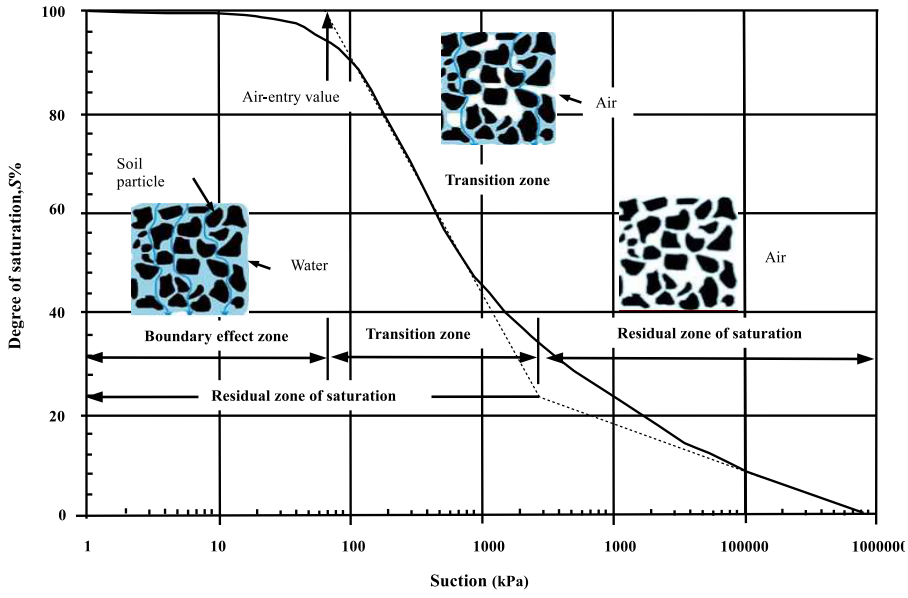

Figure 2.4: Typical zone of soil water characteristic curves, showing zones of desaturation (Vanapalli et al. 1999)

In the boundary effect zone, the water fills all the pores and soil is in a saturated condition. In the transition zone, the slope of the SWCC is steeper and the degree of saturation decreases rapidly. As a result, the saturation of the pores will decrease until such a point where a large increases in suction leads only to relatively small changes in water content. The residual zone of the SWCC can be considered as the stage where the movement of water cannot happen in the liquid phase and the water is no longer continuous.

The measurement of the SWCC may be obtained in two different ways:

(i) Taking a saturated sample and applying suction to desaturate it(desorption or drying).

(ii) Gradually wetting an initially dry sample (adsorption or wetting).

It can be noted that these two methods do not produce an identical SWCC shape and the end point of drying curve may differ from the starting point of wetting curve. This phenomenon is called hysteresis. Figure 2.5 shows a typical SWCC for a silt soil along with three mechanisms to which the hysteresis phenomenon is conventionally attributed (Fredlund and Rahardjo 1993).

(i) The shape and diameter of interconnected pores within the soil is not uniform and identical to each other. This effect is called the "ink bottle effect". As Figure 2.5 a) shows, at the same volumetric water content the drying path is governed by the small pores and a higher suction, however the wetting path is governed by the larger pores and requires small suction to achieve the same water content (Tuller and Or 2004).

(ii) There is a different contact angle between a soil particle and advancing air-water interface during drying and wetting path. Typically, the liquid –solid contact angle in adsorption is larger (Figure 2.5b).

(iii) The presence of entrapped air in the pores may also reduce the water content of the soil as the suction decreases. During wetting, some air gets trapped in the soil and therefore the volumetric water content tends towards a lower value than it had initially and cause the wetting path to differ from drying path (Tuller and Or 2004).

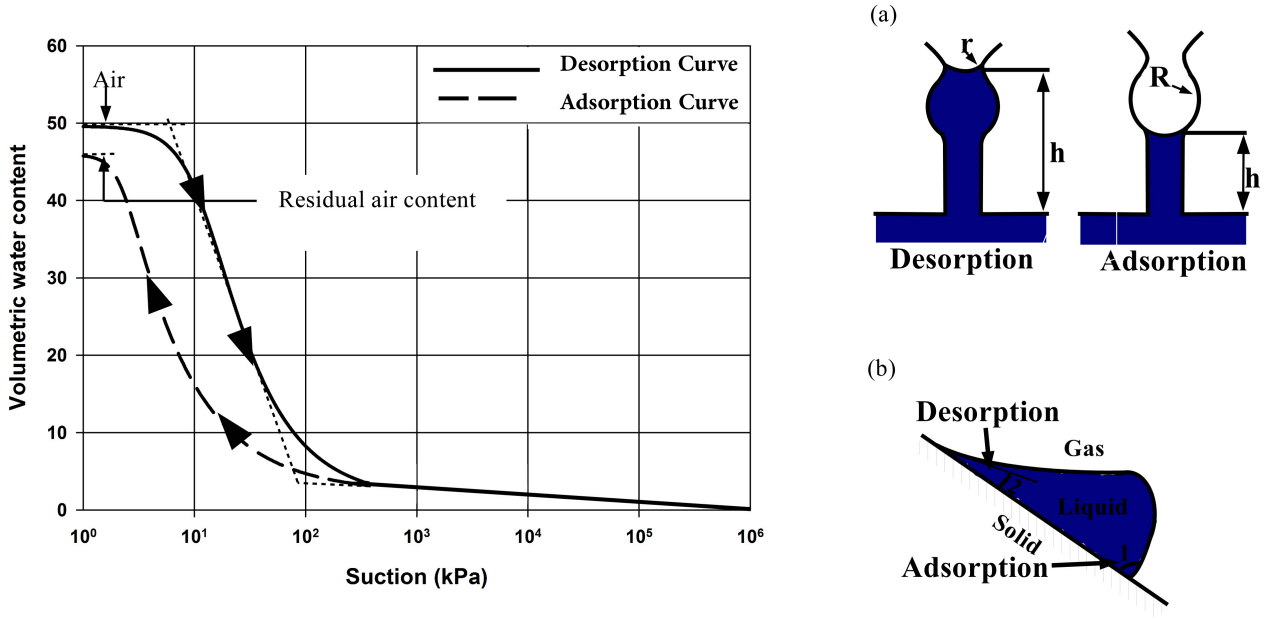

Figure 2.5: Hysteresis phenomenon in SWCC of silty soil, (a) The ink bottle effect (b) The contact angle effect (Fredlund and Rahardjo 1993)

2.5 Importance of SWCC in geotechnical engineering

The measurements of the unsaturated soil properties such as the shear strength and volume change behaviour require highly skilled technicians, intricate laboratory equipment, and can result in substantial added costs. For these reasons, the implementation of unsaturated soil mechanics for routine geotechnical engineering projects would benefit from a tool that can allow a practical and sufficiently accurate estimate this soil property. Fredlund (2004) observed that the SWCC and the saturated soil properties along with one additional soil parameter is sufficient to estimate unsaturated soil properties with a high degree of reliability and confidence.

$$\textbf{Unsaturated soil property} = [SaturatedSoilProperty]f(SWRC)^{soilparameter} \quad (2.4)$$

As an example, analysis of the flow of water in unsaturated soil based on Darcy's law requires defining the coefficient of permeability. This coefficient is significantly affected

by the degree of saturation. Burdine (1953) and Brooks and Coney (1964) indicated that the permeability function of an unsaturated soil can be obtained from its SWCC. Figure 2.6 shows the plots of a typical SWCC and the predicted hydraulic conductivity function. The key attributions such as the location and steepness in the shape of hydraulic conductivity curve are highly related to the air-entry value and steepness of its SWRC (Gitirana 2005).

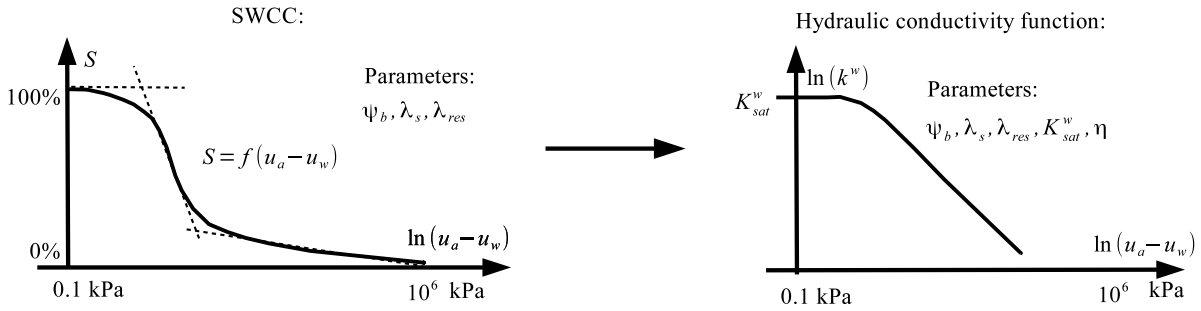

Figure 2.6: Estimating hydraulic conductivity function based on SWCC (Gitirana 2005)

In the analysis of shear strength behaviour, Vanapalli (1994) indicates that the shear strength of an unsaturated soils is significantly affected by the amount of water present within the pore space which indirectly can be related to the SWCC. Vanapalli et al. (1996) developed an approach to predict the behaviour of shear strength with respect to matric suction using the saturated shear strength parameters and the SWCC.

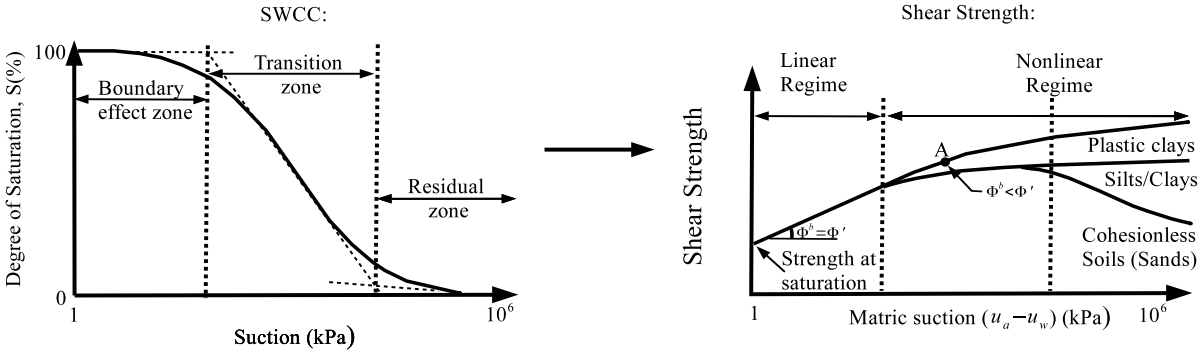

Figure 2.7: Estimating shear strength function based on SWCC (Vanapalli et al. 1996)

As Figure 2.7 shows, the air entry values (AEV) of the SWCC may be used to discretize the behavior of shear strength of unsaturated soil into two different paths:

(i) Before the AEV: The gradient of matric suction contributing to the shear strength displays a linear behaviour (Vanapalli et al. 1996).

(ii) After the AEV: As the soil starts to desaturate, the effective area of contact between the liquid phase and soil particles decreases and the air phases increases. Therefore, the relation between matric suction and shear strength becomes nonlinear (Vanapalli et al. 1996).

2.6 Methods to measure soil suction

Several methods are available for measuring the suction of a soil sample (Fredlund and Rahardjo 1993). Some of these methods can measure suction directly while other techniques can determine suction indirectly.

2.6.1 Tesiometers

Tensiometers are devices that allow direct measurement of the soil suction, or the negative pore water pressure (Figure 2.8). The negative water pressure is equal to the matric suction if the pore-air pressure is considered to be equal to atmospheric pressure ($u_a = 0$). Tensiometers are comprised of a high entry ceramic cup which is used as an interface between the system of measurement and the negative water pressure. A pressure measuring device can be a mercury manometer, a vacuum gauge, or an electronic transducer. To measure the suction of a soil specimen, the ceramic cup must be saturated with de-aired water. The saturated cup is then inserted into a pre-cored hole in the specimen. Once equilibrium is reached, the water in the Tensiometer has the same negative pressure as the pore-water within the soil. Standard Tensiometers can measure suction up to $100kPa$. Higher suction measurements are limited by cavitation problems and require other types of instruments such as the osmotic tensiometer.

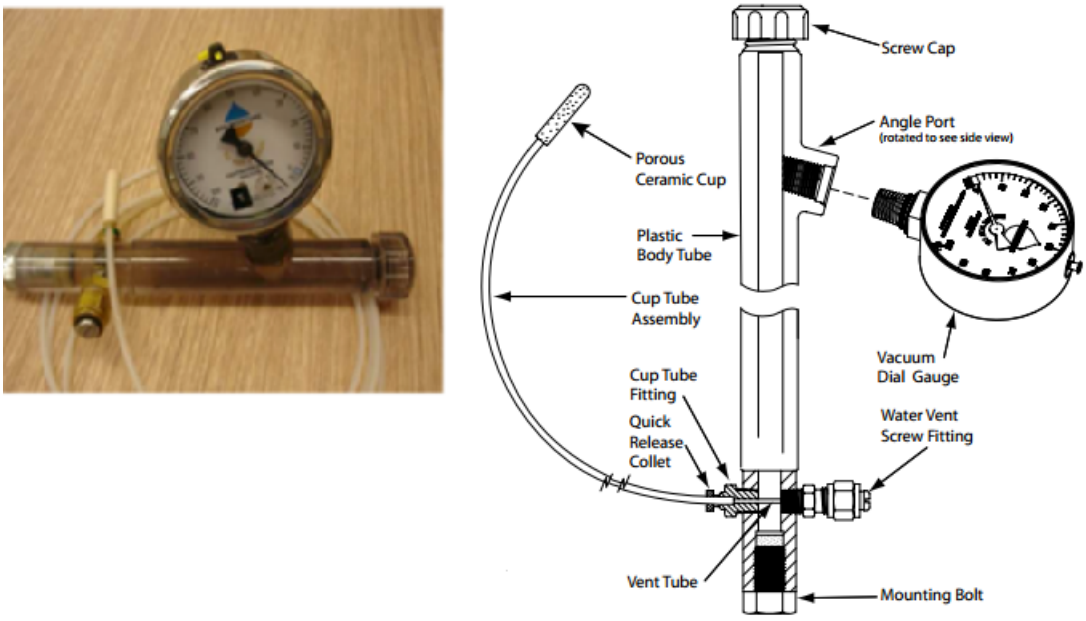

Figure 2.8: Conventional Tensiometer

2.6.2 Axis translation technique

The axis translation technique was originally proposed by Hilf (1956) and is used commonly in the determination of the SWCC in the laboratory. It is not a suction measurement technique but rather a suction control method. In this technique, the pore water is maintained under atmospheric pressure, while the air phase is subjected to a larger pressure. Thus the matric suction (u_a–u_w) is achieved by applying a positive air pressure without risk of cavitation and suction values greater than $101.3kPa$ can be achieved. Typically, in laboratory environment, the highest value of suction measurement is limited to $1500kPa$ for practical reasons .

The pressure plate and pressure membrane are common apparatus that are designed to apply a matric suction to soil specimens utilizing Axis translation technique. These devices can be used to measure the suction of multiple samples simultaneously. Figure 2.9 shows a schematic of a pressure plate device. The pressure membrane devices uses a cellulose membrane while the pressure plate uses of a porous high air-entry ceramic disk. The membrane or the ceramic disk is used as an interface to separate the specimen exposed to gaseous atmosphere and the outflow fluid. Prior to running the experiment, the ceramic disk must be saturated and any entrapped air accumulated must beremoved.

This procedure ensures a hydraulic connection between the soil-water and free water beneath of the ceramic disk. When the chosen air pressure is applied, water is allowed to be expelled from the specimens and collected in the outlet tube. The equilibrium condition is reached once no water is discharged from the apparatus. At this time, the changes of water content of each soil specimen(s) can be determined using gravimetric method by physically removing the samples from the device and weighing them.

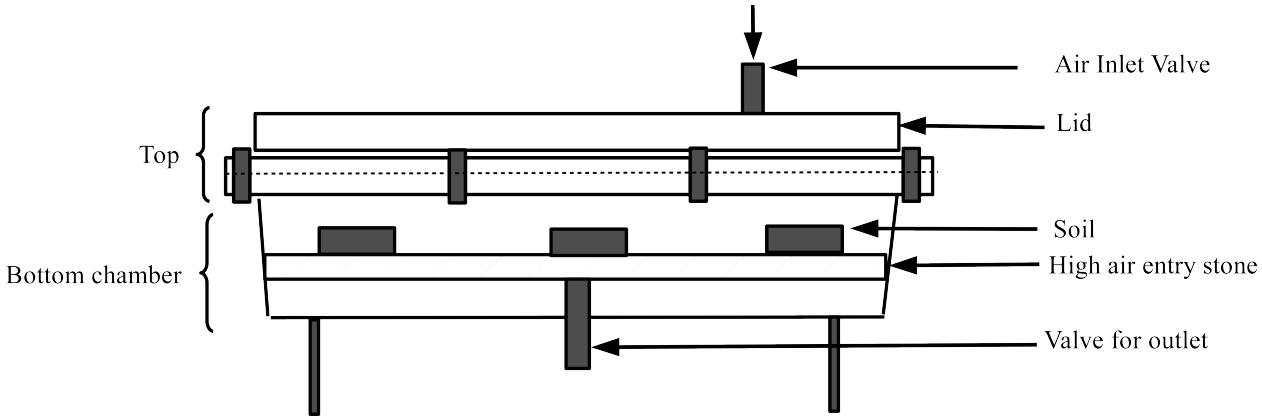

Figure 2.9: Schematic of pressure plate apparatus

2.6.3 Filter paper

The filter paper method was originally developed in the 1920's for agricultural and soil science applications and is used for the indirect measurement of the matric suction or total suction (McQueen and Miller 1974). This method has a relatively low cost and sufficient accuracy to measure suction. In this method, a filter paper can be placed directly in contact with the soil specimen to determine matric suction or indirectly in contact with the soil sample to determine the total suction (Figure 2.10). When a direct contact is used, the filter paper is located on the top of the soil sample (Bulut et al. 2001) or is buried within the sample (Houston et al. 1994) and the water from the specimen can be exchanged in the liquid phase. On the other hand, when a filter paper is indirectly in contact with the soil, the water can only be exchanged in the vapor phase. After reaching equilibrium, the suction value of the soil is determined by determining the moisture content of filter paper and using some calibration techniques which is unique for a particular type of paper.

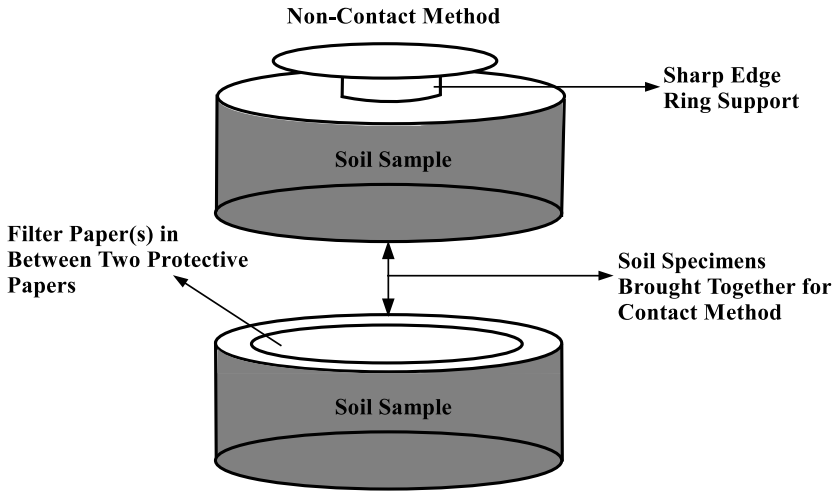

Figure 2.10: Procedure for filter paper testing (Likos and Lu 2002)

2.6.4 Psychometers

The suction of a soil sample is related to the vapor pressure of the air surrounding the pores of the soil. The thermocouple psychometers are devices that use this feature to measure the total suction by measuring the relative humidity (RH) of the air within the pores. To measure RH, a temperature gradient between a non-evaporating surface and an evaporating surface is created (Spanner 1951). To achieve this, an electrical circuit formed by thin wires of dissimilar metals is used inside the psychomotor apparatus, in a configuration called thermocouple. Prior to running the test, the soil sample must be sealed in a chamber and allowed to reach temperature equilibrium with the psychrometer. The equilibrium times typically last from hours to several days and are significantly affected by the soil suction and initial relative humidity of the device (Brown 1970; Campbell and Gardner 1971). Using Seed back effect and Peltier effect; the thermocouple psychometers can measure the total suction in a soil sample. The output result is in microvolts which are then converted into total suction using appropriate calibration curves (Tang et al. 1997).

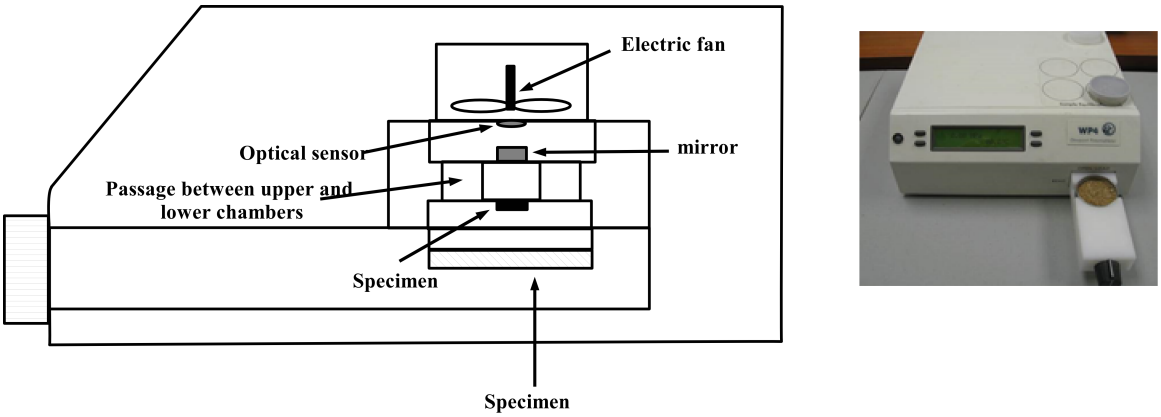

Figure 2.11: A schematic diagram of laboratory psychrometer (Fredlund et al. 2012)

2.7 Review of mathematical equations for describing the SWCC

Numerous empirical, analytical and statistical models are available in the literature to represent the mathematical formulations of the SWCC. These equations are used to fit the laboratory test results and extrapolate or interpolate where there is no experimental data. A comprehensive summary and comparison of these equations can be found in Leong and Rahardjo (1997), and Sillers et al. (2001). The common equations that are readily used in literature to estimate the shape of SWCC are summarized in Table 2.1. Depending upon the number of unknown parameters in these equations, a minimum of three to four experimental data points is required. The accuracy of the fitting analysis can be enhanced with an increase in the number of experimental data points, however.

Among these models, the van Genuchten (1980), and Fredlund and Xing (1994) equations are the most commonly used equations for engineering problems (Gerscovich and Sayao 2002; Malaya and Sreedeep 2011). In comparison with the van Genuchten (1980) equation, the model presented by Fredlund and Xing (1994) presents advantages due to its definition of the SWCC relationship for the entire range of suction (i.e. up to 1 000 000 kPa), and more flexibility in terms of its ability to fit experimental data in a wide range of suctions and requiring less iteration in to find optimum value of these parameters in different types of soils whether silt, sand, or clay (Sillers et al. 2001).

Table 2.1: SWCC equations and corresponding fixed parameters

References	Equations	Fixed Parameters
Gardner (1956)	$\theta_w = \theta_r + \frac{\theta_s - \theta_r}{1 + a_g \psi^{b_g}}$	a_g, b_g: first, and second fixed parameters
Brooks and Corey (1964)	$\theta_w = \theta_r + (\theta_s - \theta_r)(\frac{a_{bc}}{\psi})^{b_{bc}}$	a_{bc},b_{bc}: first, and second fixed parameters
Brutsaert (1966)	$\theta_w = \theta_r + \frac{\theta_s - \theta_r}{1 + (\frac{\psi}{a_b})^{n_b}}$	a_b,n_b: first, and second fixed parameters
Van Ganuchten (1980)	$\theta_w = \theta_r + \frac{\theta_s - \theta_r}{(1 + a_{vg} \psi^{b_{vg}})^{c_{vg}}}$	a_{vg}, b_{vg}, c_{vg}: first, second fixed, and third parameter
Mckee and Bumb (1987)	$\theta_w = \theta_r + (\theta_s - \theta_r) exp(\frac{a - \psi}{b})$	a,b: first, and second fixed parameters
Fredlund and Xing (1994)	$\theta_w = \theta_r + \frac{\theta_s - \theta_r}{(ln(e + (\frac{\psi}{a_f})^{n_f}))^{m_f}}$	a_f, n_f, m_f: first, second fixed, and third parameter

Recently, more studies have been directed toward developing solutions for indirectly estimating the SWCC. Fredlund (2000) indicated that estimation of SWCC by using basic soil properties rather than conventional methods is highly valuable for geotechnical engineers in preliminary steps of design and analysis. Zapata et al. (2000) divided these estimation methods into two major groups. On group of these models tries to find the statistical relationships between the structural and textural soil properties and water content versus suction values (Gupta and Larson 1979; Aubertin et al. 1998). Generally, regression analysis followed by a curve fitting is highly needed. The other group tries to develop the relationship between the parameters of the SWCC equations and the physical properties of the soil such as grain size distribution, and void ratio (Tomasella and Hodnett 1998; Perera et al. 2005). Johari et al. (2006) developed a new branch by

using artificial intelligence methods such as neural methods, and genetic programming. In this approach model is trained on an existing database to estimate the SWCC of other soils. Vanapalli and Catana (2005) propose a simplified method to estimate the SWCC for coarse-sand using one-point suction measurement and basic index properties. However, in this approach, the effect of temperature is considered negligible.

2.8 Environmental impacts on SWCC

Despite abundant research on the SWCC, the knowledge on the response of these curves to environmental factors is far from complete (Bachmann and Van der Ploeg 2002). In recent years, several studies have shown that the soil structure, stress state, compaction and temperature are influential on the SWCC behaviour. However, these effects tend to decrease at higher suction values (Zhou and Yu 2005).

2.8.1 Influence of soil structure and void ratio

The size and shape of soil particles govern the behaviour of SWCC in engineering problems (Duncan and Wright 2005). Therefore, the properties of a soil such as shear strength behaviour and volume change properties are also affected by particles size distribution. In the 1970s and 1980s, the concept of micro-structure and macro-structure of soils were introduced. The studies showed that the SWCC is highly affected by these two types of structures. The soil microstructure is described as the aggregation of very closely packed particles with small voids, whereas the soil macrostructure consist of larger particle size and wider pores. Vanapalli et al. (1996) indicated that sand or gravel are dominated by the macrostructure and tend to lose most of their water at lower suction values. However, finer soils such as clay and silt have larger capacity to keep water and more suction requires for extracting their water (Figure 2.12).

According to Malaya and Sreedeep (2011), in the range of suction from 0 to 100 kPa, the SWCC is predominantly influenced by soil structure; however, beyond this range composition and surface tension of soil is the dominant factor. C'ote and Konard (2003) studies on various types of soil indicated that the maximum pore size value or the maximum R_s in capillary theory of a soil is controlled by the fraction of finer soils rather than the coarse fraction.

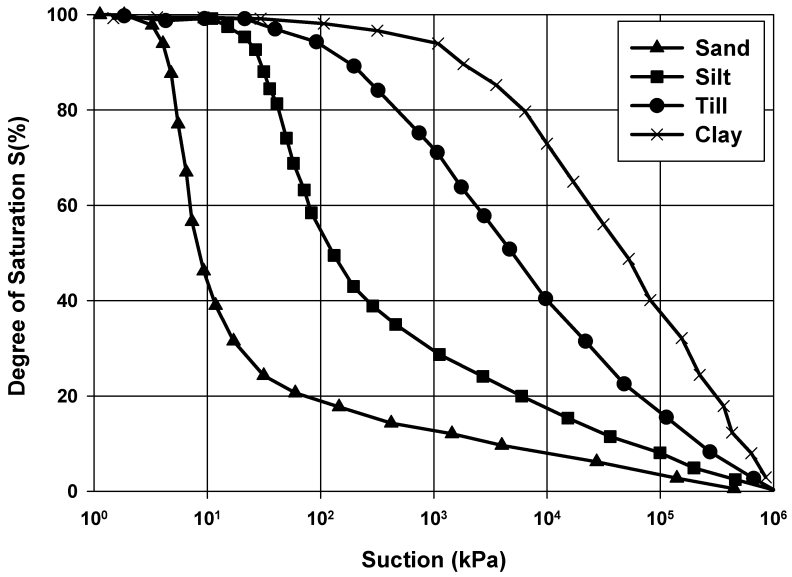

Figure 2.12: Typical SWCC for four soils (Vanapalli et al.1990)

Duncan and Wright (2005) results show that a soil with uniform ranges of pore sizes has a lower AEV. While, in well graded soils, the SWCC is smoother and the water drains more gradually. Consequentially, the soil has a higher AEV. These results are consistent with capillary theory model to estimate suction in unsaturated soils. Soil with larger radius of curvature R_s requires lower suction value to desaturate and has lower AEV .

According to Duncan and Wright (2005), the shape of the SWCC is highly influenced by the void ratio. Oedometer, pressure-plate, and shrinkage tests are the experiments used to measure the changes of void ratio in unsaturated soils (Ho et al. 1992). The experiment results by Zhou and Yu (2005) indicated that AEV is inversely related to the void ratio and expressed as:

$$S_A = ae^{-b} \tag{2.5}$$

where a and b are the fixed parameter that changes based on the soil types. Figure 2.13 shows the proposed relationship between the AEV and the overall porosity.

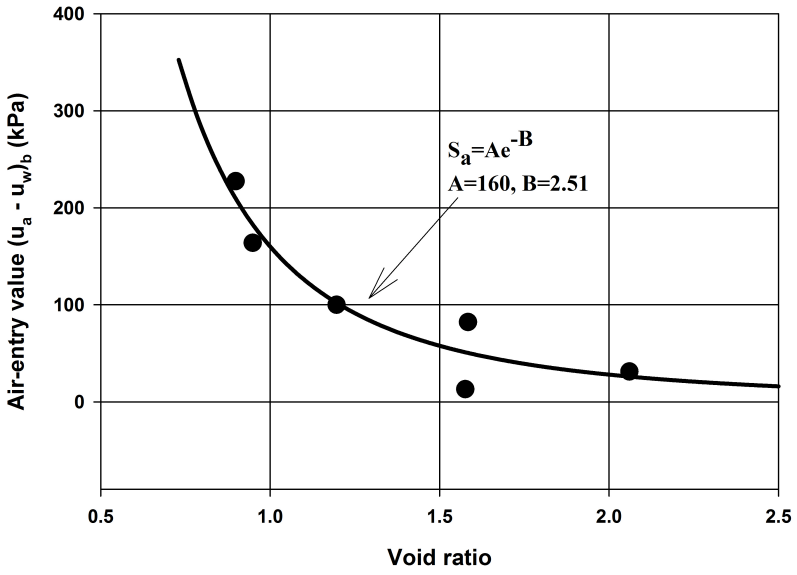

Figure 2.13: Relationship between void ratio and air-entry value (Zhou and Yu 2005)

2.8.2 Influence of liquid limit and plasticity limit

The liquid limit is defined as the minimum water content at which soil exhibits little but definite shear strength. Malaya and Sreedeep (2011) illustrates that the liquid limit in a fine-grained soil can significantly affect the SWCC. For the compacted and consolidated soils, it can be observed that when the liquid limit of soil becomes over 25%, the suction at the AEV increases up to $1000kPa$ (Malaya and Sreedeep 2011). The SWCC of fine-grained soils is also affected by the plasticity index. Obtained results by Miller et al. (2002) on clayey soils with the different plasticity index, explained that the sample with larger plasticity index can maintain higher water content at a specified suction and consequently has the higher AEV. This means the SWCC is smoother as the plasticity index is increasing.

2.8.3 Influence of compaction method and initial water content for compaction

Compacting soils is one of the frequent techniques that used in geotechnical projects such as railroad embankments, earth dams, barrier materials (Delage et al .1998; Miller et al. 2002). There are numerous factors such as initial water content, compaction

method, dry density, and energy of compaction that influence the engineering behaviour of compacted soils (Estabragh et al. 2004). Many studies have reported in the literature that compacted soils are generally in an unsaturated state and this compaction may affect their SWCC. Since the movement path of air and water through the soil is changed due to compaction, it can be expected that other properties of soil such as the soil density, shear strength, and hydraulic conductivity are also subject to such changes (Fleureau et al. 2002).

Vanapalli et al. (1999) studies on a glacial till compacted with different initial water contents show that the initial water content can significantly vary the SWCC of the same soil (Figure 2.14).

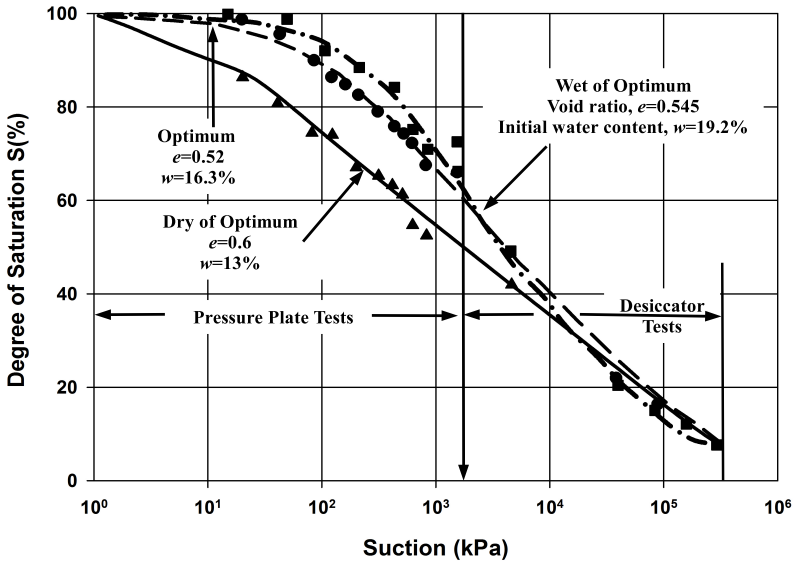

Figure 2.14: SWCC for specimens compacted at different initial water contents (Vanapalli et al. 1999)

The results also suggested that at higher suction, corresponding to the residual zone, the SWCC behaviour of these samples are very close to each other. Indeed, when the soil sample is compacted at a lower initial water content (dry of optimum), the pore space within soil particles or clods are larger and relatively low suction values are needed to extract water from the pores within the soil particles. Therefore, the rate of desaturation is relatively high and the curve has a steeper slope. On the other hand, at wet of optimum, the soil is more homogenous and the channels between the pores are more occluded. This

means that the soil sample has higher capacity to retain water and movement of water requires larger suction. In this case, the slope of SWCC is more flat (Vanapalli et al. 1999). At optimum water content, the measured SWCC of the compacted soil sample lies between SWCC of wet of optimum and SWCC of dry of optimum (Figure 2.14). This boundary can be interpreted as the margin between the occluded pores and open pores of the soil sample.

The compaction energy or compaction method either static or dynamic can also influence the SWCC behaviour. In a dynamically compacted soil, lower void ratios are typically obtained (Barden and Pavlakis 1971). It is believed that the dynamic compaction causes larger shear strains and reduces the macro pores. Miller et al. (2002) studies showed that the impact of the compaction effort is more significant in soil sample with a high plasticity index than in soil samples with a low plasticity index. In fact, a greater compaction effort induces more changes in the density and void ratio in high plasticity soil. Variation of compaction energy turns the obtained SWCCs Miller et al. (2002) into two distinct ways (Figure 2.15):

(i) Before the AEV: The soil is almost saturated and the soil sample with lowest compaction energy has more volumetric water content.

(ii) After the AEV: the soil is in a state of unsaturated condition and the water content at any given suction in the least compacted soil is less than in the more compacted soil. As a result, an inflection point is reached on the SWCC at point AEV which causes the sample with lowest compaction energy at first to be located on the top of the other samples and after the AEV, it goes below the other samples.

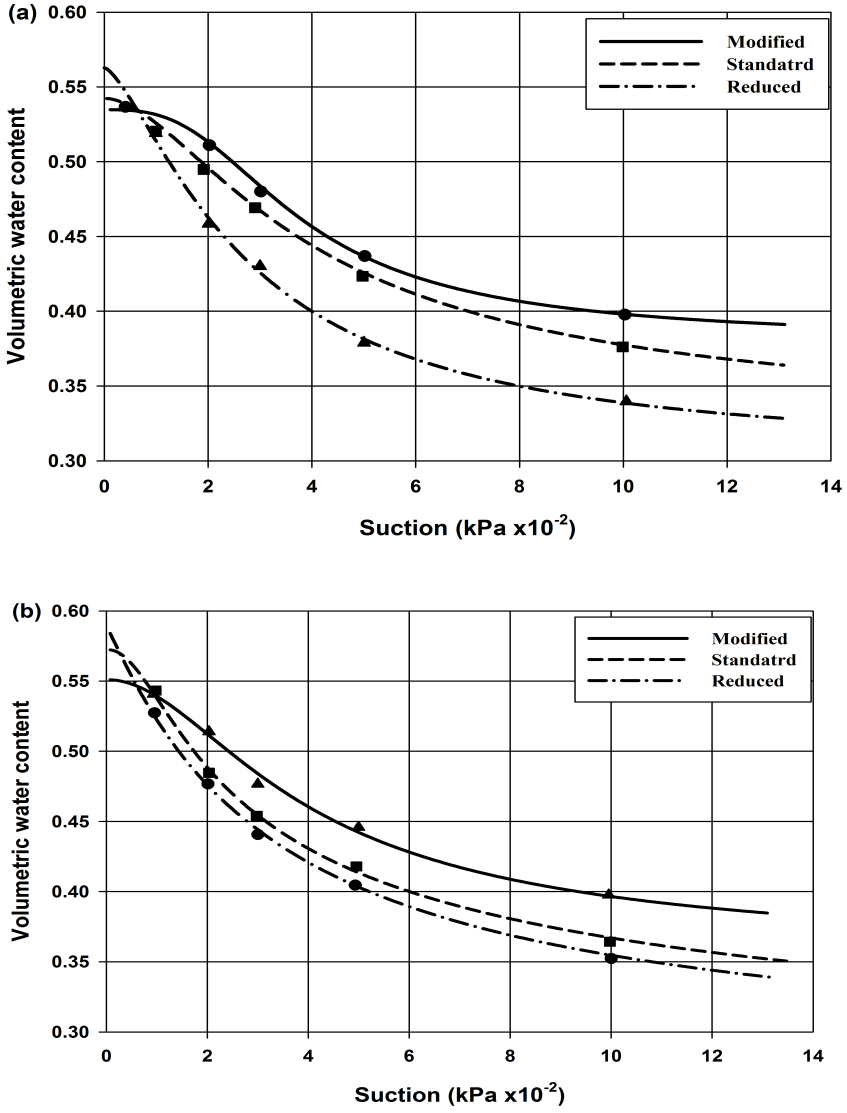

Figure 2.15: Variation in SWCC behavior due to compaction effort (a) Dry of optimum (b) Wet of optimum (Miller et al. 2002)

2.8.4 Influence of additive materials

To avoid landslide in unsaturated expansive soils, natural or chemical materials are commonly added to these soils as a form of ground improvement. However, considerable studies reported that using these materials can affect the SWCC behaviour (Rahardjo et al. 1995; Puppala et al. 2006). Hoyos et al. (2007) indicated that there is a relation

between the different proportion of cement in unsaturated soils and the AEV of SWCC. High bonding between the cement and clay particles requires higher suctions to extract water from soil samples. Therefore, in these treated soils as the proportion of cement increases, the AEV of their SWCC also increases (Hoyos et al. 2007). Dallas and Syam's (2009) observations showed that fly ash can significantly stabilize landsides of coarse-grained soils. In this method, the fly ash acts as a pozzolan or filler to decrease the void spaces among the larger size aggregate. The effectiveness of this additive is highly depending on the fraction of coarseness of soil (Malaya and Sreedeep 2011). Several studies showed that using fly ash change the behaviour of SWCC by increasing the retaining capacity of soil and the residual suction (Malaya and Sreedeep 2011). Test studies on the SWCC of bentonite-sand mixtures as a repository of high-level radioactive nuclear waste showed that the different fractions of bentonite can change the AEV of SWCC by filling a portion of the pores. Greater bentonite content results in a greater relative filling ratio of pores which in turn leads a larger AEV (Pei-yong and Qing 2009).

2.8.5 Influence of stress state and stress history

To obtain reliable SWCC, it is necessary to simulate in the laboratory the stress history that occurred in the field (Vanapalli et al. 1999). For example in a case of loading or unloading one should consider the effects of gravity through self-weight or the stresses that are applied the surface of the soil. To study the stress state effect on the SWCC, Ng and Pang (2000) used a conventional consolidation apparatus to apply a known stress history or stress state to the specimens. The results showed that when the applied pressure increases, the family of pores with large diameter will be reduced and particles are more oriented (Al-Mukhtar et al. 1996). However, the unloading process like an excavation of clayey layers changes the rearrangement of the particles and results in non-uniform pore size distribution. Experimental results by Vanapalli et al. (1998) on a compacted fine grained-soils suggested that the dry of optimum samples are more affected by stress state. Figure 2.16 shows that that the specimen in the higher equivalent pressure has a higher degree of saturation at any given suction. This means that in dry of optimum condition, because of larger void ratio or existence of macro-structure within the pores of soils, the structure of the soil sample has more potential to change. In wet of optimum conditions, however, the soil is dominated by the micro-structure and cannot change significantly in different equivalent pressures (Vanapalli et al. 1998)(Figure 2.16).

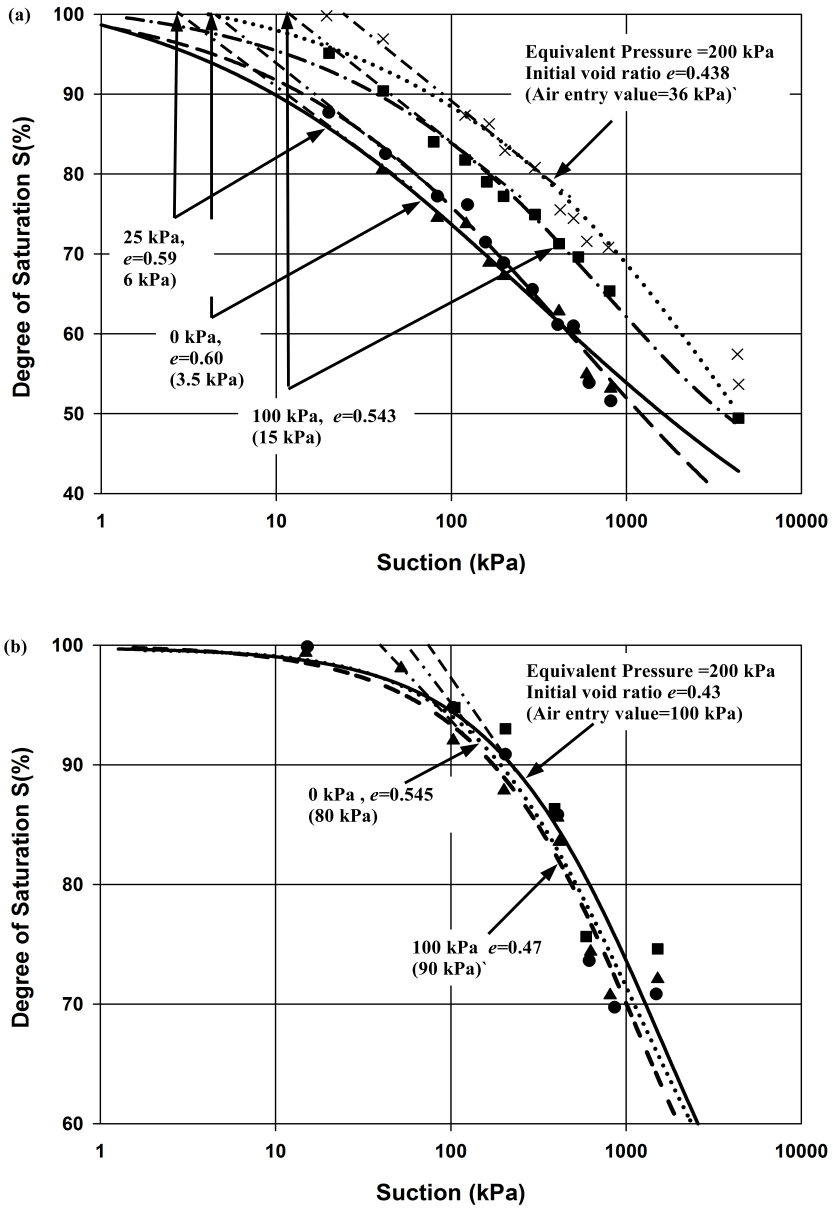

Figure 2.16: SWCC for specimens compacted at equivalent pressure of 0, 25,100,200kPa (a) Dry of optimum (b) Wet of optimum (Vanapalli et al. 1998)

Al-Mukhtar et al. (1996) mentioned that undrained and drained condition in the unloading process can also affect the pore size distribution. The results obtained on boom clay indicated that in undrained conditions, the SWCC was gradually shifted towards

the smaller pores. This means that there was rearrangement of pore space in the specimen under the applied suction which resulted in bringing the soil particles in face to face alignment and being horizontal parallel to each other. In this case the soil has the smaller pores and needs more suction to desaturate (Al-Mukhtar et al. 1996).

2.8.6 Influence of temperature and humidity

Considerable studies have shown that the temperature can affect the SWCC behaviour and hydraulic conductivity function. Experimental evidence indicates that the effect of temperature on the hydraulic conductivity is inversely proportional to the viscosity of the fluid (Haridasan and Jensen 1972; Grant 2005). Hopmans and Dane (1986a,b) indicated that the relation between the viscosity of fluids and temperature can be expressed as:

$$\mu = 661.2 \times 10^{-3} \times (T - 229)^{-1.562} \tag{2.6}$$

where T is in Kelvin. The above equation states that the viscosity of fluid decreases linearly with temperature which in turn increases the hydraulic conductivity coefficient.

While it is accepted that the effect of temperature on hydraulic conductivity can be estimated by considering the temperature effect on the viscosity of the fluid, there are still more arguments in the literature explaining the temperature effect on the SWCC. In the first attempt, King (1892) observed that temperature can significantly affect the water holding capacity of the unsaturated soils. After fifty years, Gardner (1955) by measuring the variation of capillary potential with respect to temperature in sand, sandy loam and organic soil sample noted that the suction behaviour in response to temperature decreases linearly when temperature is in the range of 0 °C to 50 °C.

On the basis of Gardner's results, Philip and De Vries (1957) proposed the first model to describe the migration of water in the liquid phase under temperature differences. Assuming a zero contact angle and using the Young- Laplace law, they expressed the variation of suction with respect to temperature as:

$$\frac{1}{p_c}\frac{dp_c}{dT} = \frac{1}{\sigma}\frac{d\sigma}{dT} \tag{2.7}$$

where p_c is the capillary pressure (Pa), σ is the surface tension at the air water interface (N/m) and, T is temperature (K). Later studies by several authors (Constantz 1991; Nimmo and Miller 1986; Grant and Bachmann 2002) have shown that using this theory

cannot completely determine variation of suction related to temperature. They postulate that additional phenomena such as the effect of occluded air bubbles, existence of the solute content and changes of contact angle need to be considered.

2.8.6.1 Effect of air bubbles

According to the SWCC behaviour, in the low suction range, the soil condition is almost saturated. This means that the liquid phase is continuous and the air is occluded in this phase in the form of bubbles. Chahal (1965), following a suggestion of Peck (1960), postulated that an increase in temperature causes the volume of entrapped air to increase and therefore to decrease the volume of the water content. Hopmans and Dane (1986b) studied this theory by experimentally measuring the SWCC of Glass beads medium and Norfolk sandy loam at two different temperatures (15 °C, and 30 °C). The obtained results indicated that contrary to Chahal's theory volume of the entrapped air decreases as the temperature increases (Figure 2.17).

Liu and Dane (1993) modified this theory and assumed that the water within pores of the soil has two forms:

(i) continuous form which contributes to the soil hydraulic equilibrium and determines the capillary potential.

(ii) isolated packets form which contributes to the temperature effect. Based on this theory, the relationship between the total water content, isolated water content, and continuous water content is defined as:

Based on this theory, the relationship between the total water content, isolated water content, and continuous water content is defined as:

$$\theta_t = \theta_s + \theta_c \tag{2.8}$$

$$\Delta\theta_t = \theta_{t,1} - \theta_{t,2} = \frac{\theta_s - \theta_{t,1}}{(\theta_{r,1} - \theta_{r,2})(\theta_s - \theta_{r,1})} \tag{2.9}$$

$$\frac{p_{c,1}(\theta_c, 1)}{p_{c,2}(\theta_c, 2)} = \frac{\sigma(T_2)}{\sigma(T_1)} \tag{2.10}$$

where θ_c is the continuous volumetric water content, θ_s is the isolated volumetric water content, θ_r is the residual volumetric water content, θ_t is the total volumetric water content, $p_{c,1}$and $p_{c,2}$ are the water pressure head values at T_1 and T_1, and $\sigma(T)$ is the surface tension at a desirable temperature. Using this theory to calculate the SWCC at desirable temperatures from the known SWCC at a reference temperature requires knowing the residual water content at both temperatures. The limitation of this model is related to the calculation of the isolated packet where it is impossible to know which fraction of liquid phase is contributing to the isolated packet at each suction value (Salager et al. 2011).

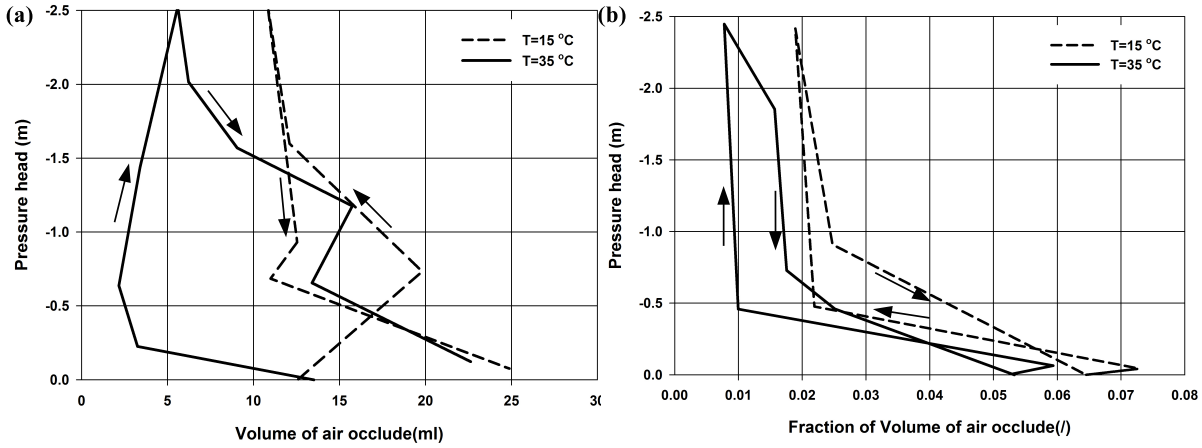

Figure 2.17: Estimated volume of entapped air as a function of tempreture (a) Glass beads medium (b) Norfolk sandy loam (Hopmans and Dane 1986b)

2.8.6.2 Effect of solute content

In compounds of natural soils, the solute can appear as mineral or in organic form. Typically, their concentration in the water phase of organic soil is around $0.01\frac{mol}{kg}$. It is well known that solutes can significantly affect the thermo-physical properties of their solution (Grant and Bachmann 2002). As a result it is reasonable to expect that the temperature can affect the liquid surface tension of these solutions more than that of pure water. Some studies on the concentration of inorganic cations in the soil solution indicated that the liquid surface tension increased with a higher concentration of this compound (Grant and Bachmann 2002). However, a reduction of liquid surface tension

was more commonly reported in literature (Anderson et al. 1995; Grant and Bachmann 2002). Singleton (1960) and Nimmo and Miller (1986) measurements of the variation of surface tension with respect to organic concentration indicated that increasing the concentration of fatty acid can decrease the surface tension by up to 30%. The results also suggested that the solubility of fatty acid as an organic compound can increase by factor of 2 or 3 when temperature is in the range of 0 °C to 60 °C.

2.8.6.3 Effect of contact angle

The wetting angle or the contact angle of a solid liquid interface in capillary tube is defined as:

$$\cos(\theta) = \frac{\sigma_{ls} - \sigma_{gs}}{\sigma_{lg}} \tag{2.11}$$

where σ_{ls} is the solid liquid interfacial tension, σ_{gs} is the gas solid interfacial tension, and σ_{lg} is the liquid gas interfacial tension. At a zero angle it can be shown that the σ_{ls} is equal to σ_{gs}. Grant and Bachmann (2002) reported that the presence of solutes may considerably affect the contact angle. The available data from literature shows that there is a significant discrepancy in behaviour of contact angle with respect to temperature which is related to the experimental difficulties in measuring this factor (Salager et al. 2011). King (1981) and Bachmann et al. (2002) studies on sand, silts and clays reported that the wetting angle tends to decrease with increasing temperature. However, She and Sleep (1998) studies showed that the contact angle increases with increasing temperature.

2.9 Models available to estimate moisture flow under the effect of temperature in unsaturated soils

In the early 1950s, attention on the physics of moisture movement in both saturated and unsaturated soils was considerable. The results of these studies indicated that when there is a temperature gradient between two ends of a sample, the moisture content of the soil sample is redistributed and water migrates from the hot boundary toward the cold boundary which is attributed mostly to changes of surface tension as a function of temperature. It is known that the thermal conductivity of a soil is related to its moisture content. This means that the redistribution of moisture content can in turn affect the

temperature distribution in the soil. Consequently, the temperature and moisture content vary until equilibrium between the moisture and temperature gradient is reached. This process which happens in a coupled manner is called Thermo-Hydraulic behaviour (TH) and can be observed in many engineering projects such as nuclear waste barriers, underground power cables, and frost heave phenomena (Hussain 1997). Philip and De Vries (1957) indicated that at equilibrium condition the liquid and vapor velocity should be equal but opposite in direction. In order to propose a numerical model to simulate thermally induced soil water movement in unsaturated soil, De Vries' (1987) studies showed that the following process needs to be taken into consideration:

(i) Heat transfer through the soil sample

(ii) Consideration of movement of different phases in unsaturated soil such as liquid water, water vapour, and dry air.

(iii) Effect of capillary forces such as surface tension and other physiochemical effects

(iv) Changes in material properties such as changes of SWCC and hydraulic conductivity as a function of temperature.

Different theories have been proposed in the literature to explain the migration of water under a fixed temperature gradient in unsaturated soils. A comprehensive summary of these theoretical formulations can be found in Alonso et al. (1987). Mathematical models used to describe this coupled behaviour can be classified into two branches:

(i) Moisture-based model that considers the moisture content (θ) as the dependent variable (Philip and De Vries 1957).

(ii) Pressure-based model that considers the capillary potential (ψ) as the dependent variable (Milly 1982 and Thomas and King 1991). In comparison with Pressure-based model, Moisture based models show less nonlinearity and are much easier to solve.

Narasirnhan (1975) indicated that the movement of water through a specimen at low degrees of saturation corresponding to residual zone of SWCC appears to be more linear. In other words, in the residual zone, the suction value may vary significantly whereas the water content of the soil or its degree of saturation tends to change more gradually. This means that a moisture-based model is more appropriate for use at low degrees of saturation.

2.9.1 Philip and De Vries model (1957)

This model is one of the traditional models that is conventionally used for describing moisture and heat transfer in unsaturated soils in response to a fixed temperature gradient. As a first attempt, Fick's law modified for unsaturated soils was only used to describe the thermally induced movement of moisture through a soil sample. However, Philip and De Vries (1957) indicated that this assumption underestimated the observed moisture movement. Therefore, they suggested considering all the interaction between water, water vapor, and the porous structure at the same time instead of using only water vapor movement (Wang et al. 2009). In this way, they divided the water movement into two

(i) Movement of water in the water phase based on the modified Darcy's law.

(ii) Movement of water in the vapor phase based on Fick's law.

In the water phase, they attributed the water movement to the changes of surface tension as a function of temperature. Philip and De Vries (1957) expressed the total moisture and heat flux formulation in one dimension under combined temperature and volumetric gradient as:

$$\frac{\delta\theta}{\delta t} = -D_\theta \nabla\theta - D_T \nabla T \tag{2.12}$$

$$C\frac{\delta T}{\delta t} = \nabla.(\lambda \nabla T) - L\nabla.(D_{\theta vap}\nabla\theta) \tag{2.13}$$

where D_θ is isothermal moisture diffusivity, D_T is the moisture diffusivity under temperature gradient,$D_{\theta vap}$ is the thermal vapor diffusivity, C is the volumetric heat capacity, λ is thermal conductivity, and L is vapor the heat of vaporization and is equal to $2.4 \times 10^6 \frac{J}{kg}$. Cassel et al. (1969) studies on the movement of water in soils in response to imposed temperature gradient showed that model of Philip and De Vries (1957) can acceptably predict the observed water movement. Further studies by De Vries (1987) indicated that adoption of this model in geotechnical problems has the following limitations:

(i) Soil should be one type (homogeneous) and isotropic.

(ii) The hysteresis, difference between wetting and drying path for estimating the SWCC, is not considered.

(iii) Water movement in the liquid phase is due to viscosity and the changes of surface tension.

(iv) Convection, caused by the tendency of hot gas to rise above colder (and denser gas), is not considered.

(v) Radiation as a heat transfer mechanism is assumed to be negligible.

(vi) The thermodynamic equilibrium is achieved only between liquid and its vapor phase.

(vii) Total pressure is constant and uniform in the whole soil (Philip and De Vries 1987).

Evgin and Svec (1988) used Philip and De Vries (1957) model to investigate the behavior of Ottawa Makenzi sand under non isothermal conditions. In this experiment, D_T is estimated by measuring the water content profile of a soil sample subjected to a constant temperature gradient and the D_θ coefficient was determined using the evaporation process that Gardner and Miklich (1962) introduced for finding thermal diffusivity under a constant heat flux.

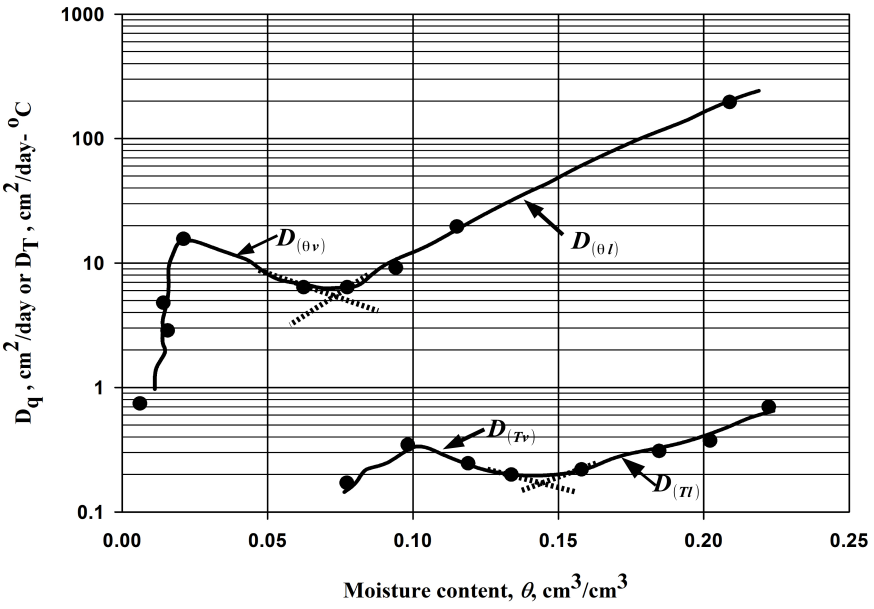

Figure 2.18: Transport coefficients as a function of volumetric moisture (Evgin and Svec 1988)

The results indicated that the curves representing the relation of D_T or D_θ versus θ had an inflection point at ($\theta = \theta_{crit}$) (Figure 2.18). This means that above ($\theta = \theta_{crit}$)the contribution of vapor diffusivity can be assumed to be negligible and below($\theta = \theta_{crit}$) the contribution of liquid flow can be ignored.

2.9.2 Milly model (1982)

Milly (1982) investigated thermally induced movement of water and heat through a vertical unsaturated Yolo light clay sample which had an initial temperature of 20 °C. To numerically simulate this experiment, Milly (1982) suggested the following formulations in which the dependent variables are the capillary potential(ψ) and temperature (T) for movement of water.

$$\rho_l s_m = \rho_l \theta + \rho_v \theta_v \tag{2.14}$$

$$\frac{\delta}{\delta t}(\theta + \frac{\rho_v}{\rho_l}\theta_a) = \nabla.((k + D_{\psi v})\nabla\psi + D_{tv}^{\psi}\nabla T) \tag{2.15}$$

where s_m is defined as total water storage per unit volume of porous media, θ_a is the volumetric air content, ρ_v is the water vapor, $D_{\psi v}$ is the suction diffusivity of vapor, D_{tv}^{ψ} is the temperature diffusivity of vapor and k is the hydraulic conductivity of unsaturated soil. Milly's derivation is commonly based on the theory of Philip and deVries. However, this approach has more advantages including consideration of hysteresis, soil inhomogeneity, and the stress strain deformation (Derek 1997).

2.9.3 Fredlund model (1980)

In this theory, the continuity equation and the constitutive relations for the soil structure, water and vapor phases were developed using Fredlund and Morgenstern (1977) theory for describing unsaturated soil behavior. Therefore, the matric suction $u_a - u_w$ and normal stress $\sigma - u_a$ are used as the stress state variable where the net normal stress can be expressed as the weight of layers of soil that is placed above the point of measurement. Dakshanamurthy and Fredlund (1981) modified the consolidation theory of Fredlund and Hasan (1979) for unsaturated soils to predict the moisture flow under the effect of the temperature with the following assumptions:

(i) The air phase is not discontinuous which means that the degree of saturation should be lower or equal to 85%. In unsaturated soils, a high degree of saturation, means there is not any air through the pores and the compressibility of fluid phase must be considered.

(ii) The coefficient of hydraulic conductivity during the derivation of equations is assumed to be constant and any formulations that to estimate this coefficient throughout the transient process can be used after calculation (Dakshanamurthy and Fredlund 1981). This assumption is not truly completely accepted because the permeability of water and air in an unsaturated soil is a function of water content or degree of saturation. However, the model addresses this by estimating its value before each step.

(iii) The volume change modulus is assumed to be constant value during movement of water.

In this model, the combination of thermal gradient and hydraulic gradient were used to simulate migration of water under effect of temperature. Moreover, the limitation of incompressible soil in Philip and De Vries does not exist. Three partial differential equations, one for the water phase, one for the air phase and the other for the heat flow are given as:

$$\frac{\delta u_w}{\delta t} = C_w \frac{\delta u_a}{\delta t} + C_v^w \frac{\delta^2 u_w}{(\delta x)^2} \tag{2.16}$$

$$\frac{\delta u_a}{\delta t} = C_a \frac{\delta u_w}{\delta t} + C_v^a \frac{\delta^2 u_w}{(\delta x)^2} + C_T \frac{\delta T}{\delta t} \tag{2.17}$$

$$\frac{\delta T}{\delta t} = \alpha \frac{\delta^2 T}{\delta x^2} \tag{2.18}$$

where, C_w is the interactive pressure constant associated with the water phase equation, C_v^w is the coefficient of consolidation for water phase, C_a is the interactive pressure constant associated with the air phase equation, C_T is the interactive thermal constant associated with the air phase equation, C_v^a is the coefficient of consolidation for air phase and α is the thermal diffusivity factor. The proposed model can be extended to two-dimensional geometric conditions.

To solve these differential equations, a finite difference method can be used. During the solution, the coefficient of hydraulic conductivity can be adjusted in each time step if the hydraulic conductivity function is known. Dakshanamurthy and Fredlund (1981) studied the flow of water though unsaturated Regina clay as a subgrade of pavements which was subjected to daily or monthly temperature fluctuation. The results indicated that the proposed model can precisely determine an excess pore-air pressure or pore-water pressure which can be adapted to estimate the swelling or shrinkage potential and this information is highly important in pavement design.

2.9.4 Thomas and King model (1991)

This model is commonly used in literature to simulate the thermo-hydro behavior of unsaturated soil because it has been validated in different type of soils either coarse-grained soil or fine-grained soil (Derek 1997). The Thomas and King (1991) model can be classified as a subset of Milly's model which considers the advection on the heat of wetting and the latent heat which occurs due to temperature effect on the vapor diffusion. Relationships are developed based on the law of conservation of mass using the derivative of the capillary potential and temperature gradient. The mathematical form of the governing equations are:

$$C_{\psi\psi}\frac{\delta\psi}{\delta t} + C_{\psi T}\frac{\delta T}{\delta t} = \frac{\delta}{\delta x}(K_{\psi\psi}\frac{\delta\psi}{\delta x}) + \frac{\delta}{\delta x}(K_{\psi T}\frac{\delta T}{\delta x}) \tag{2.19}$$

$$C_{T\psi}\frac{\delta\psi}{\delta t} + C_{TT}\frac{\delta T}{\delta t} = \frac{\delta}{\delta x}(K_{T\psi}\frac{\delta\psi}{\delta x}) + \frac{\delta}{\delta x}(K_{TT}\frac{\delta T}{\delta x}) \tag{2.20}$$

where $K_{\psi T}$ is material parameter for vapor transfers driven by temperature gradient, $k_{T\psi}$ is a material parameter for heat transfer due to capillary potential gradient, K_{TT} is a material parameter for heat transfer due to temperature gradient, $K_{\psi\psi}$ is the isothermal moisture conductivity, C_{TT} is the heat equation coefficient of rate of change of temperature,$C_{T\psi}$ is the heat equation coefficient of rate of change of capillary potential,$C_{\psi\psi}$ is the moisture equation coefficient of rate of change of capillary potential, and $C_{\psi T}$ is the moisture equation coefficient of rate of change of temperature.

The fully coupled set of these formulations are solved simultaneously using the finite element method via Galerking weighted residual approach or a finite difference time-stepping scheme. Thomas and King (1991) validated their model using the experimental

results of Ewen and Thomas (1989) on a horizontal column of sandy soil which is subjected to a fixed temperature gradient. The analysis also indicated that the proposed approach can be extended to include analysis of stress/strain relationship and therefore a complete study of thermo-hydro mechanical (THM) behaviour. Thomas et al. (1996) studies showed that the proposed formulations can be applied for flowing of water through soils near the nuclear waste disposal and unlike the Philip and De Vries (1957) model it is adequate for estimating the behavior of soil near the boundary condition.

2.10 Summary

Over the last 50 years, much effort was spent to better understand the engineering behaviour of unsaturated soils. These studies resulted in significant advances in developing a theoretical framework, experimental methods and numerical solutions. This chapter provides a review of the part of these studies that contribute to the aims of the proposed research. The concept of the effective stress, the definition of the SWCC, and its role in the prediction of other unsaturated soil properties are discussed.

The main purpose of this research is to develop a framework for interpretation and estimation of SWCC at different temperature. The theoretical background provided in this chapter is used as a tool for proposing the semi-empirical method for predicting the SWCC using soil water movement under the controlled temperature gradient. Details of the procedures for developing the suggested approach are summarized in following chapters.

Chapter 3

INTERPRETING TEMPERATURE EFFECT ON SWCC

3.1 Soil model for temperature dependence of SWCCs

3.1.1 Mathematical representation of soil water characteristic curves

During the past five decades, numerous empirical, analytical and statistical models in the literature have been proposed for the mathematical representation of the SWCC behavior (Brooks and Corey 1964; van Genuchten 1980; Fredlund and Xing 1994; Leong and Rahardjo1997). A comprehensive summary and comparison of these models can be found in Sillers et al. 2001. Among these extensive models, the Brooks and Corey (1964), van Genuchten (1980), and Fredlund and Xing (1994) equations are found to be more practical for geotechnical engineering applications purposes such as the construction and analysis of road and railway embankments, slope stabilisation, or in agriculture to find the optimum irrigation, waste containment, and solute transport in the vadoze zone (Leong and Rahardjo 1997; Stormont and Anderson 1999; Gerscovich and Sayao 2002; Malaya and Sreedeep 2011).

Table 3.1 shows the mathematical formulation of these models. A nonlinear least square fitting method can be used to obtain the fixed parameters of these equations. However, recent published literature has shown that the SWCC estimation using the

Fredlund and Xing (1994) equation has more flexibility in case of mathematical attributions (Sillers et al. 2001; Chin et al. 2010). The fixed parameters in this equation can be distinguished from the effect of the other two parameters which leads to a greater flexibility (Sillers et al. 2001). In addition, this mathematical equation can be applied over the entire range of suction from 0 to 1000000 kPa which has been supported experimentally by the results of tests on a variety of soils (Croney and Coleman 1961). Therefore, in this study, the fixed parameters of the Fredlund and Xing (1994) equation will be correlated to the temperature.

Table 3.1: Common soil-water characteristic curves equations

References	Equations
Brooks and Corey (1964)	$\theta_w = \theta_r + (\theta_s - \theta_r)(\frac{a_{bc}}{\psi})^{b_{bc}}$
van Ganuchten (1980)	$\theta_w = \theta_r + \frac{\theta_s - \theta_r}{(1+a_{vg}\psi^{b_{vg}})^{c_{vg}}}$
Fredlund and Xing (1994)	$\theta_w = \theta_r + \frac{\theta_s - \theta_r}{(ln(e+(\frac{\psi}{a_f})^{n_f}))^{m_f}}$

Note: θ is the volumetric water content, θ_s is the saturated volumetric water content, θ_r is the residual volumetric water content, a,n,m α,b, are fitting parameters and ψ is the soil suction in kPa

3.1.2 Temperature effect on the fixed parameters of the Fredlund and Xing (1994) model

To find the effect of temperature on the soil water characteristic curves capillary tube theory is used. In this theory, the pores of soil are conceptualized as a series of cylinders (Figure 3.1). This hypothesis is the basis for deriving the mathematical equations of the SWCC. The maximum height of water rise into a capillary tube can be expressed as:

$$u_a - u_w = 2\frac{\sigma^{sg} - \sigma^{ls}}{r \times \rho_l \times g} \tag{3.1}$$

where h_c is the maximum height water that rises into a capillary tube, r is the radius of

an equivalent capillary tube, σ^{sg} is the surface tension between the gas and solid, σ^{ls} is the surface tension between the liquid and the solid particles, and ρ_l is the liquid density of water.

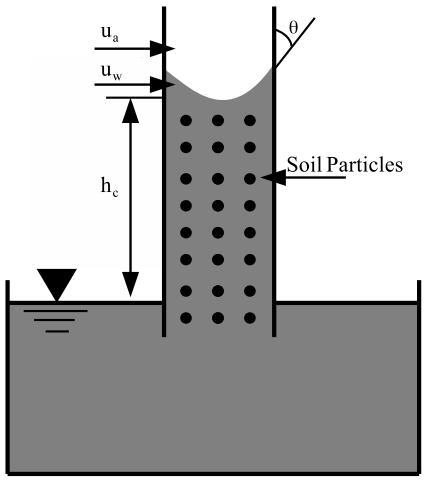

Figure 3.1: Capillary tube concept for matric suction estimation

It should be noted that in many cases the small volume of water in contact with the solid, is not formed as drops and have a contact angle which can rewritten as (Bachmann and Van der Ploeg 2002):

$$\sigma^{sg} - \sigma^{ls} = \sigma \cos(\theta) \tag{3.2}$$

where σ is the surface tension between liquid and gas, and θ is a contact angle. Generally, the relationship between the liquid-air surface tension and temperature can be written as (Bachmann and Van der Ploeg, 2002):

$$\sigma = 0.117 - 0.000153 \times T \tag{3.3}$$

where T is the temperature in Kelvin. The correlation between the liquid density and temperature is given as (Keshky, 2011):

$$\rho_l = 658.2 + 2.509 \times T - 4.606 \times 10^{-3} \times T^2 \tag{3.4}$$

Where ρ_l is the liquid density ($\frac{kg}{m^3}$). By applying the capillary model in unsaturated soils, the relation of capillary pressure to the temperature is obtained as:

$$h_c = \frac{2 \times \sigma \times \cos(\theta)}{r \times \rho_l \times g} \Rightarrow (h_c)_T = \frac{2 \times (0.117 - 0.000153 \times T) \times \cos(\alpha)}{r \times (658.2 + 2.509 \times T - 4.606 \times 10^{-3} \times T^2) \times g} \quad (3.5)$$

where h_c is the maximum height water will rise to in a capillary tube, and r is the radius of an equivalent capillary tube. The contact angle is assumed to be constant. This condition simplifies the estimation of the effect of temperature on the soil water characteristic curves.

Assuming the constant given values for θ_s and θ_r, in the differential form of the van Genuchten equation (1980) and solving this equation as function of α, it can show that this fixed parameter is related to maximum height of the water in capillary tube by:

$$\alpha = \frac{1}{h_c}((\frac{\theta - \theta_r}{\theta_s - \theta_r})^{\frac{-1}{m}} - 1)^{1/n} \rightarrow \alpha \approx \frac{1}{h_c} \quad (3.6)$$

By substituting Eq.3.5 into Eq.3.6, α can be expressed as a function of temperature as follows:

$$\alpha_T \approx \frac{1}{(h_c)_T} \approx \frac{r \times (658.2 + 2.509 \times T - 4.606 \times 10^{-3} \times T^2) \times g}{2 \times (0.117 - 0.000153 \times T) \times \cos(\theta)} \quad (3.7)$$

By knowing the parameter α at $T = 20\,^{\circ}\mathrm{C}$, the changes of α at other temperatures can be found by:

$$\frac{\alpha_T}{\alpha_{T=20\,^{\circ}\mathrm{C}}} = \frac{(658.2 + 2.509 \times T - 4.606 \times 10^{-3} \times T^2)}{(0.117 - 0.000153 \times T)} \times$$

$$\frac{(0.117 - 0.000153 \times (20 + 273.15))}{(658.2 + 2.509 \times (20 + 273.15) - 4.606 \times 10^{-3} \times (20 + 273.15)^2)} \Rightarrow$$

$$\alpha_T = \alpha_{T=20\,^{\circ}\mathrm{C}} \times 7.22 \times 10^{-5} \times \frac{(658.2 + 2.509 \times T - 4.606 \times 10^{-3} \times T^2)}{(0.117 - 0.000153 \times T)} \quad (3.8)$$

In the present study, the contact angle in this equation is assumed to be constant.

This condition simplifies the estimation of the effect of temperature on the SWCC due to difficulties in measuring the contact wetting angle (Wu et al. 2004 and Salager et al. 2006). Moreover, the parameters n and m, in Eq. 3.6 are related to the slope of the transition zone and hence the void size distribution. As a result, they can be considered to not significantly influenced by the change of temperature. This assumption is consistent with the published experimental data of Wu et al. (2004), Salager et al. (2006) in which the measured SWCC at two different temperatures have similar slopes and are parallel to each other.

To illustrate the influence of temperature on the SWCC based on this model, four different soils from literature have been modelled using the van Genuchten (1980). The values of the van Genuchten parameters for these soils at room temperature (20 °C) are listed in Table 3.2. Figure 3.2 to Figure 3.5 shows the SWCC generated at various temperatures for the soils of Table 3.2 by modifying α for temperatures between 1 to $100°C$. From the figures, it can be seen that there is an offset of the SWCC towards a lower matric suction, which impliest that at a constant matric suction, the water content of the soil decreases. Also apparent from the figures is the fact that the temperature effect has a larger impact on the SWCC of granular materials than on that of finer soils.

Table 3.2: Parameter of α, n, m for each type of soil that calculated at $T = 20\,°\mathrm{C}$ (van Genuchten, 1980)

Soil name	$\theta_s(cm^3)$	$\theta_r(cm^3)$	α	n	m
Hygiene sandstone	0.25	0.153	0.0079	10.4	0.90
Silt Loam G.E.3	0.396	0.131	0.00423	2.06	0.51
Guelph Loam	0.52	0.218	0.0115	2.76	0.64
Beit Netofa Clay	0.446	0	0.00152	1.17	0.14

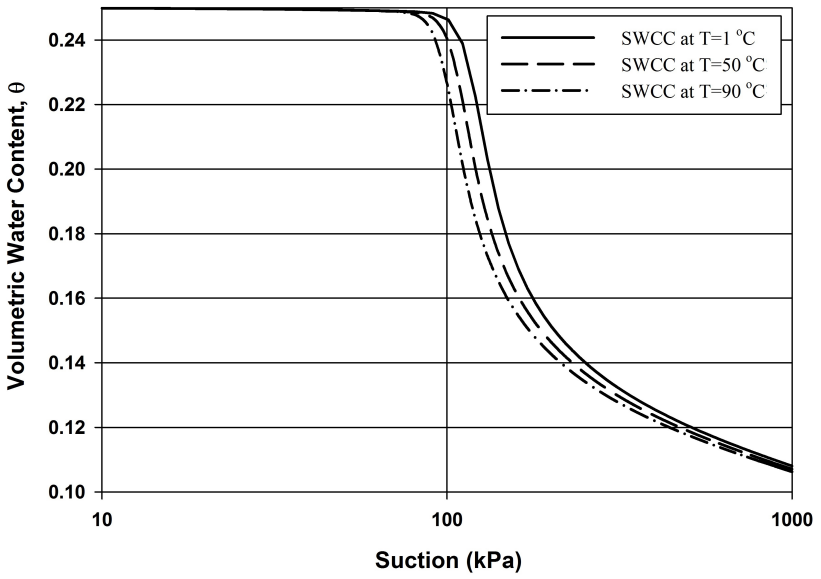

Figure 3.2: SWCC curves for Hygiene sandstone T= 1, 50, and 90 °C.

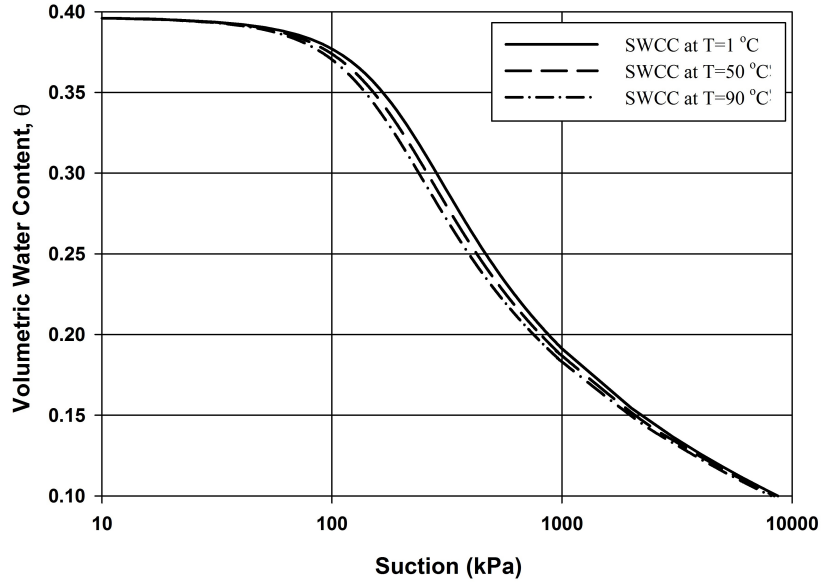

Figure 3.3: SWCC curves for Silt Loam G.E.3 T= 1, 50, and 90 °C.

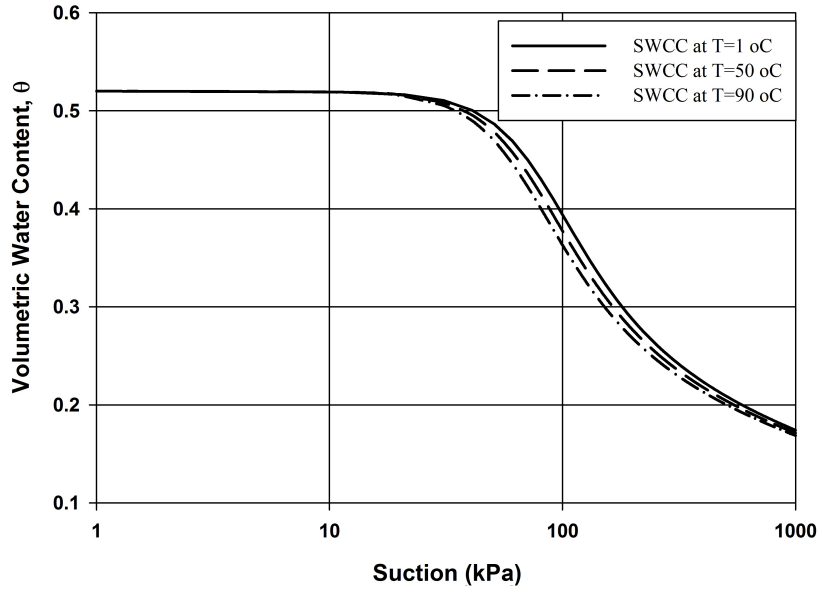

Figure 3.4: SWCC curves for Guelph Loam T= $1, 50$, and $90\,^{\circ}$C.

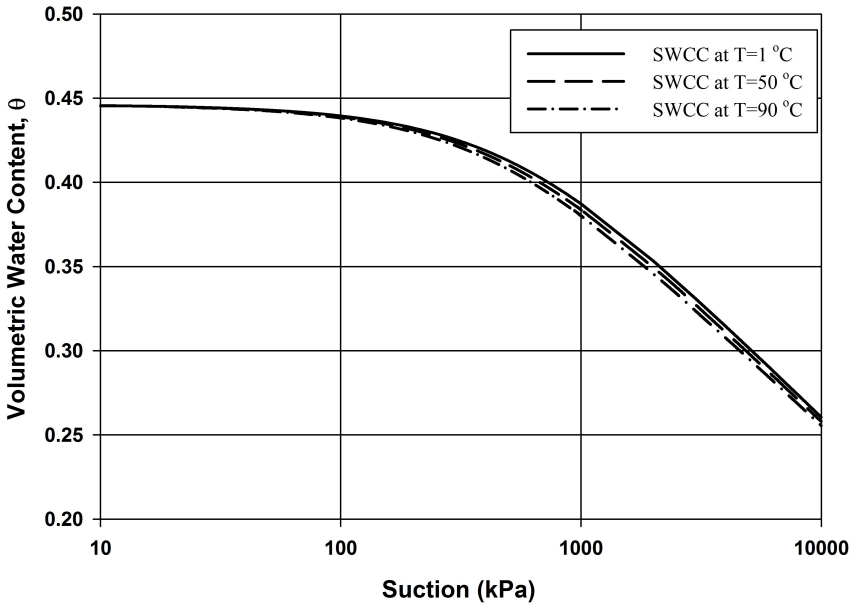

Figure 3.5: SWCC curves for Beit Netofa Clay T= $1, 50$, and $90\,^{\circ}$C.

In the Fredlund and Xing (1994) model, the parameters, a, n, and m are not directly tied to physically measurable quantities. However, the n and m parameters are generally associated with the shape of the slope of the SWCC while the a parameter is associated with the air entry value. While a is generally larger than the air entry value (it corresponds not to the air entry value but with the point of inflection), Fredlund and Xing (1994), have observed that it is close to the air entry value for small values of m. Therefore it is expected that a similar approach as used to calculate α as a function of temperature should also be applicable.

Since a is directly related to suction, then it is expected that a is proportional to $\frac{\sigma_T}{\rho_T}$. Therefore, variation of a with temperature will be expressed as the inverse of Eq. 3.8.

$$a_T = a_{(T=293.50)} \times 13840.45 \times \frac{(0.117 - 0.00153 \times T)}{(658.2 - 2.509 \times T - 4.606 \times 10^{-3} \times T^2)} \tag{3.9}$$

3.2 Materials and test methods

3.2.1 Material selection and characterization

The soils used in this study consist of a Industrial sand which was super fine sand and Unimin silica sand 7030 which was the commercial sand. The sand is named No. 7030, meaning 30% retained on 70 mesh ($0.212mm$) and the measured geometric mean of the sand particles was equal to $0.20mm$. The Unimin silica sand 7030 was obtained from Merkley Supply Ltd, Ottawa, Canada and Industrial sand was obtained from Target Products Ltd, Burnabby, Canada. The grain size distributions are given in Figure 3.6. The soil properties of both sands are presented in Table 3.3 with their basic geotechnical properties. Both these soils were obtained from Merkley Supply Ltd. in Ottawa. The geotechnical index properties of theses soils were determined in accordance with ASTM standards. The soils considered consist of particles with sizes ranging from 0.049 to $0.61mm$.

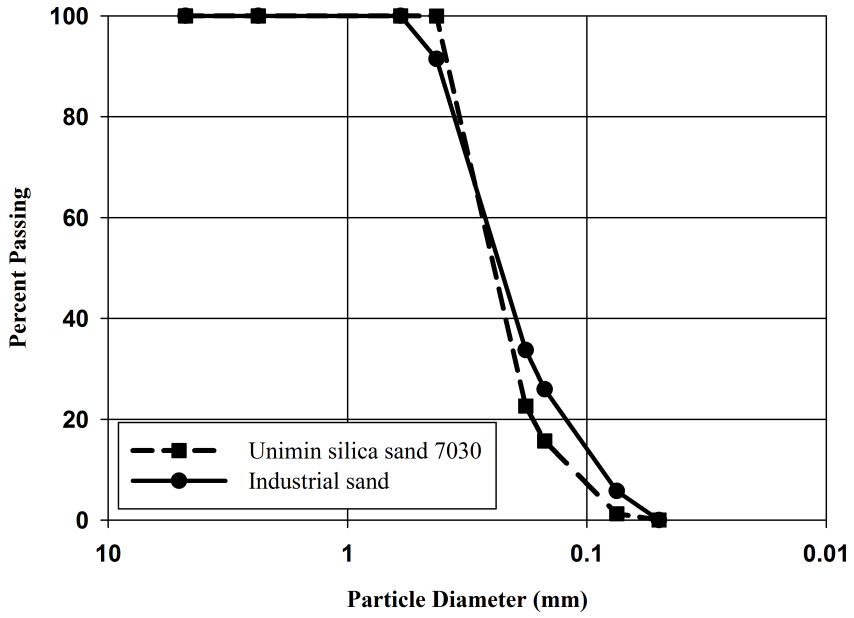

Figure 3.6: Grain size distribution of the studied soils

Table 3.3: Tested soils properties

Soil Property	Unimin Silica Sand 7030	Industrial Sand
Specific gravity, G_s	2.65	2.69
Optimum water content, $w_opt(\%)$	14.6	15.2
Maximum dry unit weight, $\gamma_{dry-max}, (kN/m^3)$	16.8	17.7
Void Ratio, e	0.63	0.56
$D_{60}, (mm)$	0.22	0.29
$D_{30}, (mm)$	0.18	0.17
$D_{10}, (mm)$	0.12	0.10
Coefficient of uniformity, C_u	1.83	2.9
Coefficient of curvature, C_c	1.23	0.99

3.2.2 Experimental methods

To explore the temperature effect on the SWCC, experiments were carried out using a Tempe cell device which was immersed into a controlled temperature water bath to control the ambient temperature during the test. Three different temperatures were considered, namely: $4\,^{\circ}\text{C}, 20\,^{\circ}\text{C}, 49\,^{\circ}\text{C}(\pm 1\,^{\circ}\text{C})$.The temperature control at $20\,^{\circ}\text{C}$ and $49\,^{\circ}\text{C}$ is achieved by using a commercial hydrometer bath used for the standard hydrometer used to determine the grain-size distribution of fine particles. The $4\,^{\circ}\text{C}$ temperature was controlled by using a mixture of water and ice cubes.

As shown in Figure 3.7, the Tempe cell consists of a removable high air entry disk enclosed within a pressurized cell. The air entry disk is used as an interface to separate

the specimen exposed to gaseous atmosphere and outflow water thus allowing control of the matric suction by maintaining the air pressure and water pressure (and therefore the matric suction) at two different values. The Tempe cell allows the measurement of the SWCC by application of the axis-translation technique, in which a positive air pressure is applied instead of a negative pore water pressure (Richards 1931; Hilf 1956). Using this technique, it is possible to achieve any desired matric suction without risk of cavitation. As indicated by Bocking and Fredlund (1980), Marinho et al. (2008), and Airò Farulla and Ferrari (2005), the axis-translation technique also presents challenges associated with the formation of bubbles coming out of solution below the ceramic disk, The higher air pressures applied within the cell cause an increase in the amount of air dissolved in the water within the specimen. When water diffuses through the ceramic disk, this air comes out of solution and accumulates below the ceramic disks. Accumulation of these air bubbles below the ceramic disk, affects the measurement of the water exchanges in and out of the specimen (Infante Sedano 2006). This problem is highlighted when the air–water interface is continuous, which is typically observed in specimens with a degree of saturation below 90% (Vanapalli et al. 2008). Therefore, it is essential to flush water below the ceramic disk to collect the bubbles so that they may be eliminated and the water volume change correctly measured.

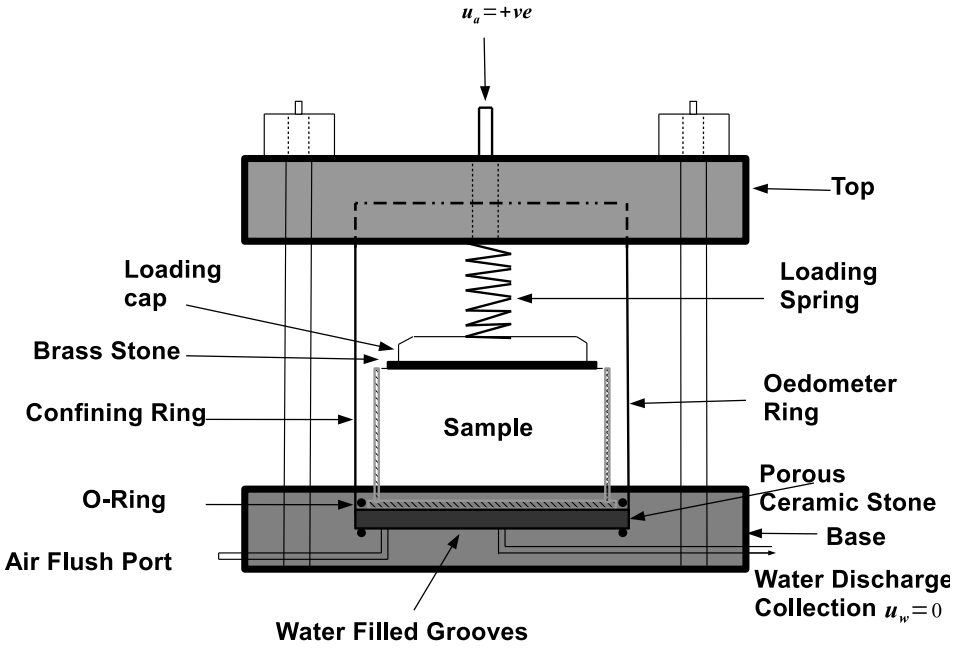

Figure 3.7: Schematic of a Tempe cell used in the study

In this experiment, a ceramic disk with an air entry value (AEV) of $300kPa$ is used. The maximum matric suction applied during the tests is $30kPa$, well below the AEV of the disk. A volume gauge, consisting of a tube open to atmosphere is located 500 mm below the mid-point of the specimen. This elevation difference is taken into account when calculating the applied matric suction. The volume gauge allows a volume measurement of $\pm 0.006ml$. The maximum volume change that can be monitored with this tube is of $6ml$, and therefore a system of water storage in the form of a pair of syringes ($1ml$, and $60ml$ respectively) connected to the system through a set of ball valves has also been provided (Figure 3.8).

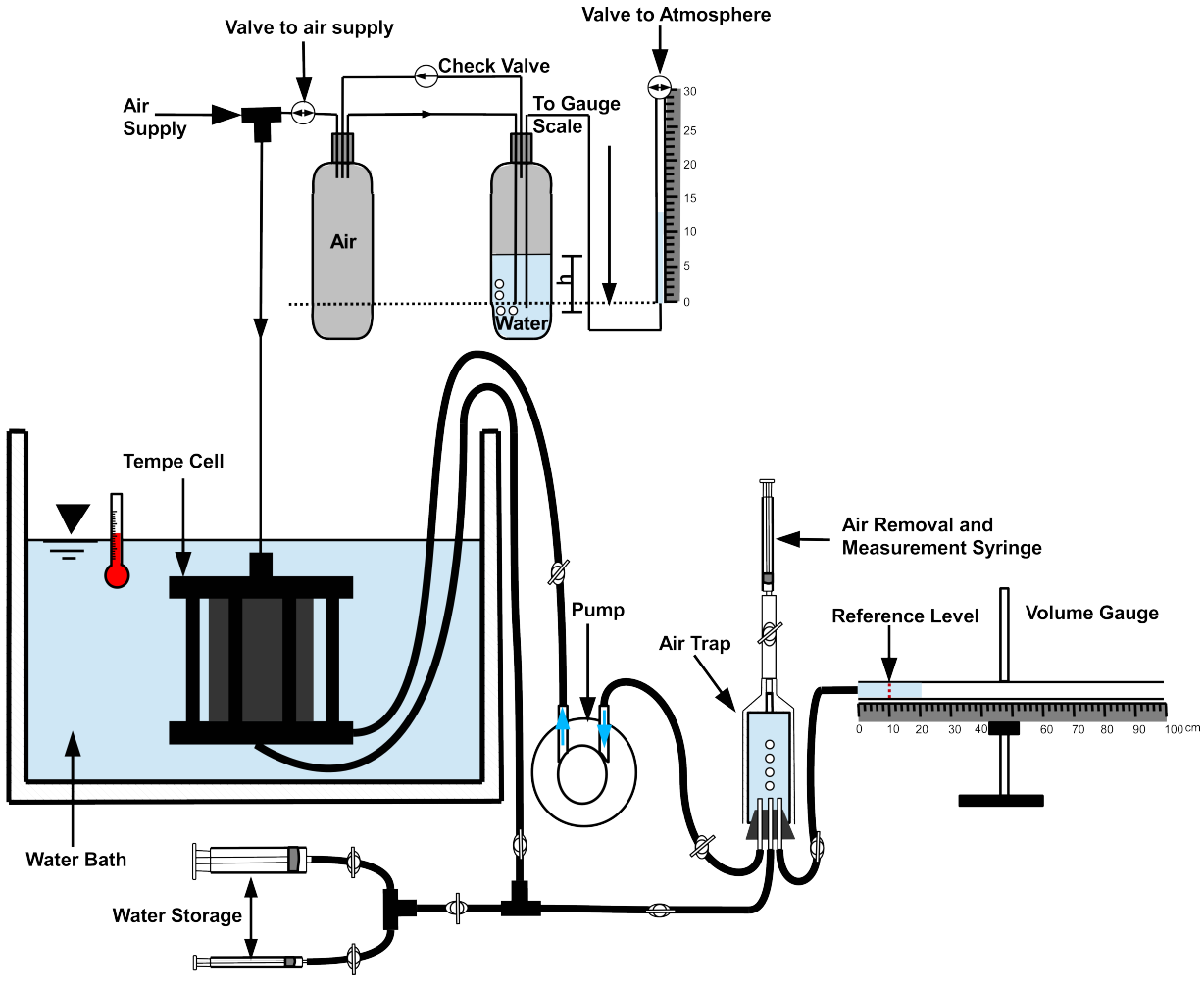

Figure 3.8: Schematic details of an experiment setup

Before starting the test, the high air entry disk is removed from the Tempe cell and soaked for 24 hours in an attempt to saturate the disk. With the porous disk in place, the connections are made to the water lines which allow water movement and flushing to be undertaken. This disposition allows not only the water content change of the specimen to be monitored but also to dispose of the air bubbles that accumulate below the disk through diffusion (Romero 2001; Vanapalli et al. 2008).

An inline pump allows water to be circulated through the system in which an air-trap is included to allow the capture and removal of the air bubbles that will eventually collect below the ceramic disk. Before any water volume change is taken, the de-airing pump is activated allowing the air to collect within the air trap. The volume gauge is then read, before and after the air accumulated in the air trap is extracted through a syringe installed at the summit. Since the syringe is used to bring the water level in the air trap to a fixed level, and since the volume gauge is read before and after this procedure, the actual volume of water expelled from the specimen is thus effectively measured as well as the volume of air that was removed. Additional details about the procedures and the design of diffused air-volume system can be found in Infante Sedano et al.(2007b).

3.2.3 Sample preparation

To prepare the soil sample the dry soil was compacted in three layers with a thickness of $10mm$ inside the confining ring with a $64mm$ diameter and a height of $30mm$ which is placed inside the Tempe cell device on the saturated high air entry disk. To achieve uniform compaction, a $460gr$ tamping rod is dropped from $50mm$ height from the center of each layer inside the Tempe cell chamber and each layer received 20 blows. The height of the achieved specimen is $27mm$. After preparation the soil specimen the loading spring and loading cap are placed on the top of the sample. The acrylic Tempe cell is then sealed using 5 bolts connecting the upper and bottom caps which ensure a positive seal with the O-rings separating them from the cell walls.

As indicated above, temperature control is achieved by immersing the Tempe cell within a temperature controlled bath. For the 20 °C and 49 °C temperatures a commercial thermostatic bath with microprocessor-based temperature control with an integrated heater and chiller is used. The control processor in the thermo bath provides a consistent bath temperature accurate to within 0.1% of input span ±1 °F. The water bath is fully-insulated and includes a circulating pump, which ensures a constant water temperature throughout bath. This system can effectively control the temperature in a range going

from 10 °C to 49 °C.

Since the lower target temperature (4 °C) is below the temperature range that can be achieved with the controlled bath, it was necessary to use another temperature control system. A cooler filled with water and ice provided an environment which could be maintained at the target temperature, through phase change latent energy exchanges, within ±1 °C with minimal external intervention. This was verified by continuous monitoring of the temperature within the bath. Figure 3.9 shows the Tempe cell immersed in the water and ice mixture.

Figure 3.9: Tempe cell submerged in an ice-water

Once immersed in the controlled temperature bath, the unsaturated soil sample is saturated by applying back pressure to the water phase. This is achieved by opening the $60ml$ syringe to atmosphere and raising the water level to $500mm$ above the mid-point of the soil specimen. Saturating the soil from bottom of the sample is ensures that a hydraulic connection is maintained between the soil-water and the free water outside the Tempe cell and ensures that the air from the specimen is gathered towards the surface of the soil (Fredlund and Rahardjo 1993). Typically, specimens are saturated within a period of 24 hours using the above technique.

Once apparent saturation of the specimen is observed based on observing a thin layer

of water on the soil surface and and saturation is verified by phase relation calculations, the overflow $60ml$ syringe is isolated from the system, using the set of valves available, and the volume gauge is connected to the outflow of the specimen (Figure 3.8). The air pressure corresponding to the desired matric suction is then applied and the volume of water expelled from the specimen is then measured. Since the pore water pressure within the volume gauge is equal to the atmospheric pressure, the applied air pressure, $+500mm \times \gamma_w$, corresponds to the matric suction causing the water drainage.

Conventional pressure regulators commonly available in the laboratories do not have the required sensitivity to measure the relatively low pressures that are of interest in the study of unsaturated coarse grained soils (Infante Sedano et al. 2007a). Hence, to measure the applied air pressure within the range of interest for this study, a simple, economical, and accurate pressure measuring device was built based on the method presented by Infante Sedano et al.(2007a). This device is built using two plastic bottles, the second of which is partially filled with water which overflows into a pressure gauge consisting of an air-filled tube sealed at the end (Figure 3.8). As the pressure increases in the bottles the water level rises in the gauge compressing the air within. The ideal gas law is used to calculate the resulting pressure based on the compression of the air phase. This technique which is based on Boyle's law is able to measure the applied suction in the range of 0.1 to $30kPa$. with a precision of $0.1kPa$.

Once the desired matric suction is applied, the volume of water expelled is continuously monitored within the volume gauge using digital imaging, at $720pHD$, until equilibrium is achieved. For these soils specimen used in this study, a time period of two or three days is required to achieve equilibrium conditions. Typically, the equilibration time is dependent on the type of soil, thickness of soil specimen, applied suction and the coefficient of permeability of the soil specimen and the high-air entry disk (Isimenmen 2002).

Figure 3.10 illustrates a typical set of readings of water volume expulsion as a function of time obtained for a suction increment from 5 to $6kPa$ for Unimin silica sand 7030 at 4 °C and 49 °C. The small breaks in these curves correspond to the flushing of air bubbles. The small recorded drop in volume is equal to the actual removed volume of air. Given the small magnitude of the observed drop it can be effectively assumed to be negligible for this particular suction increment. It can be observed that at lower temperatures the time to reach equilibrium increases. This can be explained by the effect of temperature on the viscosity of water, which, in turn, affects the value of the hydraulic conductivity.

At the end of the test, soil specimens are removed and the final water content values

are determined by oven-drying the soil specimen. The water content related to the other data points of the SWCC are determined from back calculations based on the volume mass properties of the soil. Typically, 6 to 8 data points are required to provide the key features of the SWCC (i.e., the air-entry value and the different zones of unsaturation). In this experiment, for each temperature, 10 to 11 data points were collected.

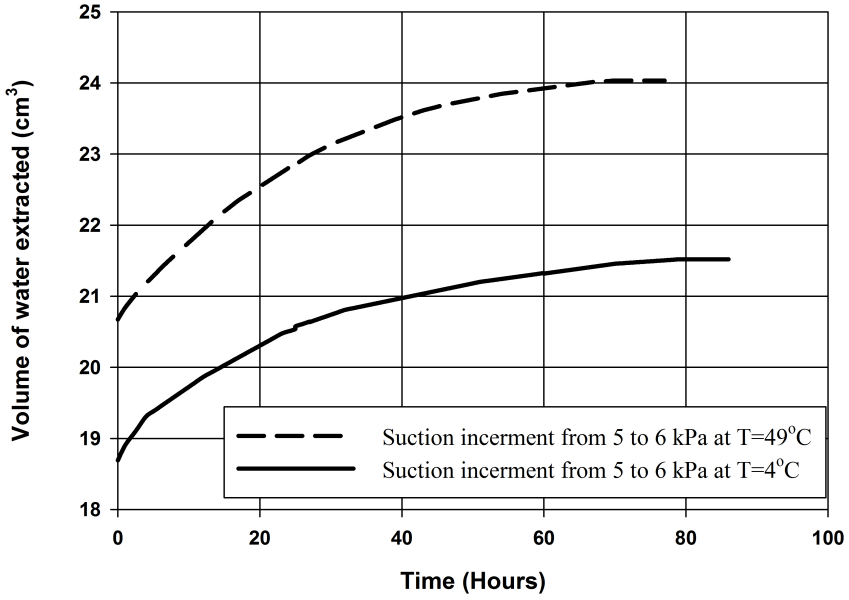

Figure 3.10: Measurement of water extracted in Unimin Silica Sand 7030

3.3 Result and Discussion

The SWCC determined experimentally at the reference temperature (20 °C) are shown in Figure 3.11 and Figure 3.12 for the two types of sand tested. The experimental data points are illustrated together with the best fit curve using the Fredlund and Xing model (1994). Also shown in the figures is the predicted SWCC based on the method proposed by Vanapali and Catana (2005) using the grain size distribution of the soil and a one point matric suction measurement. The data point used in the Unimin silica sand 7030 had a matric suction ,$(u_a - u_w)$ of $6kPa$ at a degree of saturation of S=30%. For the Industrial sand sand the matric suction used was $(u_a - u_w)$=$6kPa$ at a degree of saturation S=45%.

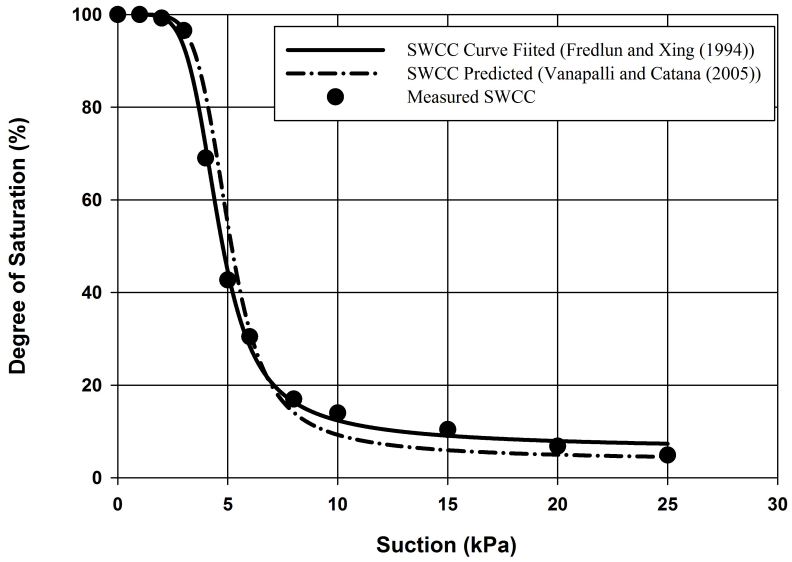

Figure 3.11: Measured and Predicted SWCC by Vanapali and Catana (2005) method for Unimin Silica Sand 7030

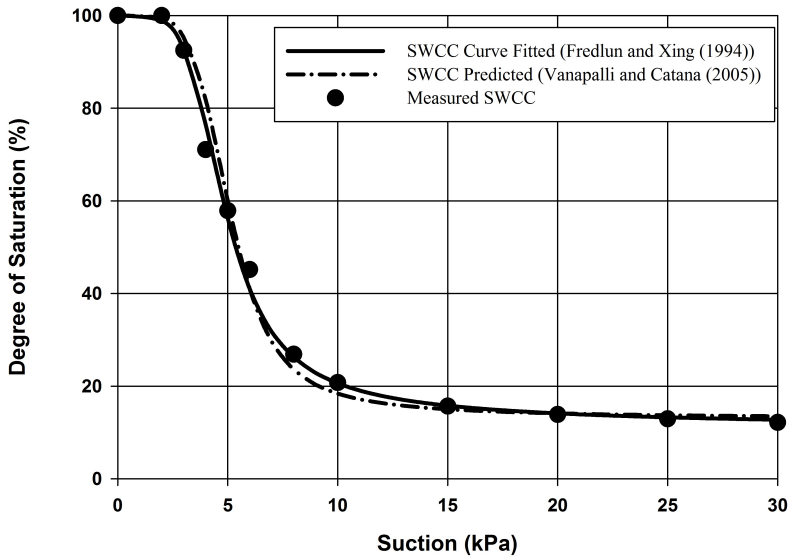

Figure 3.12: Measured and Predicted SWCC by Vanapali and Catana (2005) method for Industrial Sand

The calculated air entry value for the Unimin Silica Sand 7030 and Industrial sand is approximately in the range of 4.2 to 4.7 and 4.3 to 4.9 kPa respectively. In both soils, there is a steep transition zone in the suction range 4.5 to 10 kPa. Such behaviour is consistent with the nature of coarse-grained soils (Fredlund et al. 2012).

In order to estimate the SWCC at two other temperatures (4 °C, 49 °C), Eq. 3.9 is used to calculate the a parameter of the Fredlund and Xing equation at these temperatures. As Figure 3.13 to Figure 3.16 show, the calculated results based on the proposed model are very close to the experimental data points for both the hot (49 °C) and cold (4 °C) ambient temperatures.

Since only the air entry value has been modified, for both soils, it can be seen that the curves remain parallel to each other with only an offset along the suction axis. At any given suction, it can also be seen that the SWCC at a higher temperature corresponds to a lower degree of saturation. This is consistent with the observed experimental results and is attributed mostly to the changes in the surface tension (σ) and fluid density.

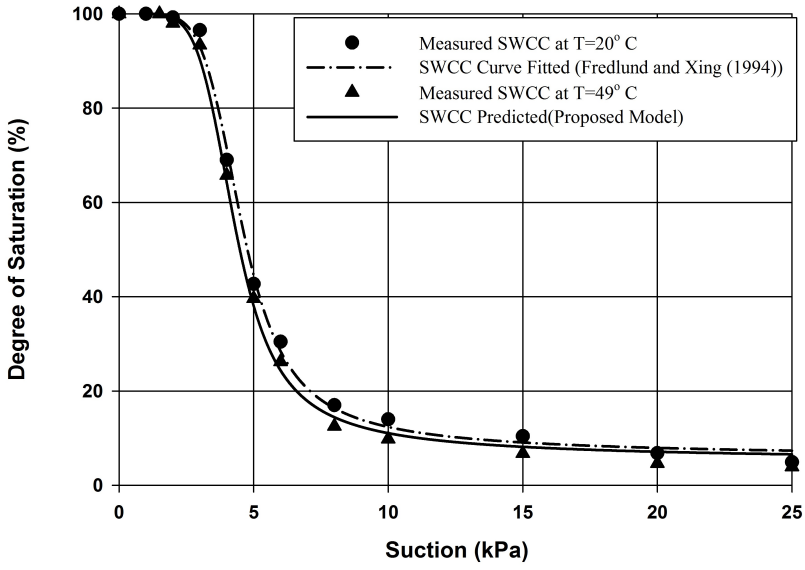

Figure 3.13: Water characteristic curves: experiments and modeling at T=49 °C for Unimin Silica Sand 7030

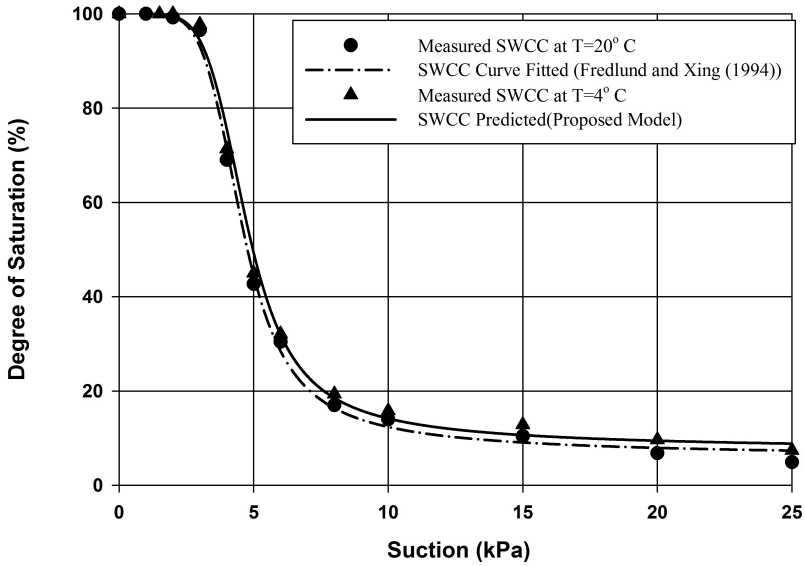

Figure 3.14: Water characteristic curves: experiments and modeling at T=4 °C for Unimin Silica Sand 7030

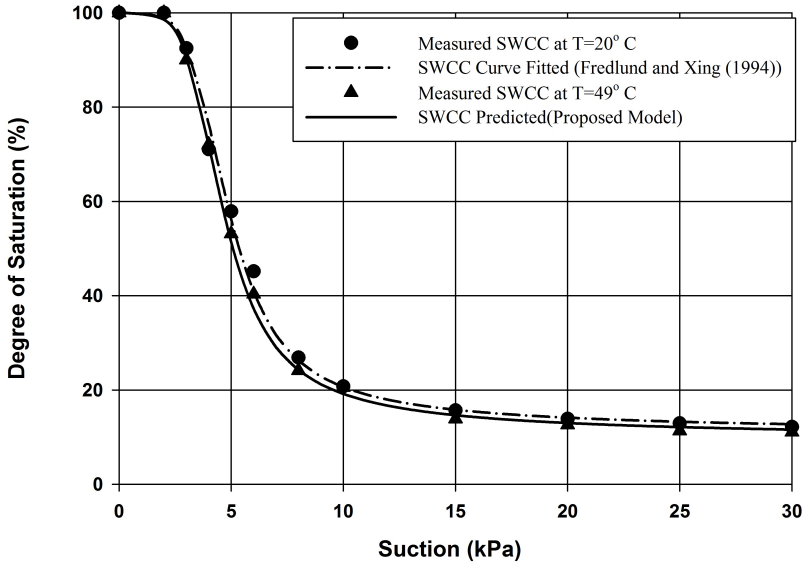

Figure 3.15: Water characteristic curves: experiments and modeling at T=49 °C for Industrial Sand

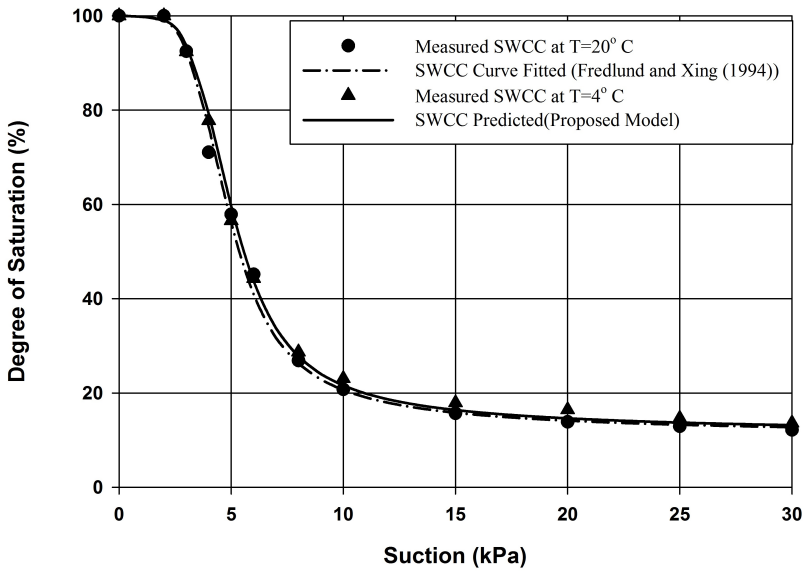

Figure 3.16: Water characteristic curves: experiments and modeling at T=4 °C for Industrial Sand

A comparison between the estimated SWCC and the measured results (Figure 3.13 to Figure 3.16) shows a good agreement between the predicted and measured SWCC at 4 °C, and 49 °C. The small error between the measured data and the proposed model can be explained considering error within the numerical approximation. Moreover, the difference in surface tension with respect to temperature can vary in the presence of organic material which contains surfactants such as fatty acid (Schnitzer and Desjardins 1969; Chen and Schnitzer 1978). The surface tension of the liquid phase decreases linearly with increasing concentration of the fatty acid (Nimmo and Miller 1986). It has been shown that solubility of fatty acid can increase by a factor of $2-3$ between 0 and 60 °C (Singleton 1960). However, in this experiment, both soils are composed of non-organic minerals. The measured organic content in the Unimin silica sand 7030 and Industrial sand is below 0.002%, 0.005% respectively. In addition, the experiments were conducted using distilled water and as a result should have minimal solute concentration, and this effect is not expected to affect the results.

Validation of the proposed method was conducted for fine grained soils, such as clay and silt. In this case, the proposed model has been applied to the SWCC test results presented by Salager et al. (2006) on two types of clay, namely ceramic and boom clay.

The imposed temperatures were 20 °C and 60 °C for ceramic clay and 22 °C and 80 °C for boom clay respectively. The ceramic clay has dry density equals to $1870\frac{kg}{m^3}$, and its void ratio is 0.464. The saturated water content is 16.9% at 20 °C. The boom clay is low-swelling clay with composition of $20-30\%$ kaolinite, illite $20-30\%$, and $10-20\%$ smectite. Its liquid limit is 56%, and the plasticity limit is 29% (Salager et al. 2006).

Figure 3.17 and Figure 3.18 show the measured and estimated SWCC for ceramic clay and boom clay and ceramic clay at 20 °C, 60 °C and 22 °C, 80 °C respectively.From these figures, it can be noted that the calculated retention curves are fairly close to the measured experimental curve at the same temperature. The results of this comparison support the validity of the proposed method for fine-grained soils as well as coarse-grained soils.

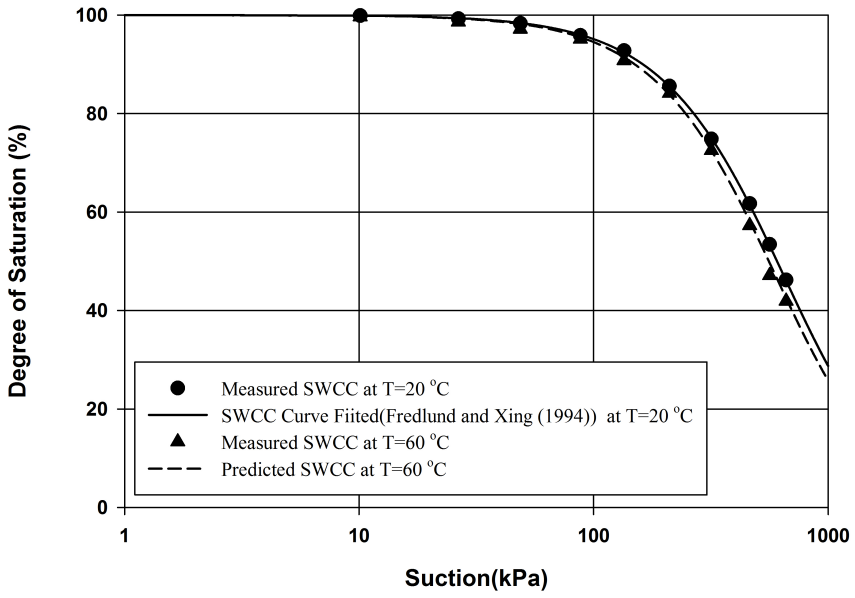

Figure 3.17: SWCC: experiments and proposed model for Ceramic clay (Salager et al. 2006)

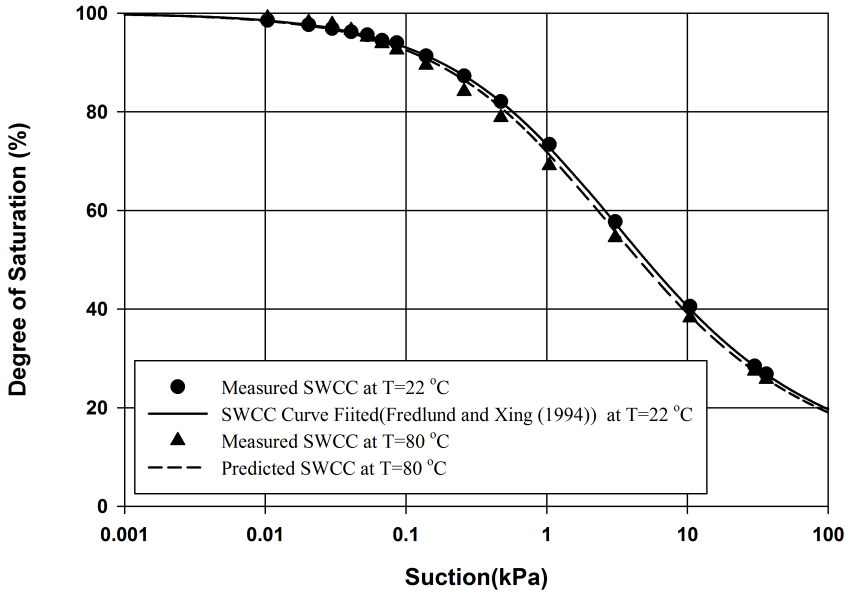

Figure 3.18: SWCC: experiments and proposed model for Boom clay (Salager et al. 2006)

3.4 Parameter Sensitivity Analysis for the proposed approach

The proposed approach of estimating the changes in the SWCC with respect to temperature assumes that the temperature affects the a parameter exclusively, while n and m remain at the same value as for the SWCC at 20°C. In this section, a range values of the independent variable of theFredlund and Xing model (a, n, and m) is selected. A comparison of the predicted SWCC and the fitted SWCC at 4 °C and 49 °C for Unimin Silica Sand 7030 and Industrial Sand are fitted independently to the Fredlund and Xing model is presented(Figure 3.19 and Figure 3.26). They can be seen to agree fairly well with the assumption of constant n and m under the effect of temperature.

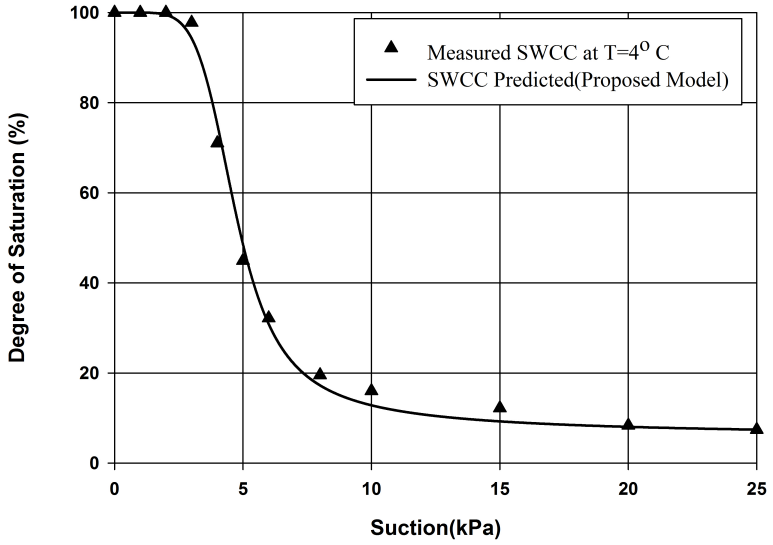

Figure 3.19: SWCC of Unimin Silica Sand 7030 at 4 °C using proposed method

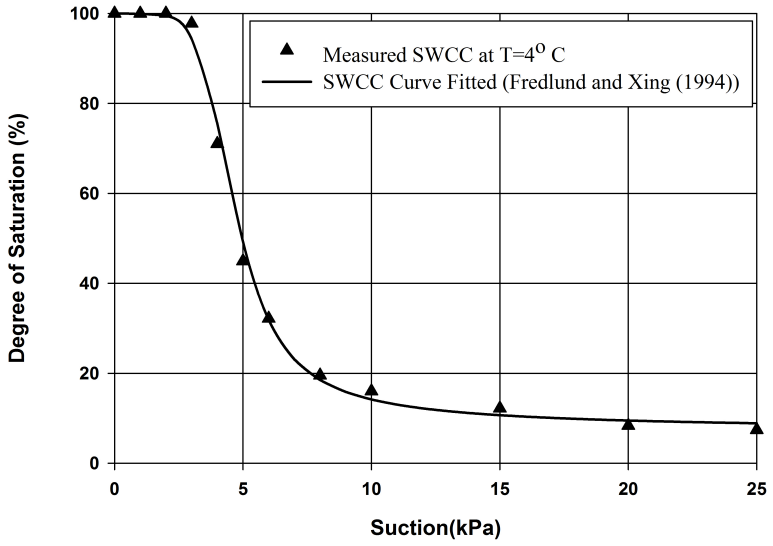

Figure 3.20: SWCC of Unimin Silica Sand 7030 at 4 °C using Fredlund and Xing method

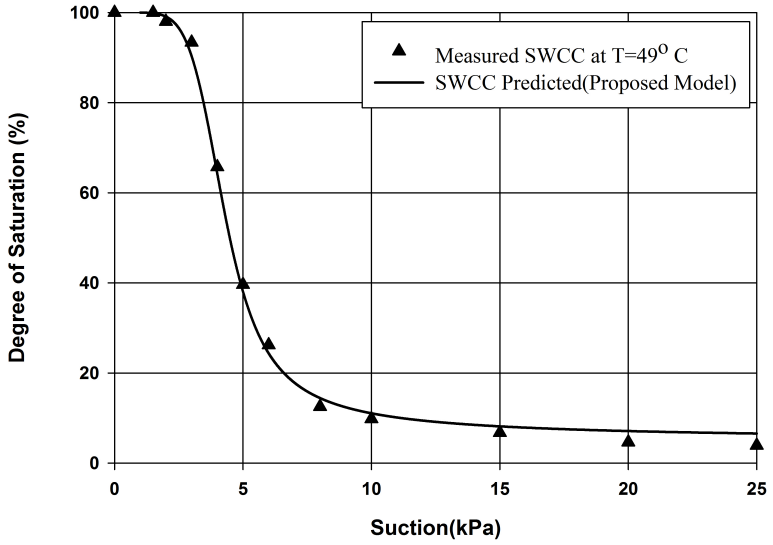

Figure 3.21: SWCC of Unimin Silica Sand 7030 at 49 °C using proposed method

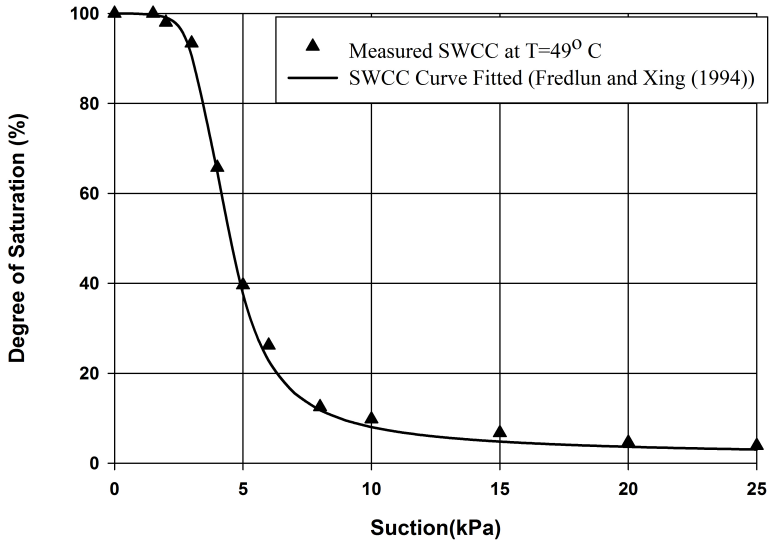

Figure 3.22: SWCC of Unimin Silica Sand 7030 at 49 °C using Fredlund and Xing method

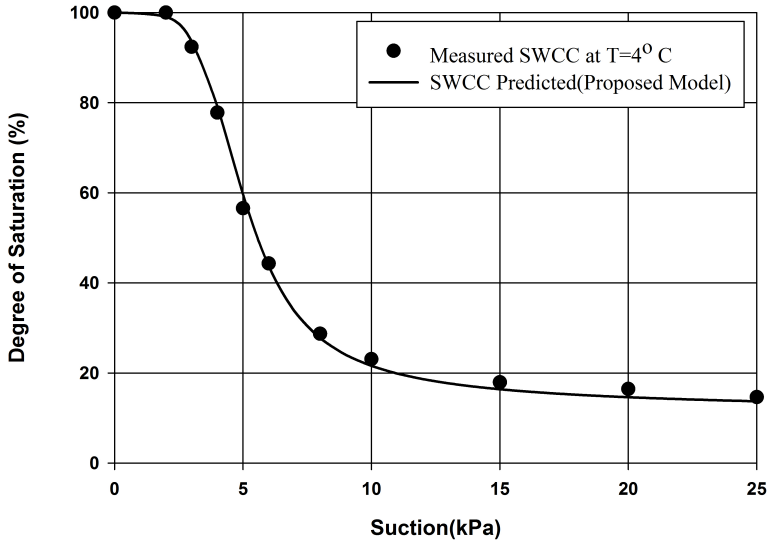

Figure 3.23: SWCC of Industrial Sand at 4 °C using proposed method

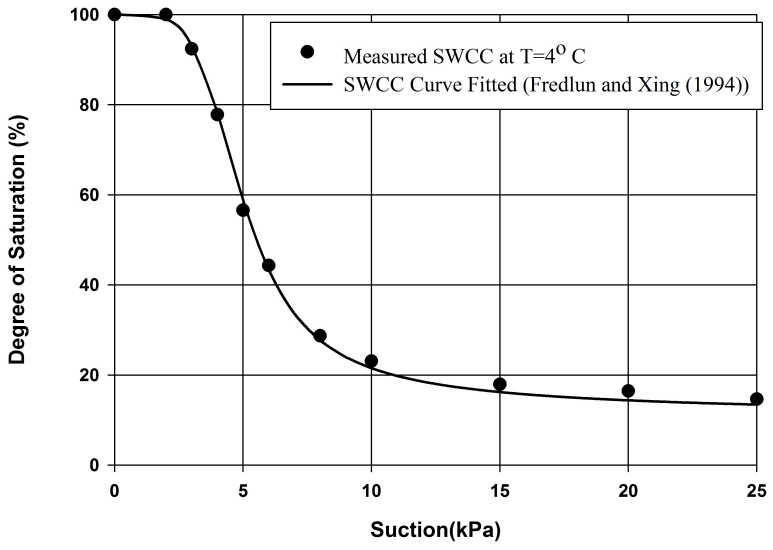

Figure 3.24: SWCC of Industrial Sand at 4 °C using Frelund and Xing (1994) method

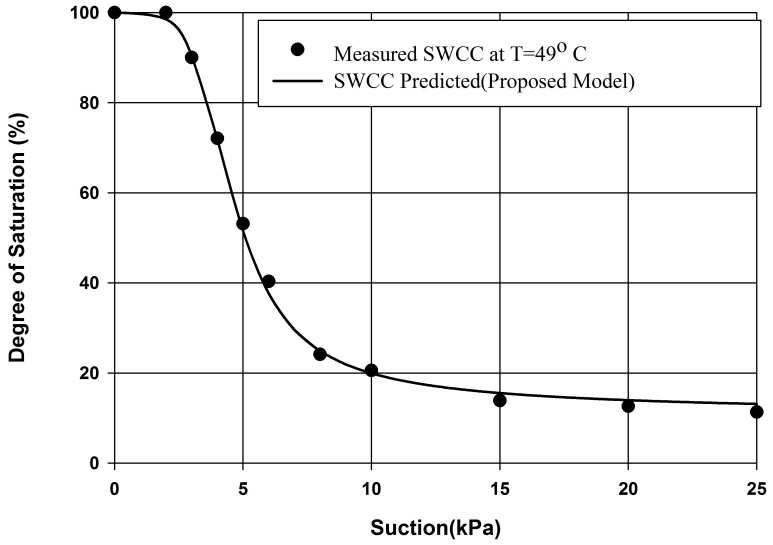

Figure 3.25: SWCC of Industrial Sand at 49 °C using proposed method

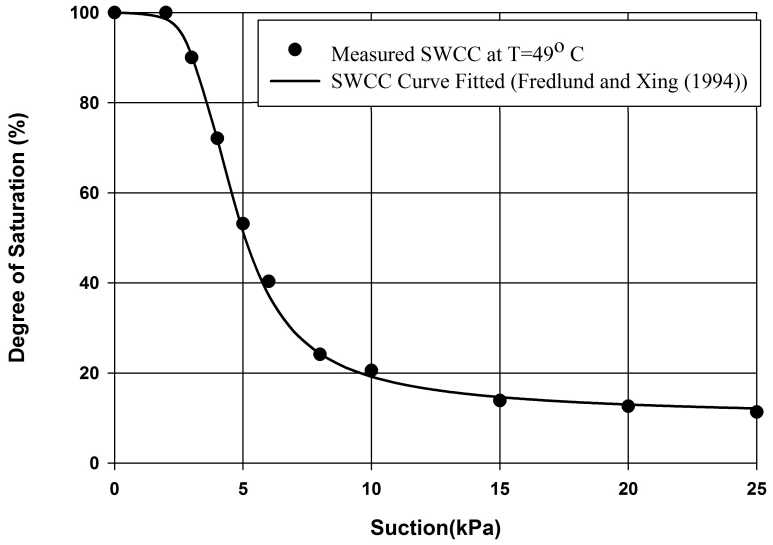

Figure 3.26: SWCC of Industrial Sand at 49 °C using Frelund and Xing (1994) method

Table 3.4 presents the parameters obtained by fitting the Fredlund and Xing model to the data at various temperatures compared to the values used with the proposed approach. It can be concluded that the parameter a at temperatures other than 20 °C can be estimated well using the proposed equation (Eq. 3.8), and that the assumption of a constant value for n, and m is not unreasonable. For Unimin Silica Sand 7030, it can be observed that the parameters n and m vary between 6.081 to 6.116 and 1.478 to 1.485, respectively. For the Industrial Sand, the same parameters vary between 4.884 to 4.900 and 1.452 to 1.459. It can be concluded that these variables are not significantly affected by the temperature which is consistent with the observed shape of the SWCC at different temperatures, where the slope of the transition zone and the residual zone remain parallel.

Table 3.4: Calculation of the fixed parameters (a, n, m)at different temperatures using Fredlund and Xing fitting method and proposed approach

		Fredlund and Xing(1994)			Proposed Approach	
Studied Soils	Fixed Parameters	T=4 °C	T=20 °C	T=49 °C	T=4 °C	T=49 °C
Unimin	a	4.240	4.111	3.890	4.251	3.923
Silica Sand	n	6.112	6.116	6.081	6.116	6.116
7030	m	1.485	1.480	1.478	1.480	1.480
Industrial	a	4.435	4.301	4.061	4.443	4.056
Sand	n	4.896	4.900	4.884	4.900	4.900
	m	1.456	1.459	1.452	1.459	1.459

3.4.1 Effect of fixed parameters on the shape of SWCC

Figure 3.27 to Figure 3.32 depict plots of the Fredlund and Xing (1994) model varying either the a, n, or m parameters while maintaining the other two constant and equal to the fitting parameters of the experimental data plotted on the same figure (n equal to 6.49 and m equal to 1.5 for Unimin Silica Sand 7030 and for Industrial sand these values are 5.14 and 1.66 respectively).

As can be seen in Figure 3.27 to Figure 3.28, variations of the a parameter result in the most severe changes in the position of the SWCC (for a a given range of parameter values) while the curves remain largely parallel to each other. This is the observed behaviour reported in literature and observed in the current experimental program.

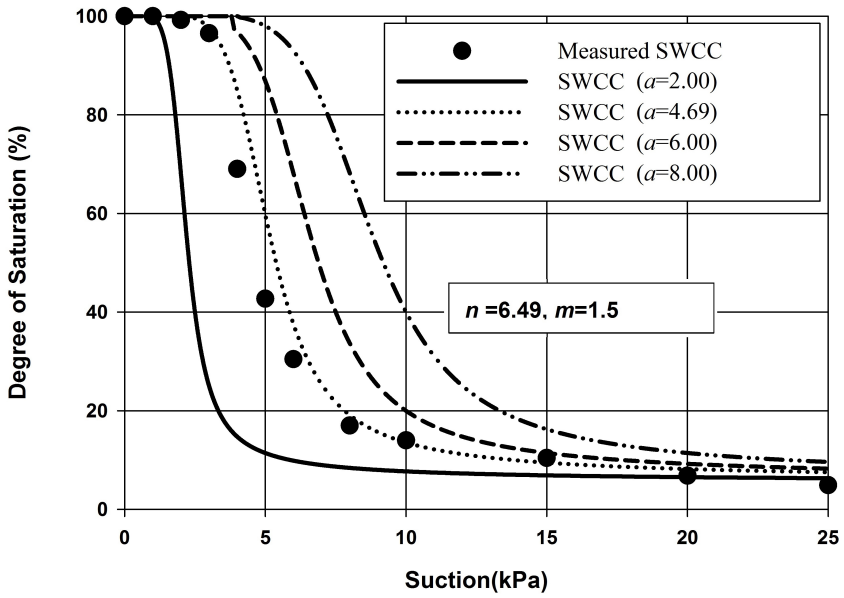

Figure 3.27: SWCC using Fredlund and Xing method for Unimin Silica Sand 7030 (n and m constant and a varying)

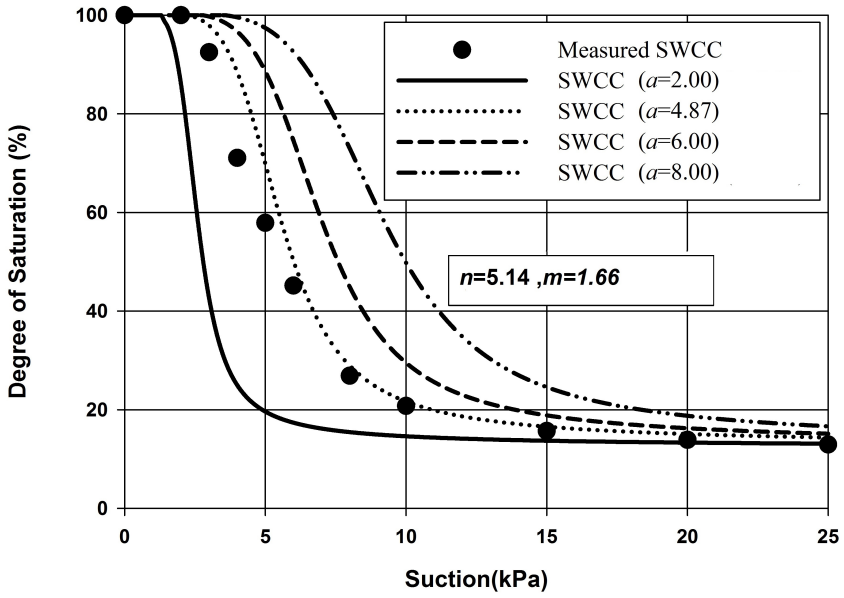

Figure 3.28: SWCC using Fredlund and Xing method at $20°C$ for Industrial Sand (n and m constant and a varying)

When the n parameter is changed, Figure 3.29 and Figure 3.30, with a and m constant (a equal to 4.69 and m equal to 1.5 for Unimin Silica Sand 7030 and for Industrial sand these values are 4.87 and 1.66 respectively), the SWCC has a clear change of slope in the transition zone which is generally related to the pore size distribution index of soil (Sillers et. al 2001), and all SWCC meet at a common point along the curve. This behaviour has the smallest correspondence with the observed behaviour of the experimental specimens.

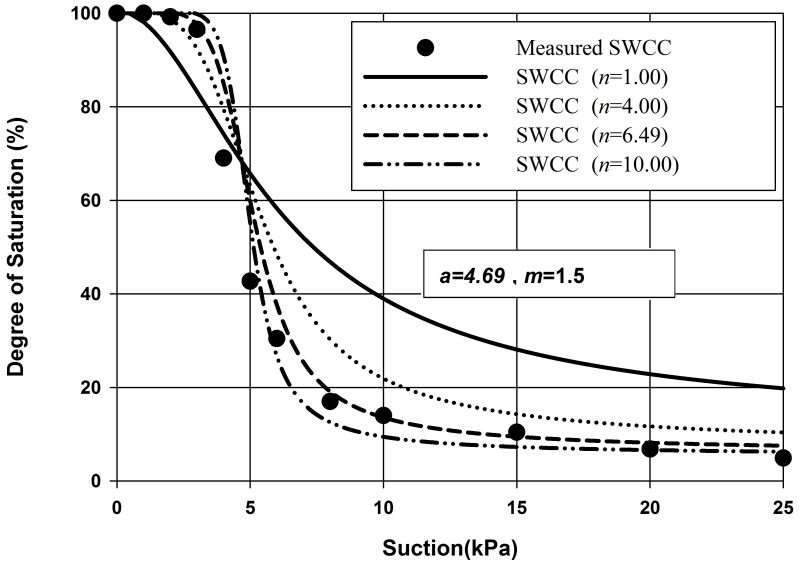

Figure 3.29: SWCC using Fredlund and Xing method at $20°C$ for Unimin Silica Sand 7030 (a and m constant and n varying)

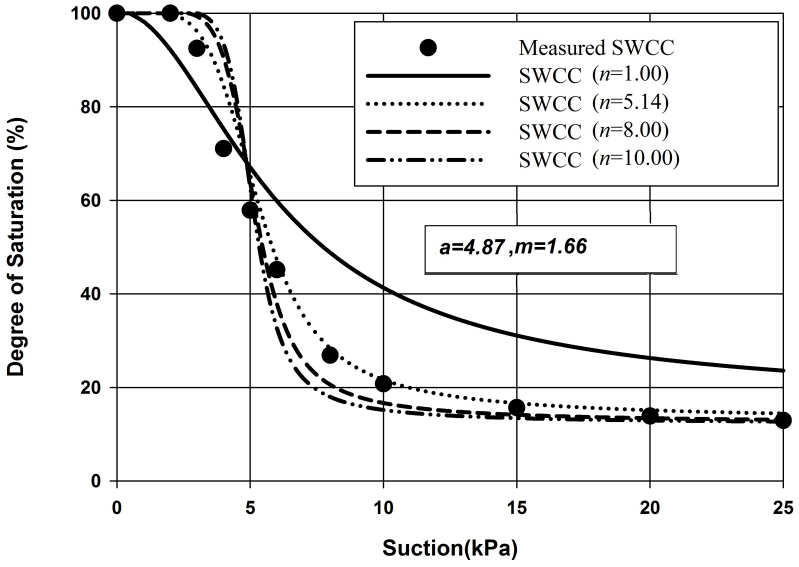

Figure 3.30: SWCC using Fredlund and Xing method at $20°C$ for Industrial Sand (a and m constant and n varying)

Figure 3.31 and Figure 3.32 illustrate the Fredlund and Xing (1994) model with constant parameters a and n (a equal to 4.69 and n equal to 6.49 for Unimin Silica Sand 7030 and 4.87 and 5.14 for Industrial sand respectively) and varying the parameter m. The parameter m is related to the asymmetry of the curve around the inflection point. Typically small values of m can result in an intermediate slope of SWCC in the boundary effect zone and steeper slope in the residual zone. However the effect of m on the transition zone slope is not as marked as the effect of the parameter n, and its main effect is on the apparent residual degree of saturation in the residual zone. The relatively parallel SWCC suggest that the m parameter might also be a factor resulting in the observed behaviour of the SWCC under various temperatures, however, given that the values of the fitted parameter m in Table 3.4 do not show a definite trend under the influence of temperature, its effect can be assumed to be relatively small, and for now will be neglected.

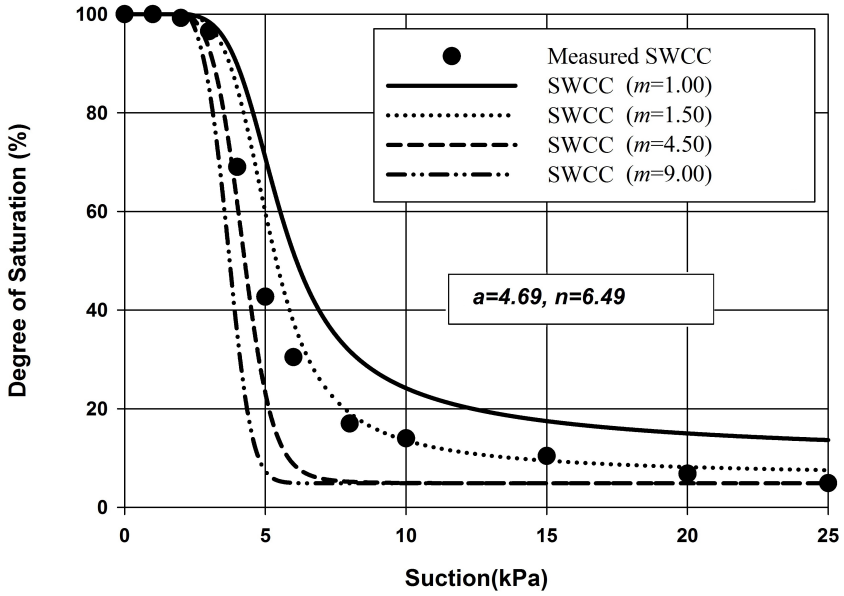

Figure 3.31: SWCC using Fredlund and Xing method at $20°C$ for Unimin Silica Sand 7030 (a and n constant and m varying)

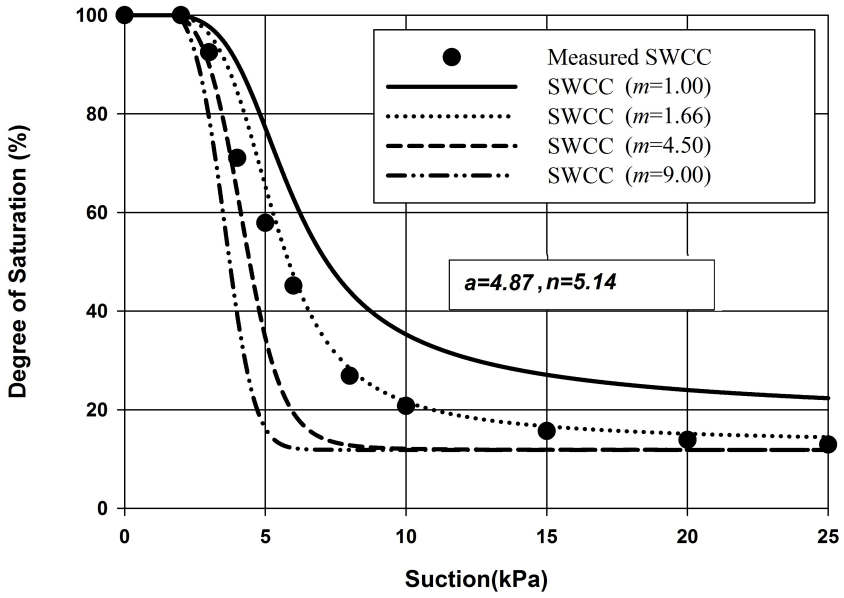

Figure 3.32: SWCC using Fredlund and Xing method at $20°C$ for Industrial Sand (a and n constant and m varying)

3.5 Summary and Conclusion

The current study has presented a simple method based on first principles to describe the effect of temperature on the SWCC. A relationship was developed relating the parameter a of the Fredlund and Xing (1994) equation and the temperature gradient. The proposed method allows the SWCC determined at a known temperature to be corrected for other temperatures. Experiments conducted on two coarse grained sands at three different temperatures and the results taken from the literature on two fine grained soils were used to validate the procedure. There is a good comparison between the measured data and the estimated SWCC with the proposed procedure. The results of this study are consistent with the observed behavior of unsaturated soils under a thermal gradient where the degree of saturation of the soil increases at the cold boundary and decreases at the hot boundary. The results of this experiment also indicate that at a given water content the suction value decreases with increasing temperature which is attributed mostly to the changes in the surface tension (σ) and fluid density. The reliability and the degree of confidence of the proposed method may further be enhanced by conducting experiment on soils with higher organic contents as well as inorganic soils.

Chapter 4

ESTIMATION OF THE SWCC USING SOIL WATER MOVEMENT UNDER TEMPERATURE GRADIENT

4.1 Introduction

During the few decades, many attempts have been made to the simplified develop empirical methods for estimation of the SWCC. The first group of these predictive models is based on calculating the water content at selected matric suction values statistically (Gupta and Larson 1979; Aubertin et al. 1998). To find these formulations, generally substantial regression analysis followed by a curve fitting method is necessary (Johari et al. 2006; Zapata et al. 2000).

The second group of these approaches is based upon estimating the SWCC using the link between physical attributes of soils and the SWCC equations (Haverkamp and Parlange 1986; Fredlund et al. 1997). If it is assumed that the soil contains an interconnected set of pores that are randomly distributed, the grain size distribution then can be used to estimate the pore-size distribution. This means that the distribution of water content within pores can be estimated at desirable suction values (Chin et al. 2010).

The last group of estimation methods which is considered in this study is based on developing relations between soil properties such as grain size distribution or index properties and fitting parameters of the SWCC equation (Tomasella and Hodnett 1998; Perera

et al. 2005). Among recent approaches, Vanapli and Catana (2005), developed a method to estimate the SWCC of coarse-grained soils using and grain size distribution and the measurement of one data point on the SWCC (ie., matric suction and corresponding water content). This method is more flexible due to the fact that it is not solely based on basic soil properties.

While much attention has been given to estimating the SWCC indirectly with regression analysis, relatively less has been done regarding using available published experimental results which may lack an explicit SWCC, but may provide other means of assessing it indirectly. Experimental evidence by Taylor and Cavazza (1954), Philip and De Vries (1957), Sutor (1969), Evgin and Svec (1988), Bach (1992), Mohamed et al. (1992), Wang and Su (2010) and many other researchers indicate that when there is a temperature gradient, the soil moisture is redistributed and migrates from the boundary with higher temperature towards the zone with a lower temperature. This suggests that considering effect of temperature on the SWCC may be used in the cases where a temperature and moisture profile exists to estimate the SWCC of the tested soil, thus increasing the value of the available data sets. In all of the papers listed above, while a temperature and moisture profile is available for the tested soils, SWCC or suction were not measured, therefore the ability to estimate the SWCC using the soil water movement in response to temperature can prove a valuable tool.

4.2 Suggested approach to estimate the fixed parameters of the Fredlund and Xing Equation (1994)

4.2.1 The *a* parameter of Fredlund and Xing (1994)

Vanapalli and Catana (2005) presented a method based on regression analysis on 14 different coarse grained soils with data from grain size distribution to estimate the a parameter of the Fredlunad and Xing (1994) equation. In this method, the fixed parameter a is inversely related to the dominant particle size where increasing the diameter results in a lower a parameter and lower AEV. The mathematical formulation is given as:

$$a = \frac{1.33}{de^{0.86}} \tag{4.1}$$

where d_e is the dominant particle size in mm. According to Zamrin's equation the

dominant particle size in a soil can be expressed as(Vukovic and Soro 1992):

$$\frac{1}{d_e} = \sum_{i=1}^{i=n} \Delta g_i \frac{ln(\frac{d_i^g}{d_i^d})}{d_i^g - d_i^d} \tag{4.2}$$

where d_i^g , d_i^d are the maximum and minimum grain diameters of the corresponding fraction. If the curve of the grain size distribution is viewed as a broken curve then Δg_i is the difference in cumulative relative weight for a particle size increment. Figure 4.1 indicates the procedure of calculating dominant particle size distribution.

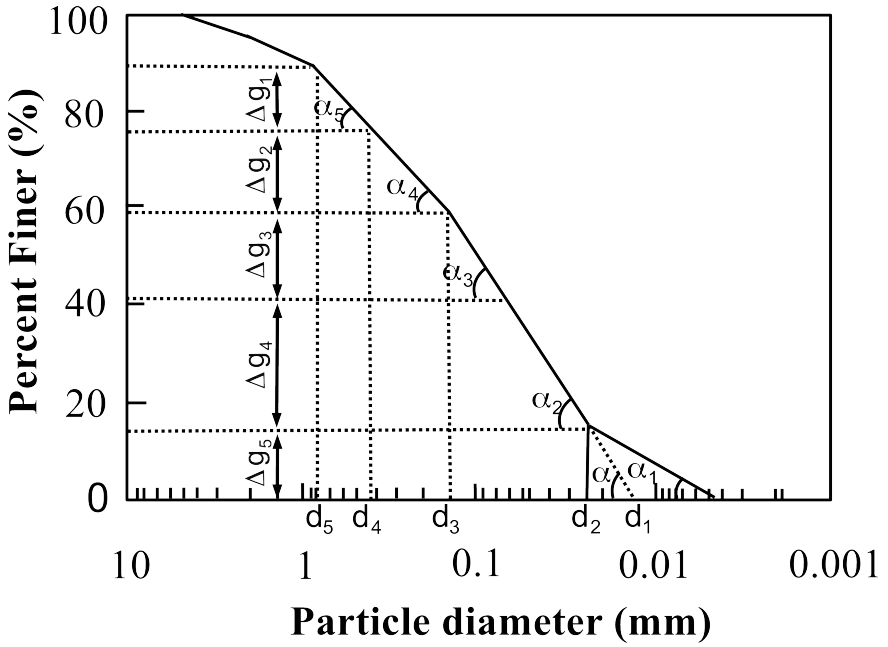

Figure 4.1: Schematic for calculating the dominant particle size diameter (Vanapalli and Catana 2005)

It can be observed that when the material is uniform, the range of the dominant particle size is larger and the a parameter becomes smaller. On the other hand, a higher value of the a indicates that the soil is well graded and the water drains more gradually. Siller et al. (2001) showed that the overall shape of the SWCC is not affected by changing the a parameter. However, once its value increases, the curve is offset along the suction axis. The shift of the curve along the suction is consistent with the expected changes in SWCC under the effect of temperature. Experimental results of Hopmans and Dane (1986), and Salager et al. (2006) on Norfolk sandy loam and clay loam respectively at

two different temperatures showed that at a given volumetric water content, the suction decreases with an increase in temperature. An increase of temperature causes the SWCC to migrate to the left with a lower AEV and a parameter. This may be accounted for by applying the capillary tube theory and assuming that the pores in the soil can be effectively represented by a series of tubes. If it is hypothesized that the wetting angle is constant with regard to temperature, changes of the SWCC due to temperature would then be attributed mostly to the changes of the surface tension (σ) and fluid density (ρ_l) (Grifoll et al. 2005; Keshky 2011), it can showed that the a parameter of the Fredlund and Xing equation can be expressed as (Chapter 3):

$$a_T = a_{(T=293.50)} \times 13840.45 \times \frac{(0.117 - 0.00153 \times T)}{(658.2 - 2.509 \times T - 4.606 \times 10^{-3} \times T^2)} \tag{4.3}$$

where a_T is the Fredlund and Xing a parameter at desirable temperature, T (in K), and $a_{(T=293.50)}$ is the value of the a parameter at $T = 293.50K$ (20 °C). By substituting Eq. 4.3 into Eq. 4.4, the a parameter can be expressed as a function of the grain size distribution and temperature as follows:

$$a_T = \frac{1.33}{de^{0.86}} \times a_{(T=293.50)} \times 13840.45 \times \frac{(0.117 - 0.00153 \times T)}{(658.2 - 2.509 \times T - 4.606 \times 10^{-3} \times T^2)} \tag{4.4}$$

4.2.2 The n parameter of Fredlund and Xing (1994)

The slope of the SWCC, in the transition zone, is consistent with the pore size distribution of the soil which can be affected by the initial water content, the dry density, and the compaction method (Estabragh et al. 2004). Sillers et al. (2001) indicated that a change of pore size index varies the inclination of SWCC in the transition zone which consequently changes the n parameter of Fredlund and Xing equation. It can be observed that as the soil becomes finer, this parameter is affected more by mineralogy and surface activity of the soil particles (Duncan and Wright 2005). However, in a coarse-grained soil, the n parameter is mostly governed by the shape, size and distribution of pore space (Chin et al. 2010). Yang et al. (2004) indicated that as the soil becomes coarser, the slope of its grain-size distribution curve is steeper and consequently the slope of the measured SWCC will be sharper. Based on these observations, Vanapalli and Catana

(2005) estimated the n parameter of a coarse -grained soil as following expression:

$$\frac{7.78}{(C_u \times e)^{1.14}} \tag{4.5}$$

where C_u is the coefficient of uniformity that is representative of particle size distribution or the pore size distribution for coarse-grained soils and e is the void ratio which introduces the effect of compaction into the estimation of the SWCC (Vanapalli and Catana 2005). Due to dependency of the parameter n on the void size distribution, its value can be assumed to remain unaffected by temperature. This assumption is in agreement with the published experimental data of Wu et al. (2004), and Salager et al. (2006) in which the measured SWCCs at different temperatures have approximately identical slopes.

4.2.3 The m parameter of Fredlund and Xing (1994)

The m parameter of the Fredlund and Xing model is related to the asymmetry aspect of the SWCC. Changing this parameter rotates the sloping portion of the curve which is located at the residual zone (Leong and Rahardjo 1997). To find this parameter, Vanapalli and Catana (2005) proposed to use one-point measurement of the SWCC which shifts the SWCC such that it passes through the measured point. However, no suitable single suction range was reported for the one-point SWCC measurement (Chin et al. 2010).

4.3 Proposed method to estimate the m parameter

If it is assumed that the soil specimen with uniformly distributed initial moisture content is subjected to a constant temperature gradient between its two end boundaries, the moisture content at the cold boundary will increase and it will decrease at the hot boundary. Ewen and Thomas (1989) indicated that the migration of water can be mathematically modelled by considering changes of surface tension in capillary forces. In order to relate the fixed parameter of the Fredlund and Xing equation to the migration of water under non isothermal conditions, the moisture content and suction profile at steady state need to be estimated or measured. The experimental results of Wang and Su (2010) showed that the final distribution of moisture content is highly dependent on the initial moisture content, the soil density, and the temperature difference which implies changes to the a and n parameters in the Fredlund and Xing equation. Therefore, if it is assumed that

the suction value corresponding to the temperature along the soil specimen has a known value at steady state, the water content profile can then be back calculated by applying the Fredlund and Xing equation and Eq.(4.4) simultaneously.

At steady state condition, the moisture distribution of the soil along the soil sample is stable and the water potential which is equal to sum of the thermal potential and matric potential at different points of the specimen should have a constant value (Wang and Su 2010). This means that at steady state, the liquid and vapour velocities are essentially equal to each other (Derek 1997). This statement can be used as a hint to estimate the suction profile. By considering the vapour and liquid movement formulations given by Thomas (1992), Roshani and Infante Sedano (2013) indicated that for a horizontal soil sample that is subjected to a temperature gradient, the following equation can be used to estimate the suction profile:

$$(k(\theta,T)-k_{v\psi})\frac{\delta\psi}{\delta x}=k_{vT}\frac{\delta T}{\delta x} \tag{4.6}$$

where, $\frac{\delta\psi}{\delta x}$ is a gradient of matric suction or matric potential, $\frac{\delta T}{\delta x}$ is a gradient of temperature or thermal potential, $k_{v\psi}$, k_{vT} are the isothermal vapour conductivity and non-isothermal vapour conductivity respectively and relate to the vapour movement, and $k(\theta,T)$ is the hydraulic conductivity of the unsaturated soil in which the effect of temperature is considered, and can be calculated based on the modified van Genuchten (1980) equation (Touma 2008) as:

$$k(\theta,T)=\frac{661.2\times10^{-3}\times(T_r-229)^{-1.562}}{661.2\times10^{-3}\times(T-229)^{-1.562}}\times k_s\times(\frac{\theta-\theta_r}{\theta_s-\theta_r})^{0.5}\times[1-(1-(\frac{\theta-\theta_r}{\theta_s-\theta_r})^{\frac{n-1}{n}})^{1-\frac{1}{n}}]^2 \tag{4.7}$$

where k_s is the saturated hydraulic conductivity that can be measured by conventional tests, n is the fixed parameter which is related to pore size distribution and can be estimated by Eq. 4.5 and T_r is the reference temperature. Thomas and King (1991) give the following equations separately to estimate the $k_{v\psi}$ and k_{vT}:

$$k_{vT}=D_{atm}\frac{v\eta}{\rho_l}\frac{\nabla T_a}{\nabla T}(h\beta-\rho_0\frac{g\psi h}{RT^2})=D_{atm}\frac{v\eta}{\rho_l}\frac{\nabla T_a}{\nabla T}(h\beta-\rho_0\frac{e^h h}{T}) \tag{4.8}$$

$$k_{v\psi}=D_{atm}\frac{v\eta\rho_0 h}{\rho_l RT} \tag{4.9}$$

where:

$$D_{atm} = \frac{5.893 \times 10^{-3} \times T^{2.5}}{10^5}(\frac{m^2}{s}) \tag{4.10}$$

$$\rho_0 = \frac{1}{194.4 \times exp(-0.06374 \times (T-273) + 0.1634 \times 10^{-3} \times (T-273)^2)} \tag{4.11}$$

$$h = exp\frac{\psi g}{RT} \tag{4.12}$$

$$v = \frac{10^5}{10^5 - \rho_0 \times h \times R \times T} \tag{4.13}$$

$$\beta = \frac{dp_0}{dT} \tag{4.14}$$

In these equations, ρ_l is the liquid density which is equal to $998\frac{kg}{m^3}$, R is the specific gas constant for the water vapour ($461.5\frac{J}{kgk}$), D_{atm} is the molecular diffusivity of the water vapour in the air, v is the mass flow factor, ρ_0 is the density of the saturated water vapour, h is the relative humidity, η is the porosity of the soil, β is the gradient of saturated water vapour density with respect to temperature, T is temperature in K and $\frac{\nabla T_a}{\nabla T}$ is the ratio of mean temperature gradient in air-filled pores to the overall temperature gradient. Ewev and Thomas (1989) and Kanno et al. (1996) indicated that the following expression can generally be used for fine and coarse-grain soils:

$$\frac{\nabla T_a}{\nabla T} = \frac{1}{3}[\frac{2}{1+BG} + \frac{1}{1+B(1-2G)}] \tag{4.15}$$

where:

$$B = \frac{k_a + k_v}{k_l} - 1 \tag{4.16}$$

$$k_v = D_{atm} v h L \beta \tag{4.17}$$

$$G = \begin{array}{c} 0.333 - \frac{0.325(\eta-\theta)}{\eta}\ 0.09 < \theta < \eta \\ 0.0033 + 11.11(0.33 - \frac{0.325(\eta-0.09)}{\eta})\ 0 < \theta < 0.09 \end{array} \tag{4.18}$$

where L is the heat of vaporization and is equal to $2.4 \times 10^6 \frac{J}{kg}$, K_a is thermal conductivity of dry air ($0.00258 \frac{w}{mk}$), and K_l is thermal conductivity of liquid water ($0.6 \frac{w}{mk}$). To simplify the calculation of these parameters, the humidity may be considered as a constant value equal to one. The reason of this assumption is that the range of meaningful suction in a coarse-grained soils are well within 0 to $1500kPa$ and experiments can be carried out at a temperature gradient between 0 °C and 100 °C (Figure 4.2). As a result, it can be shown that $k_{v\psi}$, k_{vT} can be estimated with only the knowledge of the temperature profile at steady state.

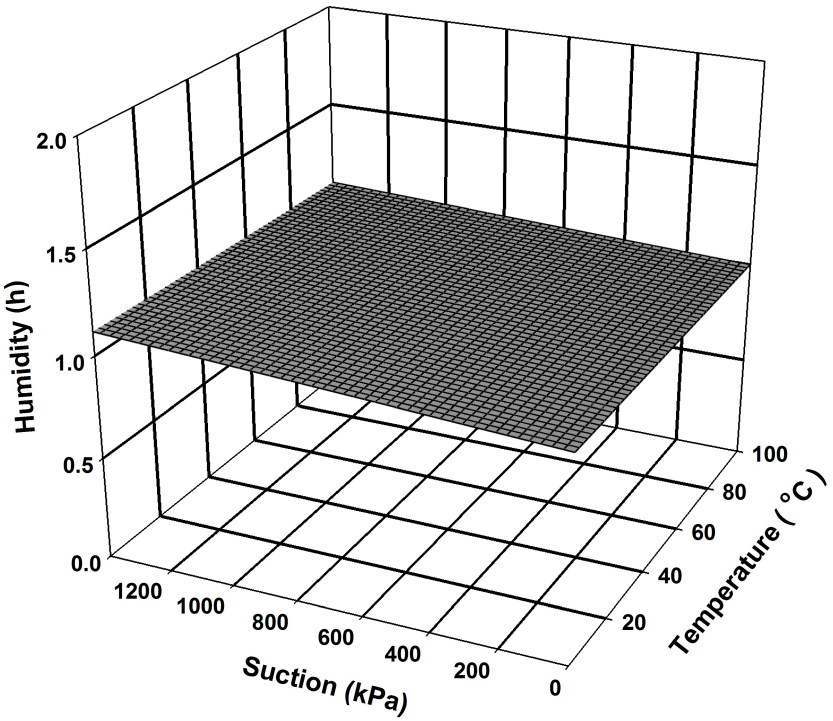

Figure 4.2: Estimated humidity (h) as a function of temperature and suction

The the m parameter described by Eq.(4.6) is obtained by assuming initial and using a trial and error procedure to find the final value. According to Fredlund and Xing (1994), the m value is typically between 0 and 10. This range is calculated based on consider-

ing the m parameter corresponding to the inflection point of the SWCC. By knowing the measured temperature and water content profile, the right hand side of (4.7) can be calculated using the finite difference method (FDM) and the value of $\frac{\delta\psi}{\delta x}$ can be estimated once the suction profile along the specimen is calculated for a given m value which requires solving a system of nonlinear Fredlund and Xing equation and Eq.(4.4) simultaneously. Since there is equality between the thermal potential (left hand side of Eq.(4.6)) and the matric potential (right hand side of Eq.(4.6)), the error of the corresponding m parameter can be estimated. Using software such as MATLAB or OCTAVE error can be minimized in repeated trials so that the optimum m value is obtained (Roshani and Infante Sedano 2013).

4.4 Materials and test methods

4.4.1 Material selection and characterization

To determine the reliability of the proposed approach, two types of coarse-grained soils; namely; Unimin Silica Sand 7030 (clean commercial sand), and Industrial sand (super fine sand) which were obtained from Merkley Supply Ltd, Ottawa, Canada and Target Products Ltd, Burnabby, Canada respectively. The grain size distributions are shown in Figure 4.3. To measure the saturated hydraulic conductivity coefficient, a TRI-FLEX II standard panel, equipped with pressure gauges and regulators, electronic pressure transducers, and graduated pipettes, was used. These tests were carried out in accordance with ASTM D5084 (ASTM 2010a) using a constant head. As a check on the accuracy of the measurement, the estimated methods proposed by Terzaghi, Zuncker, and Zamarin (Vukovic and Soro 1992), have been also used. Table 4.1 shows the summary of the results based on the estimated methods and the direct measurement. In both soils, the estimated values and measured one are in good agreement.

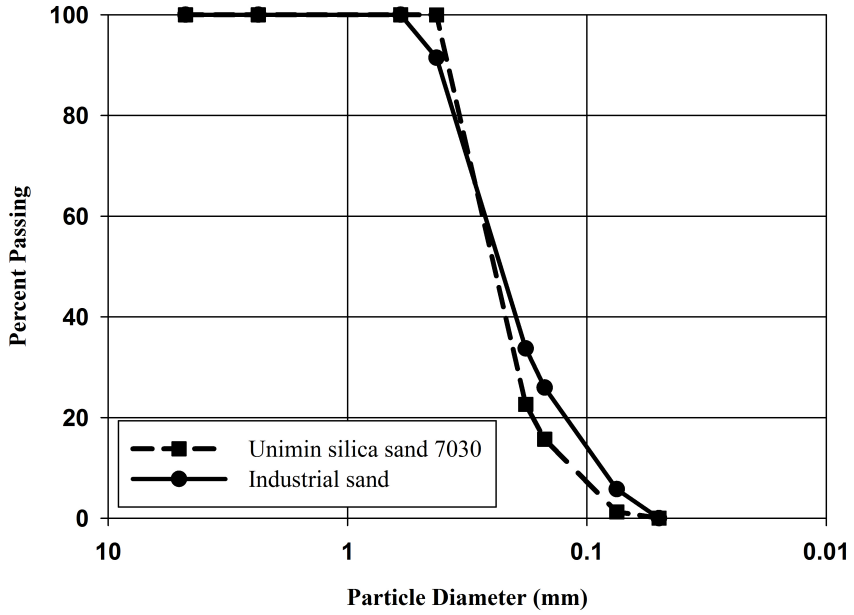

Figure 4.3: Grain size distribution of the studied soils

Table 4.1: Values of saturated hydraulic conductivity ($\frac{m}{s}$)

Methods	Unimin Silica Sand 7030	Industrial Sand
Terzaghi Method	2.1×10^{-3}	1.5×10^{-3}
Zamarin Method	1.4×10^{-3}	0.69×10^{-3}
Zunker Method	0.9×10^{-3}	1.1×10^{-3}
Measured	1.2×10^{-3}	0.92×10^{-3}

The SWCC of the above soils is determined in accordance with ASTM D 6836 (ASTM 2002) using a Tempe cell apparatus. The objective of this measurement is to compare the result of the proposed method to the standard method. In this test, the ceramic disk of the Tempe cell as well as the specimen are saturated, the pore water is kept

at atmospheric pressure and air pressure is raised thus applying the axis translation technique to change the matric suction. At each suction interval, the water content of the soil sample is determined by measuring the volume of the expelled from the specimen until equilibrium is reached at the specified suction. A homemade pressure gauge capable of accurate measurement of the pressure at the low range of pressure required for the SWCC of sands, and presented by Infante Sedano et al. (2007) was used in this study. At the end of the test, the gravimetric water content of the soil specimen is determined by oven drying the soil sample. The information related to the other data points of the SWCC can be found from back calculation based on the volume mass properties of the soil. Figure 4.4 shows the resulting SWCC for Industrial sand and Unimin silica sand 7030 respectively.

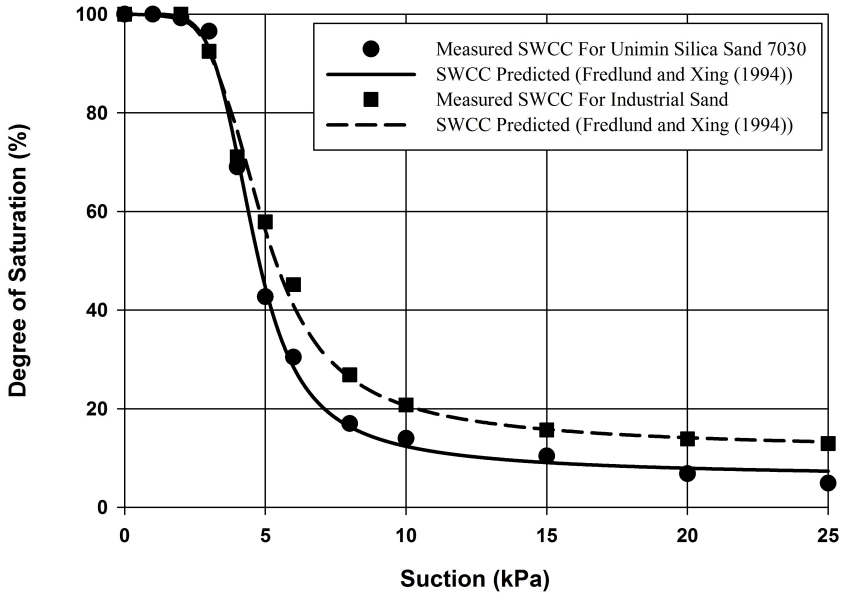

Figure 4.4: Measured SWCCs of studied soils

4.4.2 Experimental methods

The purpose of the test program is to establish the ability of the proposed approach to find the m parameter as well as the influence of the initial moisture content on the moisture profile along the specimen at thermal equilibrium. The test procedure followed in the

present study was originally inspired by the work of Evgin and Svec (1988). Figure 4.5 illustrates the schematic of experimental set-up.

In the experimental set-up used, the soil sample is formed within the testing tube and a desirable temperature difference is applied at the boundaries by circulating water in two containers that are placed in contact with the extremities of the soil specimen. A stainless steel container is fixed at one extremity while a removable container is placed at the other extremity to permit soil placement. A plastic cylinder surrounding the soil specimen has an inner diameter of $65mm$ and length of $210mm$ and forms the inner wall and a $150mm$ (outer) diameter $\times 210mm$ cardboard tube forms the outer wall of the specimen enclosure. To thermally insulate the specimen and the spaces between these tubes, commercial gap-filler foam which has a thermal diffusivity of $1.06 \times 10^{-7} \frac{m}{s}^2$ is used.

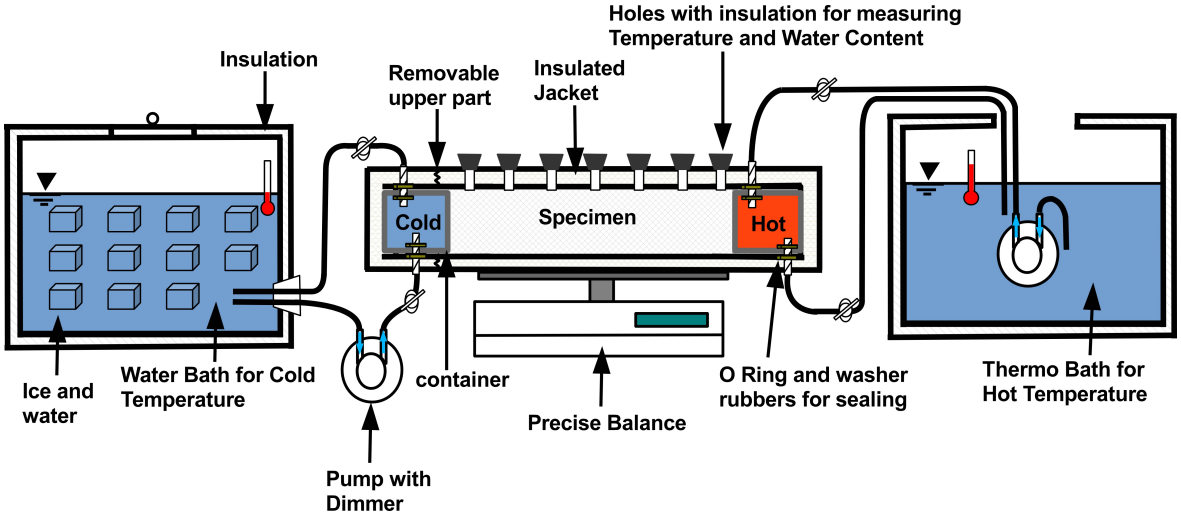

Figure 4.5: Schematic of temperature controlled SWCC determination set-up

Two hydraulic pumps are used to circulate the water from the thermal baths with controlled temperature to the containers at the ends of the specimen. Dimmer switches are used to adjust the flow rate of the pumps and help control the boundary temperature. Temperature control at the hot end is provided with a commercial thermostatic bath which is designed to provide ambient temperature throughout the unit by using a microprocessor-based temperature control with an integrated heater and chiller. The control processor in the thermal bath provides a consistent bath temperature of $20°C$ ($68°F$) accurate within 0.1% of input span ($\pm 1°F$). The temperature can be set between $10°C$ ($50°F$) and $49°C$ ($120°F$). The water bath is fully-insulated and includes

a circulating pump, which ensures a constant water temperature throughout the bath. For this experiment the temperature of the hot end is kept at 46 °C $\pm(0.1)°C$. The cold temperature at the other boundary is provided by using a water and ice mixture that is placed in a custom designed cooler. The latent heat of the phase change between ice and water provides an effective means of controlling the temperature within the insulated vessel with a minimum of external intervention. Using this approach, the temperature at the cold end of the sample is maintained at 2 °C $\pm(1)°C$

Seven ports, holes 20 mm in diameter, are provided along the length of the specimen to allow for temperature readings to be taken during the experiment, and samples for water content measurements to be extracted at the end of the test. Since the infra-red thermometer used in the experiment measures temperature by monitoring the photons emitted from the surface under observation, it is important to minimize the number of possible stray high energy photons from surfaces warmer than the target surface that might reach the sensor. To achieve this, aluminium tubes, $43mm$ in length, are kept in ice water until a reading is to be taken, at which point one tube is inserted into the temperature measurement port. This way, the only warm surface that can provide photons to the unit is the specimen itself. To ensure consistency in the readings, one aluminium tube is kept in ice for each temperature port, and is placed in the hole immediately prior to the temperature measurement.

To investigate the effect of the initial water content on the moisture content profile at equilibrium, tests at three initial water contents were conducted on each soil. The water contents were chosen so that they would lie 1-Near the air-entry value of the soil (or within the tension-saturated zone), 2-Within the transition zone, and 3- Near the residual zone of the SWCC. In all of these experiments, the samples were compacted at the same compaction water content (11.2% and 9.4% for Unimin silica sand 7030 and Industrial sand respectively) to approximately the same void ratio and subjected to approximately the same temperature difference. The initial conditions of the soil specimens are summarized in Table 4.2.

Table 4.2: Initial condition of the samples

Soil Type	Sample Number	Intial gravimetric water content w (%)	Initial Degree of Saturation S(%)	Temperature Diffrence T (°C)
Unimin Silica Sand 7030	1	22.3	93.0	43.6
	2	11.2	47.3	45.3
	3	5.6	23.5	46.0
Industrial Sand	4	18.6	89.7	43.9
	5	9.4	45.2	44.5
	6	5.3	25.7	44.5

4.4.2.1 Intermediate initial water content (Transition Zone)

To prepare a uniform unsaturated soil sample, the studied soils were first oven dried and then a $17ml$ and $14ml$ quantity of distilled water was added into the $150gr$ each of dry soil to achieve the initial intermediate water content 11.2% and 9.4% for each soil respectively. Mixing of the soil and water was done carefully and any occluded soil particles were removed. This procedure is followed to achieve a homogeneous sample with the initial intermediate water content, (11.2% and 9.4% for each soil, respectively). To ensure a uniform soil-water mixture during compaction, the soil samples are put in two sealed plastic bags and stored in a humidity controlled box for 2 days. At the end of the curing period, a dynamic compaction is applied uniaxillay, by dropping a $870gr$ tamping rod with a width of $64mm$, from a height of $50mm$ from the center of each $21mm$ thick layer inside the specimen enclosure. During the compaction phase, the enclosure stands vertically.

The water content of each layer is verified by taking small samples from the soil of each layer before compaction. The results of the verification of the layers indicate that the water content of all layer were approximately equal (i.e., $\pm 0.5\%$). The variations may be attributed to random errors in measurement as well as evaporation during preparation of the layer.

After compaction, the specimen is closed by placing the upper water container and is then laid horizontally and left to rest for $24hr$ in a temperature controlled room maintained at $20 \pm 1.0\,^{\circ}\mathrm{C}$. This procedure ensures a uniform moisture distribution within the specimen before starting the test.

After 24 hr, the experiment is initiated by imposing a temperature gradient by circulating water within the two end containers under controlled temperature. The temperatures at both extremities are measured using thermistors located before on the surface of the container at the ends of the sample. Figure 4.6 indicates the typical variation of temperatures in at the two boundaries. It can be seen that only a few minutes are required to change the temperatures of the end plates from the room temperature to the desired temperature. After reaching this point, the boundary temperature is subjected to negligible variations (Figure 4.6).

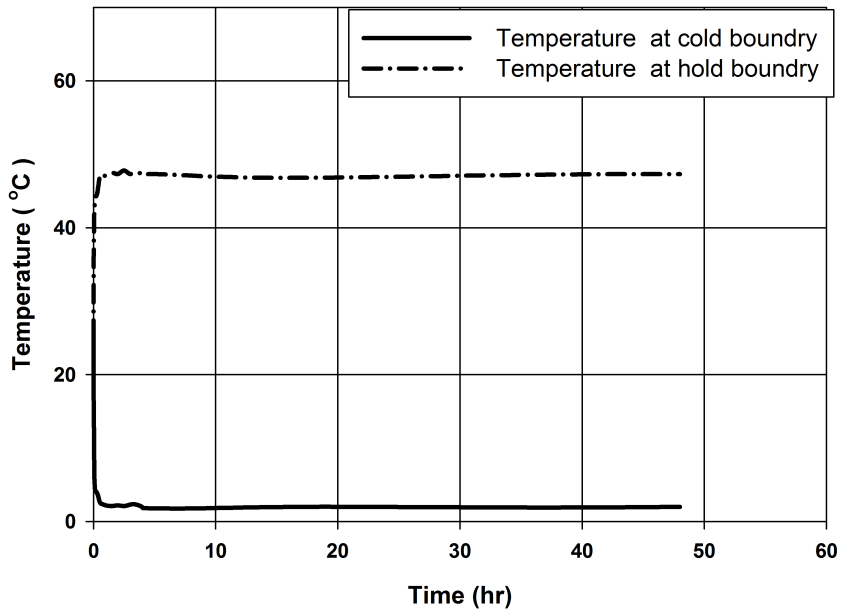

Figure 4.6: Typical temperature profile at two end boundaries

To ensure a steady state condition was achieved in the specimen, the tests are run for a period of 48 hr. based on the recommendations found in the literature (Cassel et al. 1969; Drek 1997; Thomas and King 1991). The published results for $100mm$ long columns of unsaturated Leighton Buzzard sandy soil which was subjected to a 40 °C thermal gradient shows that the time needed for the steady state was $24hr$ (Drek 1997). The saturated hydraulic conductivity of this soil is $1.1 \times 10^{-3} m/s$ which is close to the measured values of the soils investigated in the current study. Moreover, Observations by Cassel et al. (1969) for a $200mm$ long column of sandy loam which has a lower hydraulic conductivity than the soils of the present study, indicate that the time required achieve steady state was near $72hr$. The results of Thomas and King (1991) on a $200mm$ diameter column of unsaturated sand shows that the required time to reach steady state under a 40 °C temperature gradient is almost $48hr$. Figure 4.7 shows the measured temperature profile at different time intervals along the Unimin silica sand 7030 specimen (sample 2) and Figure 4.8 shows the moisture content profile at steady state of samples 2 and 5.

The measured temperature profile at steady state can be approximated by a linear function. This behaviour is consistent with the experimental results by Evgin and Svec (1988).

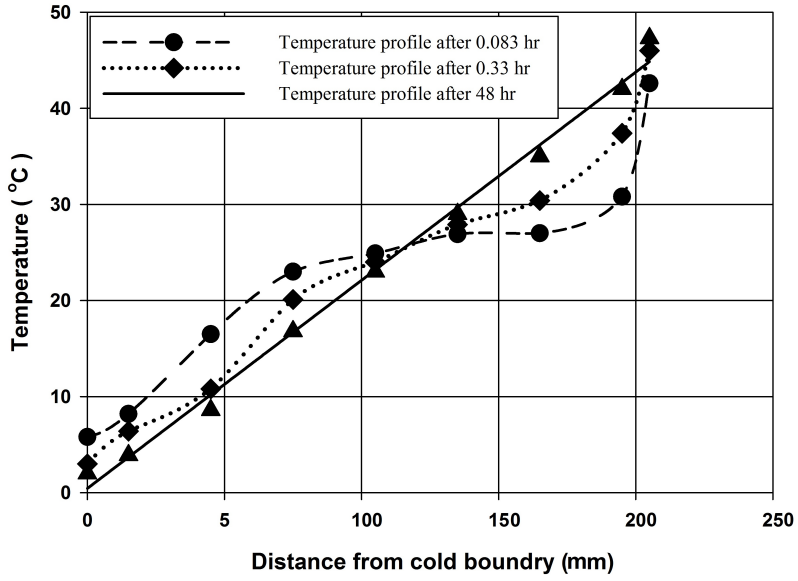

Figure 4.7: Temperature distribution along soil specimen for sample 2

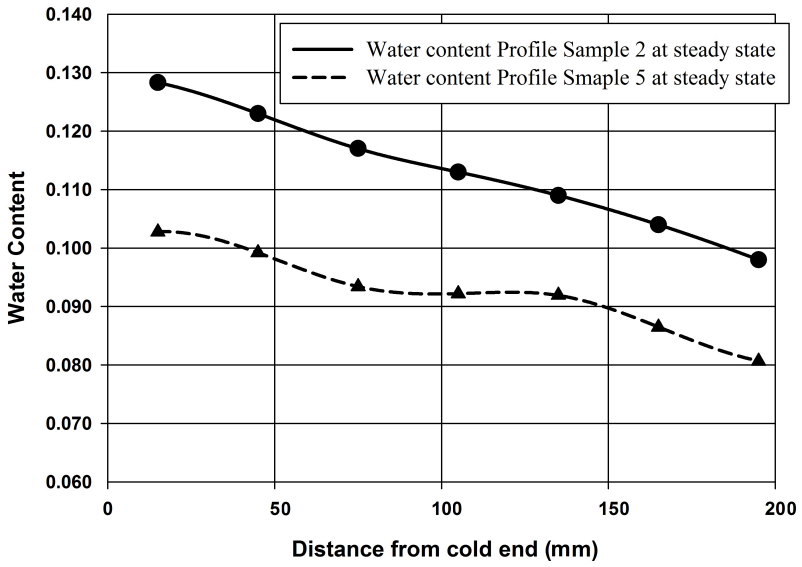

Figure 4.8: Moisture distribution along soil specimen for sample 2 and 5

4.4.2.2 Low initial water content (Residual Zone)

The second series of experiments investigates the moisture profile at steady state for specimens at a lower initial water content. To achieve the same void ratio as in the first series of experiments, the specimen are compacted at the same water content as those of the first series. The specimens are then kept horizontal to eliminate the effect of gravity moisture flow and all temperature port holes are opened to allow water loss through evaporation.

The mass of the specimen is carefully monitored as a function of time to determine the moment when the chosen initial water content is reached. Ten (10) days are required to achieve the target water content given the sample size and the small relative area of the openings which allowed evaporation. After reaching the target water content, the holes are sealed and the specimen is allowed to rest for $48hr$. Figure 4.9 and Figure 4.10 show the measured temperature profile and moisture content profile at steady state of samples 3 and 6.

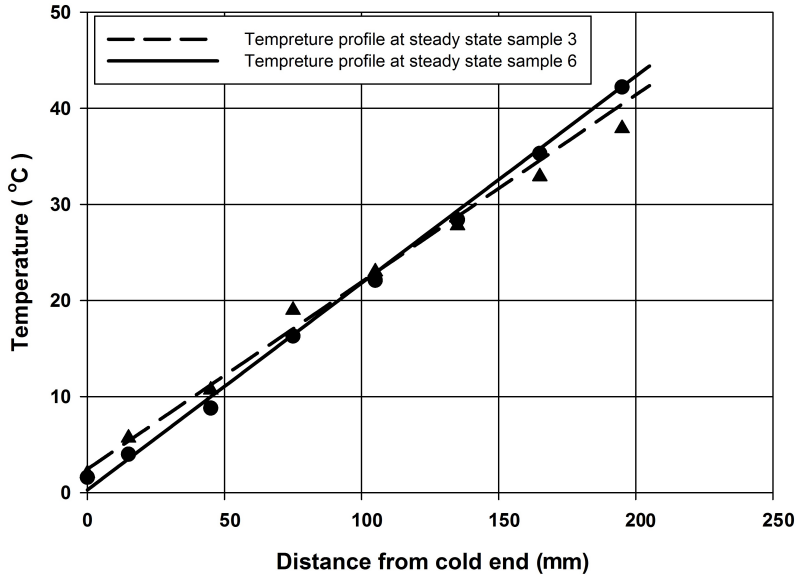

Figure 4.9: Temperature distribution along soil specimen for sample 3 and 6

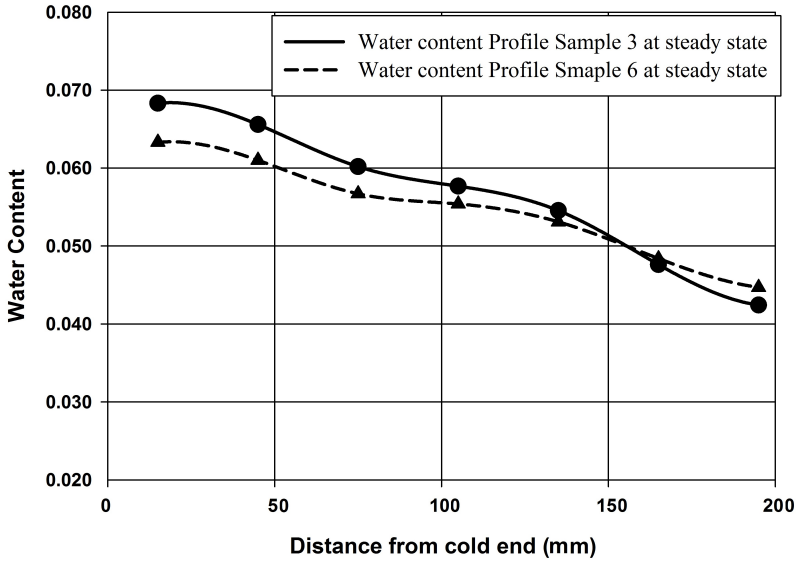

Figure 4.10: Moisture distribution along soil specimen for sample 3 and 6

4.4.2.3 High initial water content (Boundary Effect Zone)

To increase the initial moisture content in the third set of experiments, the specimens, compacted at the same water content as the previous sets, are saturated gradually by allowing water ingress from a tube inserted in the bottom port while the specimen stands upright (Figure 4.11). By maintaining the specimen vertical and allowing water ingress from the bottom the air escapes through the top of the specimen following a continuous air path and avoiding air entrapment. The elevation between the plastic water feeding tube at the midpoint of the lower port and water reservoir was adjusted to $200mm$. A filter paper barrier was used to moderate the water movement and avoid washing out of soil particles during the process. The specimen is allowed to absorb water until near saturation is inferred when water droplets form at the surface. Samples are taken to verify the water content from which, from phase relations, a degree of saturation of 90% was calculated.

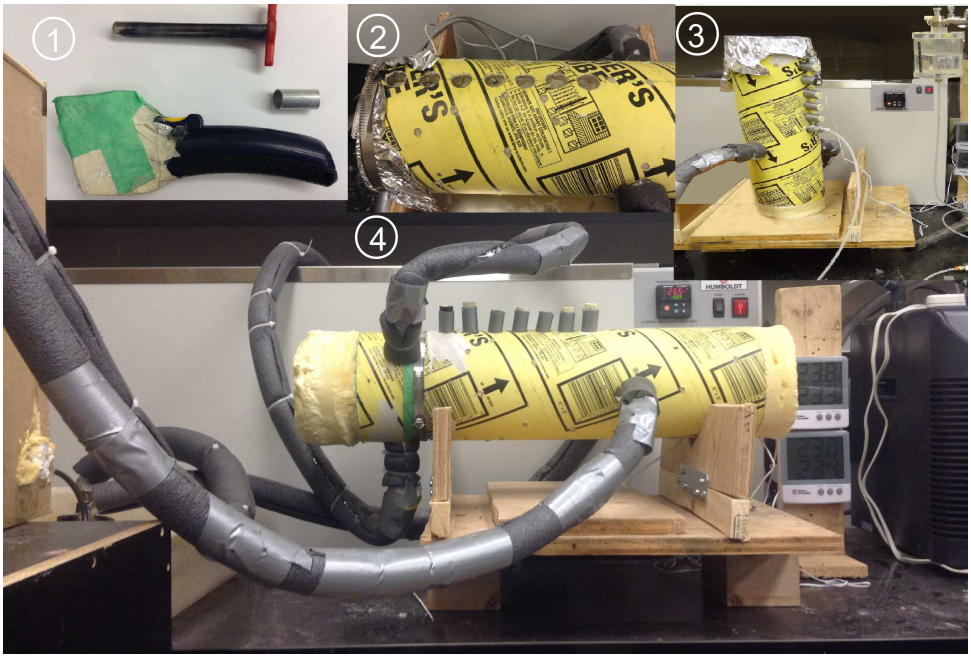

Figure 4.11: Experimental set-up: 1-Infrared thermal emissivity thermometer 2-Evaporation process 3-Saturation process 4-Running Test

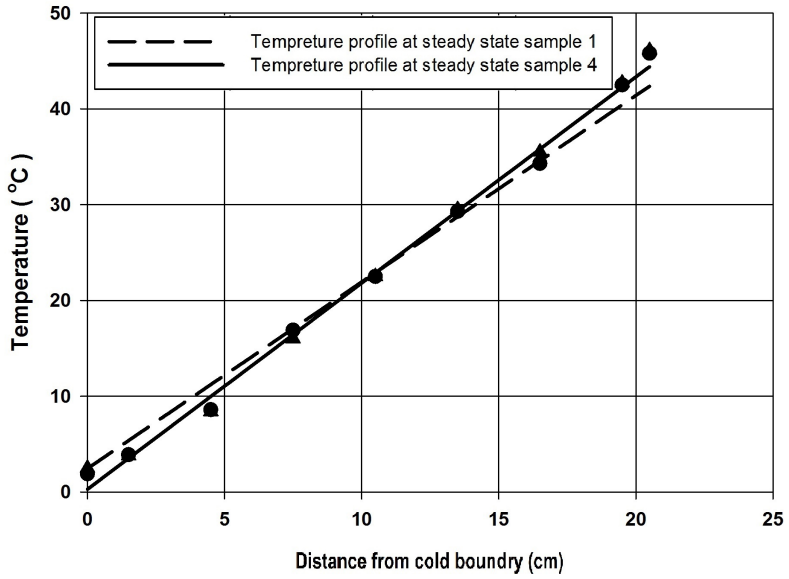

Figure 4.12: Temperature distribution along soil specimen for sample 1 and 4

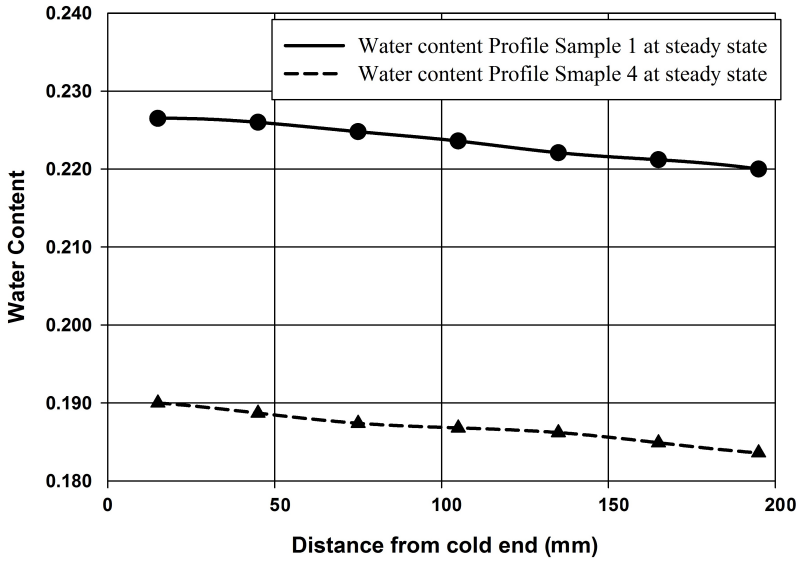

Figure 4.13: Moisture distribution along soil specimen for sample 1 and 4

4.5 Result and Discussion

Under the influence of a thermal gradient, the water in the soil is redistributed and migrates from the hot boundary towards the cold boundary which can be related mostly to changes of capillary potential.

It can be observed that, within the boundary effect zone (sample 1 and 4), where the initial water content is larger, the resulting moisture content difference between the hot and cold boundaries is smaller. However, in the transition zone (sample 2 and 5), where the initial moisture content is intermediate, the moisture content difference between the boundaries is large. In the residual zone (sample 3 and 6), where the initial moisture content is smaller, the moisture content differences between the boundaries at equilibrium is again smaller, however the difference is larger than it is within the boundary effect zone. These trends are in agreement with the studies of Wang and Su (2010) on loess soil, and can be readily explained by the slope of the SWCC which is steeper in the transition zone, and therefore a small shift along the suction axis will produce the largest change in water content.

To examine the optimum location of the initial water content in estimating the m parameter for the most reliable SWCC using the proposed method a sensitivity analysis was performed. Initially, knowledge of moisture and temperature profile at steady state for each zone is used to calculate the $k_{v\psi}$ and k_{vT} profiles which are independent from the suction value (Eq.(4.8 & 4.9)). The suction can then be evaluated along the specimen using an initial value of m selected in the range between 0 and 10 (Fredlund and Xing 1994). To solve the temperature dependent form of the Fredlund and Xing equation a simple program using a combination of bisection, secant, and inverse quadratic interpolation methods (Brent 1973) was written for MATLAB or OCTAVE and used for back-calculating the suction value.

The derivative $\frac{\delta\psi}{\delta x}$ and $\frac{\delta T}{\delta x}$ are then determined from the calculated suction and measured temperature profile using a combination of forward, backward, and central difference approximations (Chapra and Canale 2006). To find how far the desirable m, the error between the vapour velocity and liquid velocity at each point of measurements is then calculated calculated. The estimation error is quantified by calculating the index of agreement d which was originally developed by Willmort et al. 1985 to find differences between the observed and the model simulated results and is given as:

$$d = 1.0 - \frac{\sum_{i=1}^{N}(O_i - P_i)^2}{\sum_{i=1}^{N}(|P_i - O'| + |O_i - O'|)^2} \tag{4.19}$$

where O_i is the individual measured data (vapour velocity), P_i is the individual estimated data (liquid velocity for known m parameter), O' is the mean value of the measured data (vapour velocity) and N is the number of paired measured–simulated values. The value of d varies from 0.0 to 1.0, with higher values showing better agreement of liquid velocity with the vapour velocity. The interpretation of d is closely consistent with the interpretation of R^2 for the range of most values encountered (Legates and McCabe 1999).

Figure 4.14 & Figure 4.15 show the change of d as a function of the m parameter in each sample. From these simulations, it can be seen that the highest coefficient of determination d is obtained as $m = 1.5$ for Unimin silica sand 7030 and $m = 1.6$ for Industrial sand. The close value of the predicted m parameter for these soils implies a parallel slope in the portion of the SWCC within the residual zone. This is consistent with the measured SWCC results (Figure 4.4). The simulation results also suggest that as the initial moisture content moves towards the residual zone, the index of agreement decreases which can be justified by considering the characteristic of the residual zone and the higher error in determining an accurate suction in the residual zone (Fredlund et al. 2011).

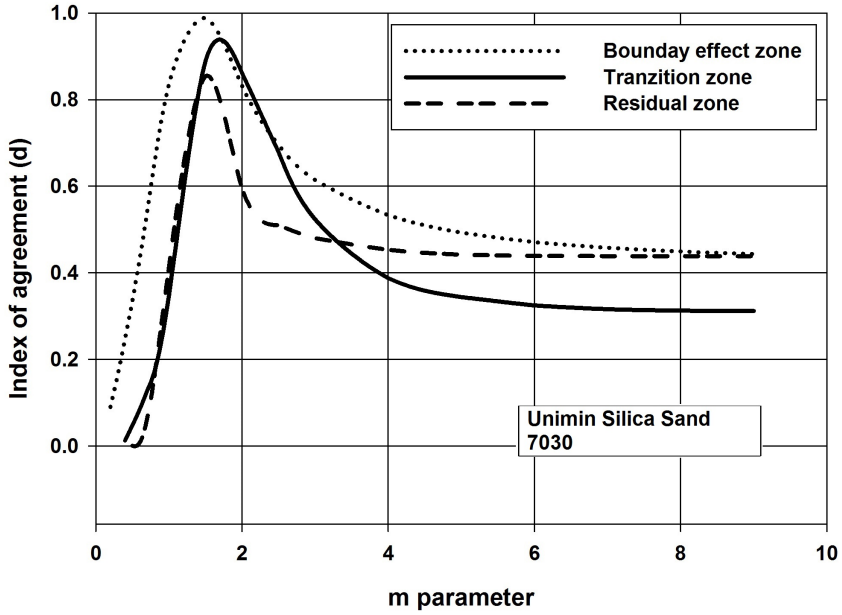

Figure 4.14: Index of agreement as function of m parameter for Unimin Silica Sand 7030

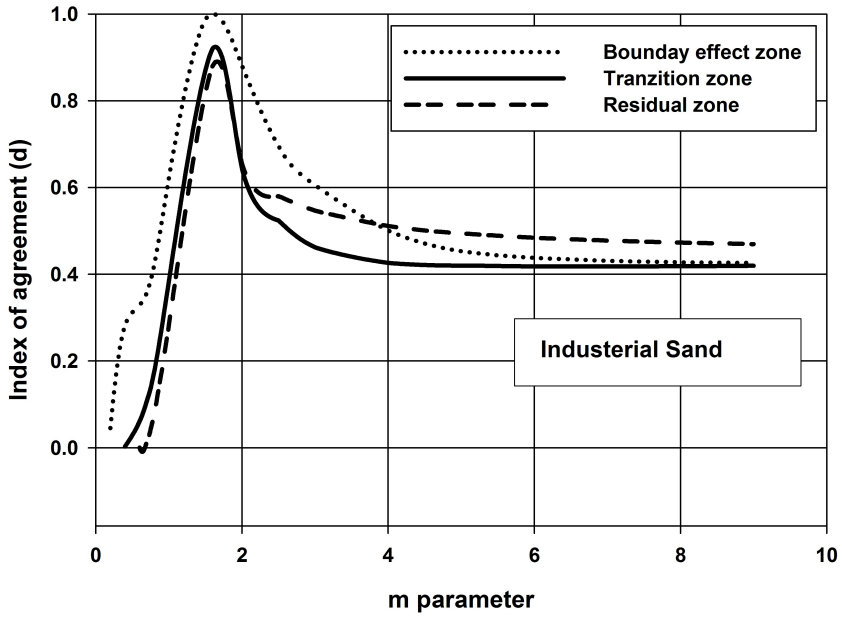

Figure 4.15: Index of agreement as function of m parameter for Industrial Sand

It should be noted that the experimental determination of the moisture content profile with an intermediate initial water content is more practical due to the more obvious moisture migration and larger moisture content differences between the two boundaries of the soil sample. Figure 4.16 presents the calculated suction profile for specimen water contents corresponding to different parts of the SWCC at the optimum m parameter for Unimin silica sand 7030. The behaviour of these curves can be interpreted considering the shape of the SWCC and equilibrium between the matric potential and thermal potential. At the hot boundary, a drop of water content increases the suction, and the rise of moisture content at the cold boundary decreases the suction as would be expected from the effects of temperature on the surface tension of water. An unbalanced suction leads to moisture movement from the colder boundary towards hotter boundary. This movement of liquid water and water vapour becomes balanced when equilibrium is reached (Joshua and Jong 1973).

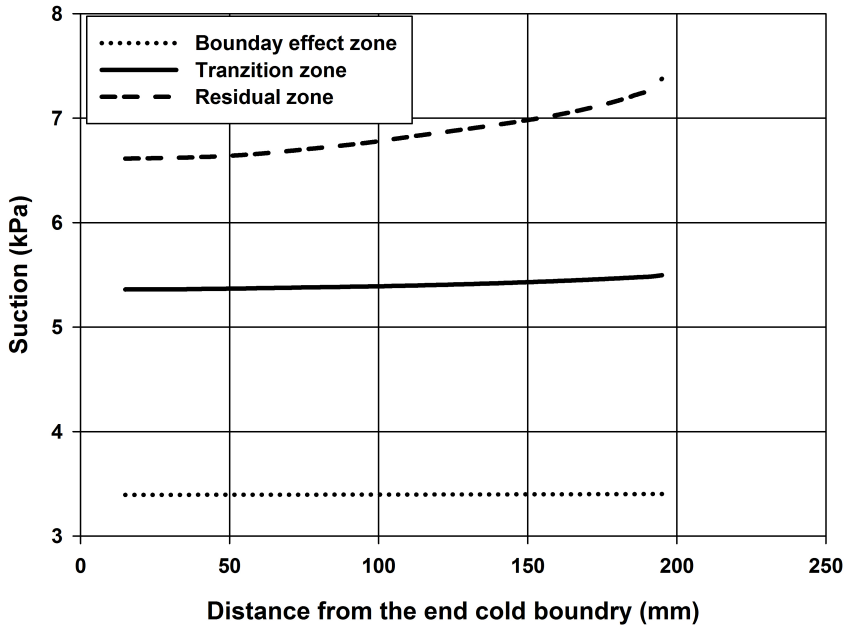

Figure 4.16: Estimated suction profile at steady state at each zone of SWCC for Unimin Silica Sand 7030 for $m = 1.5$

Figure 4.16 presents interesting considerations with respect to the behaviour of unsaturated soils under the effect of a temperature gradient. Indeed, it can be observed that in the boundary effect zone, to a lesser extend in the transition zone, the increase of water content at the cold boundary due to the water migration induced by changes in the SWCC will not result in a significant change in matric suction within the soil profile. This means that while the water content may be reduced at the hot boundary, the increase in suction may not be sufficient, due to the decrease in water content, to result in an increase of the shear strength of the soil at the hot boundary. This is an important consideration as usually a decrease in water content in an unsaturated soil is assumed to correspond to an increase in shear strength. However, when the initial water content in the soil is near the residual zone, there is a much more significant increase in suction near the hot boundary, however at that stage, the degree of saturation being much smaller, the influence of suction on the shear strength is also reduced. Clearly, then, knowledge of the behaviour of unsaturated soils under the influence of a thermal gradient can be important when assessing the behaviour of an unsaturated soil.

Figure 4.17 shows the trend of vapour velocity and liquid velocity for Unimin silica

sand 7030 at the transition zone for the optimum m value ($m = 1.5$). The liquid velocity U_L and the vapour velocity U_v are calculated from following equations (Derek 1997):

$$U_l = k(\theta, T)\frac{\delta\psi}{\delta x} \tag{4.20}$$

$$U_v = k_{v\psi})\frac{\delta\psi}{\delta x} + k_{vT}\frac{\delta T}{\delta x} \tag{4.21}$$

The gradients of ψ and T are calculated using a finite difference approximation from the estimated suction profile shown in Figure 4.16, and the corresponding temperature profile. Considering the numerical approximation used to obtain the gradients and hence the velocity profiles and in view of the small values involved, it can be observed that the vapour velocity values are generally near the liquid velocity and in opposite direction as predicted by De Vries (1958).

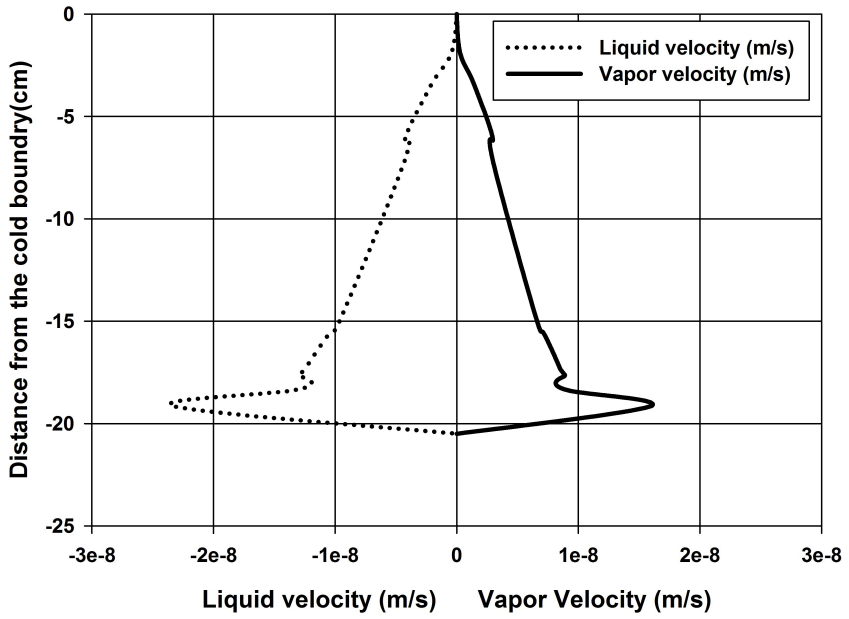

Figure 4.17: Liquid and vapour velocity profiles of Unimin Silica Sand 7030 at $m = 1.5$ for the transition zone at steady-state.

An additional soil from the literature is used to validate the proposed method of estimating the SWCC, namely Leighton Buzzard medium sandy soil which has an initial volumetric liquid content of 0.05 and is subjected to a fixed temperature of 20 °C, and 60 °C at either boundary (Drek 1997). The grain size distribution is shown in Figure 4.18 and the value of a at the reference temperature (20 °C) is estimated at $2.75kPa$, based on Eq.(4.4). The value of the parameter n, is determined as 7.5 based on the Eq.(4.5). The calculated coefficient of uniformity C_u is equal to 1.67 and the porosity of the soil is equal to 0.389.

Table 4.3 summarizes the calculated d and the estimated m parameter for this set of data. It can be seen that at $m = 6$ the highest index of agreement is obtained. Figure 4.19 to Figure 4.21 compare the predicted SWCC of Unimin silica sand 7030, Industrial sand, and Leighton Buzzard medium sand by the proposed approach, as well as the Vanapalli and Catana (2005) method, and the measured data respectively. From these figures it may be concluded that the proposed method has a good potential for predicting SWCC with reasonable accuracy.

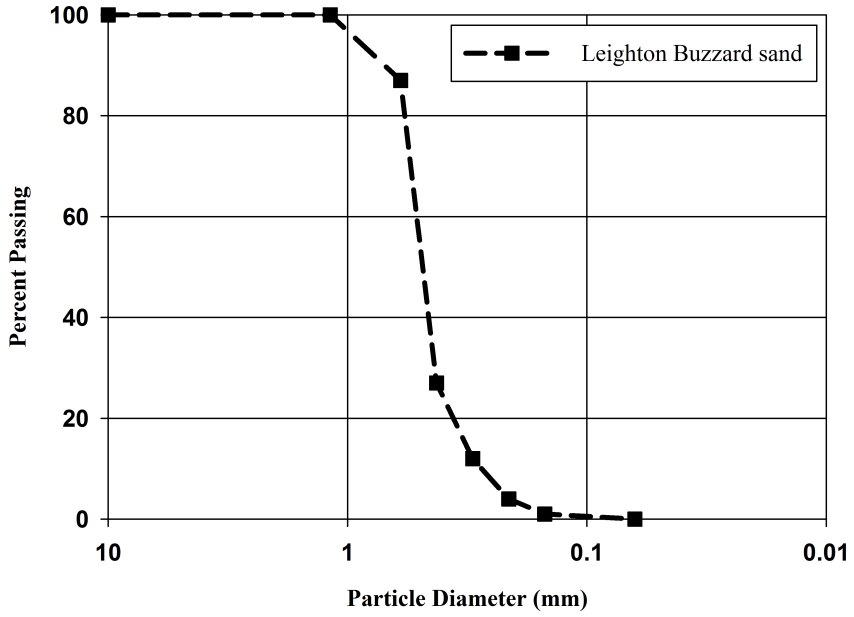

Figure 4.18: Grain size distribution of the Leighton Buzzard medium sandy soil

Table 4.3: Estimated index of agreement d at different m value (Calculation is based on the Data from Derek 1997)

m parameter	d	m parameter	d
2	0.0004	5.5	0.6860
2.5	0.0432	6	0.8628
3	0.0574	6.5	0.7532
3.5	0.0841	7.0	0.6120
4	0.1273	7.5	0.5825
4.5	0.2069	8.0	0.5959
5.0	0.3772	9.0	0.6044

Table 4.4 presents the error in suggested prediction compared with Vanapalli and Catana (2005) approach. In this table, the mean sum squared of the error $MSSE$ is defined by (Johari et al. 2006):

$$MSSE = \frac{1}{N}\sum_{i=1}^{N}(O_i - P_i)^2 \tag{4.22}$$

where O_i is the individual measured points of SWCC, P_i is the individual predicted points of SWCC, and N is the number of paired measured–simulated values. From Table 4.4 it can be concluded that the proposed method is capable of simulating SWCC more accurately and there is a good reliability between the measured data and proposed model.

Table 4.4: Performance of proposed approach and Vanapalli and Catana (2005) method

	Proposed Approach		Vanapalli and Catana (2005)	
Studied soils	d	MSSE	d	MSSE
Unimin Silica Sand 7030	0.99	0.0016	0.98	0.0023
Industrial Sand	0.98	0.0007	0.96	0.0011
Leighton buzzard sand	0.93	0.048	0.90	0.053

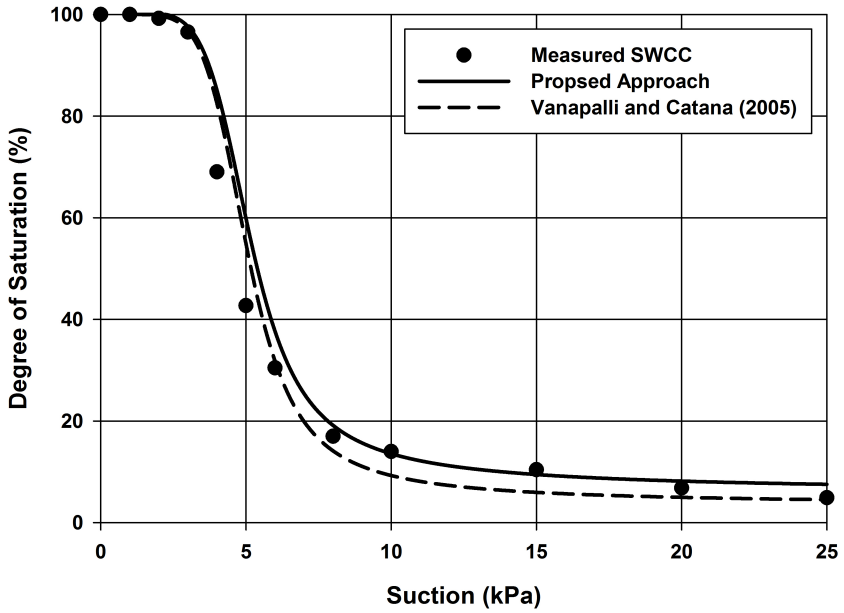

Figure 4.19: SWCC estimation for Unimin Silica Sand 7030

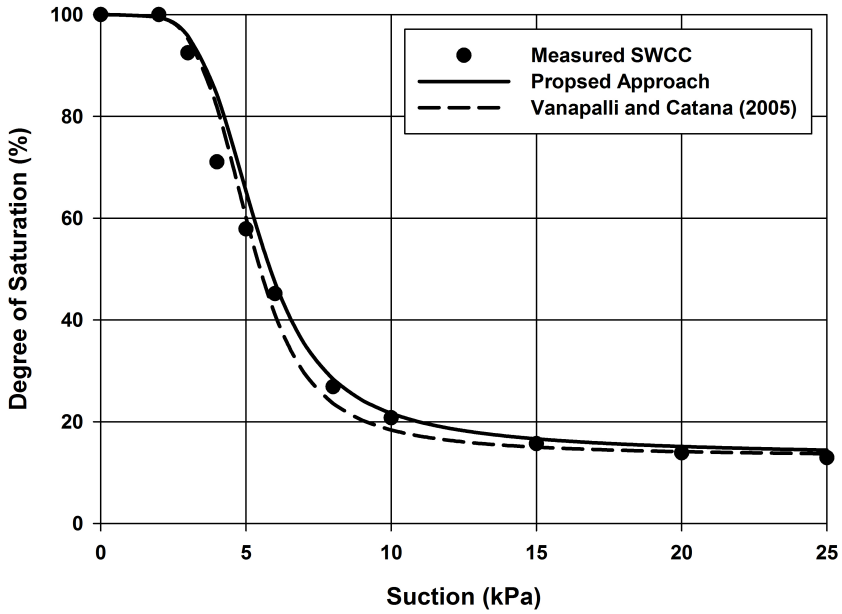

Figure 4.20: SWCC estimation for Industrial Sand

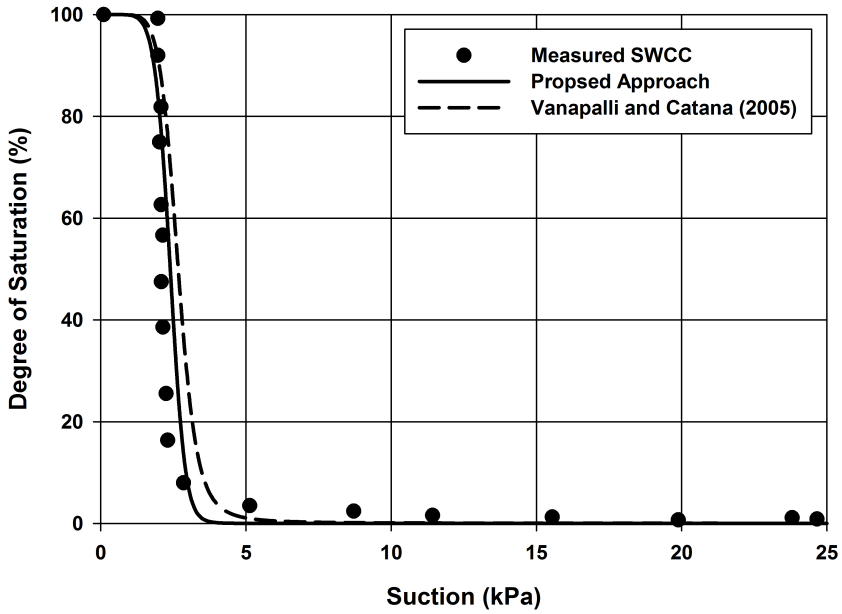

Figure 4.21: SWCC estimation for Leighton Buzzard sand (Data from Drek 1997)

4.6 Summary and Conclusion

The objective of this study was the presentation of a new technique to estimate the SWCC using the moisture content distribution at equilibrium under the influence of a temperature gradient. On the theoretical side, the water potential equation based on Thomas and King's formulation in the liquid and vapour phases for analysing steady flow conditions in unsaturated soils along with the grain size distribution were used to develop the new approach to estimate SWCC.

On the experimental side, tests were carried out on two different coarse-grained soils with different initial moisture contents and the same temperature gradient to validate the proposed approach. The results are consistent with the observed behaviour of unsaturated soils under a thermal gradient where the moisture content of the soil increases at the cold boundary and decreases at the hot boundary. The results also indicate that samples with intermediate initial water content provide a larger moisture content difference between the soil boundaries at equilibrium. Determination of SWCC using the proposed method allowed a good approximation of the SWCC. This implies that the model of the effect of temperature on the SWCC is reliable enough to allow the determination of a realistic moisture profile in an unsaturated soil subjected to a temperature gradient, which in turn allows the effect of temperature on the SWCC to be incorporated in numerical methods making use of the properties of unsaturated soils under variable temperature conditions.

Chapter 5

SUMMARY AND CONCLUSION

5.1 Introduction

The description and mathematical simulation of water movement through unsaturated soils requires knowledge of the SWCC function. However, laboratory determination of SWCC is cumbersome, costly, and needs intricate equipment. The move towards predicting the SWCC from other readily determined soil properties has therefore seen an increased adoption during the last decade. However, the effect of some environmental factors, such as the role of temperature, have still seen only limited research. The proposed research therefore had a two main objectives:

(i) To develop a method based on first principles to estimate the effect of temperature on the SWCC

(ii) To develop a method to estimate the SWCC of a coarse-grained soil when only the grain-size distribution, void ratio and moisture profile under a constant thermal gradient are available

The summary and conclusions from the studies undertaken in this thesis are summarized in the following sections.

5.2 Effect of temperature on SWCC behaviour

(i) A method has been proposed to interpret the influence of temperature on the SWCC. The method relies on capillary theory which has been used to relate void

space between particles to their ability to retain water. The relationships are developed between the fitting parameters of Fredlund and Xing (1994) equation and the temperature variable. A simple equation is proposed based on effect of temperature on air entry value (AEV) for estimating the SWCC at different temperatures with adequate degree of reliability and confidence.

(ii) An experimental program has been undertaken on two sandy soils to validate the proposed model. The experimental program used the axis translation technique to determine the SWCC of the two soils at 3 temperatures, namely $4°C$, $20°C$, and $49°C$.

(iii) Comparison of the results from the proposed method with the experimental results as well as data from the literature on fine grained soil indicate that the proposed method can successfully predict the changes of the SWCC under different temperatures.

(iv) The results of this study are consistent with the observed behavior of unsaturated soils under a thermal gradient where the degree of saturation of the soil increases at the cold boundary and decreases at the hot boundary. The measured SWCCs of each soil show that at different temperatures their SWCC retain a similar slope in the the transition zone and can be considered as offset along the suction axis relative to each other.

5.3 Estimation of SWCC of coarse-grained soils using grain size distribution and soil water profile in response to fixed temperature gradient

(i) A rational approach was proposed to estimate the SWCC of coarse-grained soils using the grain size distribution, void ratio, and the moisture profile in a soil specimen under a fixed temperature gradient. A proposed model highlighted that the water potential equation in the liquid and vapor phases can be used for analysing steady flow conditions in unsaturated soil and therefore estimating SWCC.

(ii) An experimental program was undertaken on two different sands subjected to a temperature gradient, to obtain a moisture profile at steady state. Three different initial water contents were considered such that the experiment was conducted

within the boundary effect zone (tension saturated), the transition zone, and the residual zone.

(iii) The results of the study have confirmed that there is an obvious change in the moisture content distribution of soil sample after a temperature differences is exerted on the boundaries of the sample, with the water content increasing at the cold boundary, and decreasing at the hot boundary.

(iv) The water vapour transfer contribute to an increased in suction value at the hot boundary, and a lowered suction at the cold boundary, however these changes are as large as the change in water content would make it appear. This is due to the changes that are also affecting the SWCC under the different temperatures.

(v) The comparison between the measured SWCC and estimated SWCC using the suggested approach indicated that the SWCC of coarse grained soils can be reliably estimated using one measured moisture profile under temperature gradient and simple soil properties.

5.4 Recommendations and suggestions for future studies

The recommendations and suggestion offered for future research studies are summarized in this section.

(i) The proposed techniques and models in the present thesis are developed based on limited experimental results of two coarse-grained soils. In order to develop a comprehensive techniques and models, more studies for different types of soils are necessary. For instance, performing the SWCC determination on wide range of soils including fine-grained soils would be of interest for future research.

(ii) The current study has proposed an approach to estimate the SWCC of coarse-grained soils based on migration of water under a fixed temperature gradient. However, the moisture content profile at equilibrium may be influenced by different scenario such as different boundary temperature or void ratio or different length of sample. These parameters can be investigated in additional experiments.

(iii) The estimation of the SWCC based on the moisture profile was established only on coarse-grained soils. Using more types of soils tested to include silts and clays would be most useful.

(iv) The focus of the current research was directed towards interpreting and indirectly predicting the SWCC of an unsaturated soils using temperature gradient. This approach might be generalized to indirectly estimate the other soil properties such as hydraulic conductivity or shear strength which may be affected by the SWCC.

REFERENCES

[1] Airò Farulla, C.,and Ferrari, A. 2005. *Controlled suction oedometric tests: analysis of some experimental aspects*. Advanced Experimental Unsaturated Soil Mechanics. Taylor & Francis Group, London, 43-48.

[2] Aitchison, G. D. 1965. *Soil properties, shear strength, and consolidation*. Proc. of the 6th Int. Conf. On Soil Mechanics and Foundation Engineering, 3:318-321.

[3] Al-Mukhtar, M., Belanteur, N., Tessier, D. and Vanapalli, SK.1996. *The fabric of a clay soil under controlled mechanical and hydraulic stress states*. Applied clay Science, 11:99-115.

[4] Alonso EE, Gens A. and Hight, DW. 1987. *Special problem soils. General report. In: Proc. 9th European conf. on soil mechanics and foundation engineering*. Dublin, 3:1087–1146.

[5] Anderson, M. A., Hung, A. Y., Mills, D. and Scott, M. S. 1995. *Factors affecting the surface tension of soil solutions and solutions of humic acids*. Soil science, 160(2):111-116.

[6] ASTM D5084. 2010. *Standard test methods for measurement of hydraulic conductivity of saturated porous materials using a flexible wall permeameter. ASTM standard D5084*. American Society for Testing and Materials (ASTM), West Conshohocken, Pa.

[7] ASTM D-6836. 2002.*Standard test methods for determination of the soil water characteristic curve for desorption using a hanging column, pressure extractor, chilled mirror hygrometer, and/or centrifuge*. ASTM standard D 6836. American Society for Testing and Materials (ASTM), West Conshohocken, Pa.

[8] Aubertin, M., Ricard, J. F. and Chapuis, R. P. 1998.*A predictive model for the water retention curve: application to tailings from hard-rock mines*. Canadian Geotechnical Journal, 35:55–69.

[9] Bach, L. B. 1992. *Soil water movement in response to temperature gradients: Experimental measurements and model evaluation*. Soil Science Society of America Journal, 56(1):37-46.

[10] Bachmann, J., and van der Ploeg, R. R. 2002. *A review on recent developments in soil water retention theory: interfacial tension and temperature effects*. Journal of Plant Nutrition and Soil Science, 165(4):468.

[11] Bachmann, J., Horton, R., Grant, S. A. and Van der Ploeg, R. R. 2002. *Temperature dependence of water retention curves for wettable and water-repellent soils*. Soil Science Society of America Journal, 66(1):44-52.

[12] Barbour, S. L. 1998. *Nineteenth Canadian Geotechnical Colloquium: The soil-water characteristic curve: a historical perspective*. Canadian Geotechnical Journal, 35:873-894

[13] Barden, L. and Pavlakis, G. 1971. *Air and water permeability of compacted unsaturated cohesive soil*. Journal of Soil Science, 22:302–318.

[14] Bishop, A. W. 1959. *The principle of effective stress*. Teknisk Ukeblad, 39:859-863.

[15] Bishop, A. W. and Donald, I.B. 1961. *The experimental study of partly saturated soil in triaxial apparatus*. In Proceedings of the Fifth International Conference on Soil

[16] Bocking, A. K., and Fredlund, D.G. 1980. *Limitations of the axis translation technique*. In Proceedings of the 4th international conference expansive soils, Denver, 117–135.

[17] Brent, R. 1973. *Algorithms for minimization without derivatives*. Prentice-Hall, Englewood Cliffs, New Jersey, USA.

[18] Brooks, R., and Corey, A. 1964. *Hydraulic Properties of Porous Media*. Hydrology Paper No. 3, Colorado State University, Fort Collins, CO., U.S.A.

[19] Brown, R. W. 1970. *Measurement of water potential with thermocouple psychrometers: construction and applications. Research Papers*. Intermountain Forest and Range Experiment Station, (INT-80).

[20] Brutsaert, W. 1966. *Probability laws for pore-sized distribution*. Soil Science, 101(2):85-91.

[21] Buckingham, E. 1907. *Studies on the movement of soil moisture*. U.S. Department of Agriculture Bureau of Soils, Bulletin 38.

[22] Bulut, R., Lytton, R. L., and Wray, W. K. 2001. *Soil suction measurements by filter paper*. In Proceedings of Geotechnical Special Publication Expansive Clay Soils and Vegetative Influence on Shallow Foundation, ASCE, 115:243-261.

[23] Burdine, N. T. 1953. *Relative permeability calculations from pore size distribution data*. Journal of Petroleum Technology, 5(3):71-78.

[24] Burland, J. B. 1964. *Effective stresses in partly saturated soils*. Géotechnique, 14:65-68.

[25] Campbell, G. S., and Gardner, W. H. 1971. *Psychrometric measurement of soil water potential: temperature and bulk density effects*. Soil Science Society of America Journal, 35(1):8-12.

[26] Cassel, D. K., Nielsen, D. R., and Biggar, J. W. 1969. *Soil-water movement in response to imposed temperature gradients*. Soil Science Society of America Journal, 33(4):493-500.

[27] Chahal, R. S. 1965. *Effect to temperature and trapped air on matric suction*. Soil Science, 100(4):262-266.

[28] Chapra, S. C. and Canale, R. P. 2006. *Numerical Methods for Engineers*. 5th Edition, McGraw-Hill, Inc. New York. USA.

[29] Chen, Y., and Schnitzer, M. 1978. *The surface tension of aqueous solutions of soil humic substances*. Soil Science, 125(1):7-15.

[30] Chin, K. B., Leong, E. C., and Rahardjo, H. 2010. *A simplified method to estimate the soil-water characteristic curve*. Canadian Geotechnical Journal, 47(12):1382-1400.

[31] Constantz, J. 1991. *Comparison of isothermal and isobaric water retention paths in nonswelling porous materials*. Water Resources Research, 27(12):3165-3170.

[32] Côté, J. and Konrad, J. M. 2003.*Assessment of the hydraulic characteristics of unsaturated base-course materials: a practical method for pavement engineers*. Canadian Geotechnical Journal, 40(1):121-136.

[33] Croney, D., and Coleman, J.D. 1961. *Pore pressure and suction in soils*. In Proceedings of the Conference on Pore Pressure and Suction in Soils, Butterworths, London, UK, 31-37.

[34] Dakshanamurthy, V. and Fredlund, D. G. 1981. *A mathematical model for predicting moisture flow in an unsaturated soil under hydraulic and temperature gradients*. Water Resources Research, 17(3):714-722.

[35] Dallas, N. L., Syam, N. 2009. *Recommended practice for stabilization of subgrade soils and base materials*. Texas Contractor's Final Task Report for NCHRP Project, Texas Transportation Institute, Texas A& M University, College Station, U.S.A.

[36] Davies, J.T. and Rideal, E.K. 1963. *Interfacial Phenomena*. 2nd ed., New York: Academic Press.

[37] De Vries, D. A. 1987. *The theory of heat and moisture transfer in porous media revisted*. International Journal of Heat and Mass Transfer. 30(7):1343-1350.

[38] Delage, P., Howat, M. D. and Cui, Y. J. 1998. *The relationship between suction and swelling properties in a heavily compacted unsaturated clay*. Engineering Geology Journal, 50(1):31-48.

[39] Derek M. Li. 1997. *Numerical of pressure based coupled heat and moisture flow in unsaturated porous media using the integrated finite difference method*. M.A.Sc. thesis, University of Toronto, Toronto, Canada, 166p.

[40] Duncan, J. M., Wright, G. 2005. *Soil Strength and Slope Stability*. John Wiley & Sons, Hoboken, New Jersey, USA.

[41] Edlefsen, N. E. and Anderson, A. B. 1943. *Thermodynamics of soil moisture*. Hilgardia, 15:30-298.

[42] Estabragh, A.R., Javadi, A.A., and Boot, J.C. 2004. *The effect of compaction pressure on consolidation behavior of unsaturated silty soils*. Canadian Geotechnical Journal, 41:540-550.

[43] Evgin, E. and Svec, O.J. 1988. *Heat and moisture transfer characteristic of compacted Mackenzie silt*. Geotechnical Testing Journal, 11:92-99.

[44] Ewen, J., and Thomas, H. R. 1989. *Heating unsaturated medium sand*. Géotechnique 39(3):455-470.

[45] Fleureau, J. M., Verbrugge, J. C., Huergo, P. J., Correia, A. G. and Kheirbek-Saoud, S. 2002. *Aspects of the behaviour of compacted clayey soils on drying and wetting paths*. Canadian Geotechnical Journal, 39(6):1341-1357.

[46] Fredlund, D. G. 2000. *The 1999 RM Hardy Lecture: The implementation of unsaturated soil mechanics into geotechnical engineering*. Canadian Geotechnical Journal, 37(5):963-986.

[47] Fredlund, D. G. 2004. *Use of soil–water characteristic curves in the implementation of unsaturated soil mechanics*. In Proceedings of the Third international Conference on Unsaturated soils, Recife, Brazil 3:887-902.

[48] Fredlund, D. G. and Hasan, J. U. 1979. *One-dimensional consolidation theory: unsaturated soils*. Canadian Geotechnical Journal, 16(3):521-531.

[49] Fredlund, D. G. and Morgenstern, N. R. 1977. *Stress state variables for unsaturated soils*. Journal of the Geotechnical Engineering Division, ASCE, 103(GT5):447-466.

[50] Fredlund, D. G., Morgenstern, N. R. and Widger, R. A. 1978. *The shear strength of unsaturated soils*. Canadian Geotechnical Journal, 15(3):313-321.

[51] Fredlund, D.G., and Rahardjo, H. 1993. *Soil Mechanics for Unsaturated Soils*. John-Wiley and Sons, New York, 486p.

[52] Fredlund, D. G., Rahardjo, H., Fredlund, M. D., 2012. *Unsaturated soil mechanics in engineering practice.* Technology & Engineering, Published in Canada.

[53] Fredlund, D. G., and Xing, A. 1994. *Equations for the soil-water characteristic curve*. Canadian Geotechnical Journal, 31(4): 521-532.

[54] Fredlund, D. G., Sheng, D., and Zhao, J. 2011. *Estimation of soil suction from the soil-water characteristic curve*. Canadian Geotechnical Journal, 48(2):186-198.

[55] Fredlund, M. D., Fredlund, D. G., and Wilson, G. W. 1997. *Prediction of the soil-water characteristic curve from grain-size distribution and volume-mass properties*. In Proceedings of Third Brazilian Symposium on Unsaturated Soils , Rio de Janeiro, Brazil, 13-23.

[56] Fredlund, M. D., Wilson, G. W., and Fredlund, D. G. 2002. *Use of the grain-size distribution for estimation of the soil-water characteristic curve*. Canadian Geotechnical Journal, 39(5): 1103-1117.

[57] Gardner, R. 1955. *Relation of temperature to moisture tension of soil*. Soil Science, 79(4):257-266.

[58] Gardner, W. R. and F. J. Miklich. 1962. *Unsaturated conductivity and diffusivity measurements by a constant flux method*. Soil Sci., 93:271–274.

[59] Gerscovich, D. M. S., and Sayão, A. S. F. J. 2002. *Evaluation of the soil-water characteristic curve quations for soils from Brazil*. In Proceedings of Third International Conference on Unsaturated Soils, 295-300.

[60] Gitirana Jr. and G.F.N. 2005. *Weather-related geo-hazard assessment model for railway embankment stability*. Ph.D. Thesis. University of Saskatchewan, Saskatoon, SK, Canada, 411p.

[61] Grant, S. A. and Bachmann, J. 2002. *Effect of temperature on capillary pressure*. Environmental Mechanics: Water, Mass and Energy Transfer in the Biosphere. The Philip Volume, 199-212.

[62] Grant, S. A. and Salehzadeh, A. 1996. *Calculation of temperature effects on wetting coefficients of porous solids and their capillary pressure functions*. Water Resources Research, 32(2):261-270.

[63] Grifoll, J., Gastó, J. M., and Cohen, Y. 2005. *Non-isothermal soil water transport and evaporation*. Advances in Water Resources, 28(11):1254-1266.

[64] Gupta, S. and Larson, W. E. 1979. *Estimating soil water retention characteristics from particle size distribution, organic matter percent, and bulk density*. Water Resources Research, 15(6):1633-1635.

[65] Haridasan, M. and Jensen, R. D. 1972. *Effect of temperature on pressure head-water content relationship and conductivity of two soils*. Soil Science Society of America Journal, 36(5):703-708.

[66] Haverkamp, R. T., and Parlange, J. Y. 1986. *Predicting the water-retention curve from particle-size distribution: 1. Sandy Soils Without Organic Matter1*. Soil Science, 142(6):325-339.

[67] Hilf, JW. 1956. *An investigation of pore-water pressure in compacted cohesive soils*. PhD Thesis. Technical Memorandum No. 654. United State Department of the Interior Bureau of Reclamation, Design and Construction Division, Denver, Colorado, USA

[68] Ho, D. Y. F., Fredlund, D. G., and Rahardjo, H. 1992. *Volume change indices during loading and unloading of an unsaturated soil*. Canadian Geotechnical Journal, 29(2):195-207.

[69] Hopmans, J. W. and Dane, J. H. 1986a. *Temperature dependence of soil hydraulic properties*. Soil Science Society of America Journal, 50(1):4-9.

[70] Hopmans, J. W. and Dane, J. H. 1986b. *Temperature dependence of soil water retention curves*. Soil Science Society of America Journal, 50(3):562-567.

[71] Houston, S. L., Houston, W. N., and Wagner, A. M. 1994. *Laboratory Filter Paper Measurements*. Geotechnical Testing Journal, 17(2):185-194.

[72] Houston, W.N., Dye, H.B., Zapata, C.E., Perera, Y.Y., and Harraz, A. 2006. *Determination of SWCC using one point measurement and standard curves*. In Proceedings of the 4th International Conference on Unsaturated Soils, Carefree, Ariz., 2–6 April 2006. Geotechnical Special Publication No. 147. Edited by G.A. Miller, C.E. Zapata, S.L. Houston, and D.G. Fredlund. American Society of Civil Engineers, Reston, 2:1482–1493.

[73] Hoyos, L. R., Thudi, H. R., and Puppala, A. J. 2007. *Soil-water retention properties of cement treated clay*. In Proceedings of Sessions of Geo-Denver, 4-11.

[74] Hussain, S. 1997. *Validation of coupled heat and moisture flow program in unsaturated porous media*. M.A.Sc. thesis , University of Toronto, Toronto, Canada, 91p.

[75] Infante Sedano, J. A. 2006. *A modified ring shear test device for determining the hydro-mechanical behavior of unsaturated soils*. PhD thesis. University of Ottawa, Ottawa, Canada.

[76] Infante Sedano, J. A., Vanapalli, S. K., and Garga, V. K. 2007. *A simple air pressure gauge for unsaturated soils*. Canadian Geotechnical Journal, 44(8):1013–1018.

[77] Infante Sedano, J. A., Vanapalli, S. K., and Garga, V. K. 2007a. *Modified ring shear apparatus for unsaturated soils testing*. ASTM Geotechnical Testing Journal, 30(1):39-47.

[78] Jacinto, A. C., Villar, M. V., Gómez-Espina, R., and Ledesma, A. 2009. *Adaptation of the van Genuchten expression to the effects of temperature and density for compacted bentonites*. Applied Clay Science, 42(3):575-582.

[79] Jennings, J. E. B. and Burland, J. B. 1962. *Limitations to the use of effective stresses in partly saturated soils*. Géotechnique, 12(2):125-144.

[80] Johari, A., Habibagahi, G. and Ghahramani, A. 2006. *Prediction of soil–water characteristic curve using genetic programming*. Journal of Geotechnical and Geoenvironmental Engineering, 132(5):61-665.

[81] Joshua, W. D., and Jong, E. D. 1973. *Soil moisture movement under temperature gradients*. Canadian Journal of Soil Science, 53(1):49-57.

[82] Kanno, T., Kato, K., and Yamagata, J. 1996. *Moisture movement under a temperature gradient in highly compacted bentonite*. Engineering geology, 41(1):287-300.

[83] Keshky, M.E. 2011. *Temperature effect on the soil water retention characteristic*. Master of Science Thesis, Presented in Partial Fulfillment, Arizona State University, Arizona, U.S.A.

[84] King, F.H. 1892. *Observations and experiments on the fluctuations in the level and rate of movement of ground water on the Wisconsin Agricultural experiment station farm, and at Whitewater*. Wisconsin. U.S. Weather Bureau Bulletin 5, 67-69.

[85] King, P. M. 1981. *Comparison of methods for measuring severity of water repellence of sandy soils and assessment of some factors that affect its measurement*. Soil Research, 19(3):275-285.

[86] Koorevaar, P., Meaelilt, G., and Dirksen, C. 1983. *Element of soil physics*. Elsevier publishers B.V.(North-Holland), Amsterdam, The Netherlands.

[87] Legates, D. R., and McCabe, G. J. 1999. *Evaluating the use of "goodness-of-fit" measures in hydrologic and hydroclimatic model validation*. Water Resources Research, 35(1):233-241.

[88] Leong, E. C. and Rahardjo, H. 1997. *Review of soil-water characteristic curve equations*. Journal of Geotechnical and Geoenvironmental Engineering, 123(12):1106-1117.

[89] Likos, W. J. and Lu, N. 2002. *Filter paper technique for measuring total soil suction*. Transportation Research Record: Journal of the Transportation Research Board, 1786(1):120-128.

[90] Liu, H. H., Bodvarsson, G. S., and Dane, J. H. 2006. *Temperature dependence of large-scale water-retention curves: a case study*. Hydrogeology Journal, 14(8):1403-1408.

[91] Lu, N. and Likos, W. J. 2004. *Unsaturated soil mechanics*. J. Wiley Pub.

[92] Malaya, C., and Sreedeep, S. 2011. *Critical review on the parameters influencing soil-water characteristic curve*. Journal of Irrigation and Drainage Engineering, 138(1):55-62.

[93] Marinho, F. A. M., Take, W. A., and Tarantino, A. 2008. *Measurement of matric suction using tensiometric and axis translation techniques*. Geotechnical and Geological Engineering, 26(6):615-631.

[94] Marshall, T. J. 1958. *A relation between permeability and size distribution of pores*. Journal of Soil Science, 9(1):1-8.

[95] McKee, C. R. and Bumb, A. C. 1987. *Flow-testing coalbed methane production wells in the presence of water and gas*. SPE formation Evaluation, 2(4):599-608.

[96] McQueen, I. S., and Miller, R. F. 1974. *Approximating soil moisture characteristics from limited data: Empirical evidence and tentative model*. Water Resources Research, 10(3):521-527.

[97] Miller, C.J., Yesiller, N., Yaldo, K., Merayyand, S. 2002. *Impact of soil type and compaction conditions on soil water characteristic*. Journal of Geotechnical and Geoenvironmental Engineering, ASCE, 128:733-742.

[98] Milly, P. C. D. 1982. *Moistue and heat transport in hysteresis, inhomogeneous porous media: A matric head- based formulation and numerical model*. Water Resources Research, 18(3):489-498.

[99] Mohamed, A. M. O., R. N. Yong, and B. Kjartanson.1992. *Temperature and moisture distributions in a clay buffer material due to thermal gradients*. MRS proceedings, Cambridge University Press, 294.

[100] Mualem, Y. 1976. *A new model for predicting the hydraulic conductivity of unsaturated porous media*. Water resources research, 12(3):513-522.

[101] Narasirmhan, T. N. 1975. *An unified numerical model for saturated-unsaturated ground water flow*. Ph. D. Dissertation, University of California, Berkeley, California, U. S .A.

[102] Ng, C.W.W. and Pang, Y.W. 2000. *Influence of stress state on soil-water characteristics and slope stability*. Journal of Geotechnical and Geoenvironmental Engineering, 126 (2):157–166.

[103] Nimmo, J. R. and Miller, E. E. 1986. *The temperature dependence of isothermal moisture vs. potential characteristics of soils*. Soil Science Society of America Journal, 50(5):1105-1113.

[104] Peck, A. J. 1960. *Change of moisture tension with temperature and air pressure: Theoretical*. Soil Science, 89(6):303-310.

[105] Pei-yong, L. and Qing, Y. 2009. *Test study on soil-water characteristic curve of bentonite-sand mixtures*. Electron Journal of Geotechnical Engineering, 14:1-8.

[106] Perera, Y. Y., Zapata, C. E., Houston, W. N. and Houston, S. L. 2005. *Prediction of the soil-water characteristic curve based on grain-size-distribution and index properties*. Advances in pavement engineering (ed. EM Rathje), Geotechnical Special Publication, 130:49-60.

[107] Philip, J. R. and De Vries, D. A. 1957. *Moisture movement in porous materials under temperature gradients*. Transactions, American Geophysical Union, 38:222-232.

[108] Puppala, A.J., Konnamas, P. and Vanapalli, S.K. 2006. *Soil-water characteristic curves of stabilized expansive soils*. Journal of Geotechnical and Geo environmental Engineering, 132(6):736-751.

[109] Rahardjo, H., Lim, T.T., Chang, M.F. and Fredlund, D.G. 1995. *Shear strength characteristics of a residual soil*. Canadian Geotechnical Journal, 32:60-77.

[110] Richards, L. A. 1931. *Capillary conduction of liquids through porous mediums*.Physics, 1(5):318-333.

[111] Richards, S. J. 1965. *Soil suction measurements with tensiometers. Methods of soil analysis Part 1: Physical and Mineralogical properties, Including Statistics of measurement and Sampling*. 153-163.

[112] Romero, E. 2001. *Controlled-suction techniques*. In Proceedings of forth Simposio Brasilerio de Solos Nao Saturadoes, ABMS, Porto Alege, 533-542.

[113] Roshani, P, and Infante Sedano, J. A. 2013. *Using grain size distribution and moisture profile under non-isothermal conditions to determine the SWCC of coarse grained size soils*. In proceedings of the Geo Montreal Conference, Montreal, Qc, Canada.

[114] Salager, S., Jamin, F., El Youssoufi, M. S., and Saix, C. 2006. *Influence de la température sur la courbe de rétention d'eau de milieux poreux*. Comptes Rendus Mécanique, 334(6):393-398.

[115] Salager, S., Rizzi, M. and Laloui, L. 2011. *An innovative device for determining the soil water retention curve under high suction at different temperatures*. Acta Geotechnica, 6(3):135-142.

[116] Schnitzer, M., and Desjardins, J. G. 1969. *Chemical characteristics of a natural soil leachate from a humic podzol*. Canadian Journal of Soil Science, 49(1):151-158.

[117] She, H. Y., and Sleep, B. E. 1998. *The effect of temperature on capillary pressure saturation relationships for air water and perchloroethylene water systems*. Water Resources Research, 34(10):2587-2597.

[118] Sillers, W. S., Fredlund, D. G., and Zakerzadeh, N. 2001. *Mathematical attributes of some soil water characteristic curve models*. In Proceedings of Unsaturated Soil Concepts and Their Application in Geotechnical Practice Conference, Springer Netherlands, 243-283.

[119] Singleton, W.S. 1960. *Solution porperties*. Wiley Interscience, 609–682, NY, U.S.A.

[120] Spanner, D. C. 1951. *The Peltier effect and its use in the measurement of suction pressure*. Journal of Experimental Botany, 2(5):145-168.

[121] Stormont, J. C., and Anderson, C. E. 1999. *Capillary barrier effect from underlying coarser soil layer*. Journal of Geotechnical and Geoenvironmental Engineering, 125(8):641-648.

[122] Sutor, J. 1969. *Soil moisture distribution function in non-isothermic conditions.*Water In The Unsaturated Zone Proc Wageningen Symp. 2:790-800

[123] Tang, X., J. Graham, and A.W.L. Wan. 1997. *Measuring total suctions by psychrometer in triaxial tests*. In Proceedings of the XIV th International Conference on Soil Mechanics and Foundation Engineering, Hamburg, Germany. 1:213–216

[124] Taylor, S. A., and Cavazza, L. 1954. *The movement of soil moisture in response to temperature gradients*. Soil Science Society of America Journal,18(4):351-358.

[125] Terzaghi, K. 1936. *The shear resistance of saturated soils*. In Proceedings of the first International Conference On Soil Mechanics and Foundation Engineering, 1:54-56.

[126] Thomas, HR. 1992. *On the development of a model of coupled heat and moisture transfer in unsaturated soil*. Canadian Geotechnical Journal, 29:1107–1112.

[127] Thomas, H. R., He, Y., Sansom, M. R., and Li, C. L. W. 1996. *On the development of a model of the thermo-mechanical-hydraulic behaviour of unsaturated soils*. Engineering Geology Journal, 41(1):197-218.

[128] Thomas, H.R., King, S.D. 1991. *Coupled temperature/ capillary potential variations in unsaturated soil*. ASCE Journal of the Engineering Mechanics Division, 117:2475-2491.

[129] Tomasella, J. and Hodnett, M. G. 1998. *Estimating soil water retention characteristics from limited data in Brazilian Amazonia*. Soil Science, 163(3):190-202.

[130] Touma, J. 2008. *Comparison of different capillary models to predict the hydraulic conductivity from the water retention curve*. European Journal of Soil Science, 60(4):671–680.

[131] Tuller, M., and Or, D. 2004. *Retention of water in soil and the soil water characteristic curve*. Encyclopedia of soils in the environment, 4:278-289.

[132] van Genuchten, M. T. 1980. *A closed-form equation for predicting the hydraulic conductivity of unsaturated soils*. Soil Science Society of America Journal, 44(5):892-898.

[133] Vanapalli, S. K. 1994. *Simple test procedures and their interpretation in evaluating the shear strength of an unsaturated soil*. PhD Thesis, Dept. of Civil Eng., University of Saskatchewan, Saskatoon, Canada.

[134] Vanapalli, S. K. and Catana, M. C. 2005. *Estimation of the soil–water characteristic curve of coarse-grained soils using one point measurement and simple properties*. In Proceedings of an International Symposium on Advanced Experimental Unsaturated Soil Mechanics, Roma, Italy, 401-410.

[135] Vanapalli, SK., Fredlund, D.G. and Barbour, SL. 1996. *A rationale for an extended soil-water characteristic curve*. Canadian Geotechnical Journal, 1:457–464.

[136] Vanapalli, S. K., Fredlund, D. G., and Pufahl, D. E. 1999. *The influence of soil structure and stress history on the soil–water characteristics of a compacted till*. Geotechnique, 49(2):143-159.

[137] Vanapalli, S.K., Fredlund, D. G., Pufahl, D. E., and Clifton, A. W. 1996. *Model for the prediction of shear strength with respect to soil suction*. Canadian Geotechnical Journal, 33(3):379-392.

[138] Vanapalli, S. K., Nicotera, M. V., and Sharma, R. S. 2008. *Axis translation and negative water column techniques for suction controls*. Journal of Geotechnical and Geological Engineering, 26(6):645-660.

[139] Vanapalli, S.K., Pufahl, D.E. and Fredlund, D.G. 1998. *The effect of stress state on the soil-water characteristic behavior of a compacted sandy-clay till*. In Proceedings of the 51st Canadian Geotechnical Conference, Edmonton,Canada, 87-94.

[140] Villar, M. V., and Gómez-Espina, R. 2007. *Retention curves of two bentonites at high temperature*. In Experimental Unsaturated Soil Mechanics, Springer Berlin Heidelberg, 267-274.

[141] Vukovic, M., and Soro, A. 1992. *Determination of hydraulic conductivity of porous media from grain-size composition*. Water Resources Publications. Littleton Colorado, USA.1: 83.

[142] Wang, T. H., and Su, L. J. 2010. *Experimental study on moisture migration in unsaturated loess under effect of temperature*. Journal of Cold Regions Engineering, 24(3):77-86.

[143] Wang, W., Kosakowski, G. and Kolditz O. 2009. *A parallel finite element scheme for thermo-hydro-mechanical (THM) coupled problems in porous media*. Computers and Geosciences Journal, 35:1631–1641.

[144] Williams, P.J. 1982. *The surface of the Earth, an introduction to geotechnical science*. Longman Inc., New York.

[145] Willmott, C. J. 1981. *On the validation of models*. Phys. Geogr.,2:184-194.

[146] Wu, W., Li, X., Charlier, R., and Collin, F. 2004. *A thermo-hydro-mechanical constitutive model and its numerical modelling for unsaturated soils*. Computers and Geotechnics, 31(2):155-167.

[147] Yang, H., Rahardjo, H., Leong, E.-C., and Fredlund, D.G. 2004. *Factors affecting drying and wetting soil-water characteristic curves of sandy soil*s. Canadian Geotechnical Journal, 41(5): 908-920.

[148] Zapata, C. E., Houston, W. N., Houston, S. L., and Walsh, K. D. 2000. *Soil-water characteristic curve variability*. Geotech. Spec. Pub. (99):84-124.

[149] Zhou, J., and Yu, J. L. 2005. *Influences affecting the soil-water characteristic curve*. Journal-Zhejiang University Science, 6(8):797.

Appendix A

Figures of Study

Table A.1: Typical Analysis of Industrial Sand

Mineral	$\%wt$	Chemical Oxide	$\%wt$
Quartz	60	Silica (SiO_2)	68
Feldspar	20	Calcium (CaO)	4
Chloride	10	Alumina (Al_2O_3)	14
Iron Oxide	5	Iron (Fe_2O_3)	5
Hornblende	5	Magnesium (MgO)	2

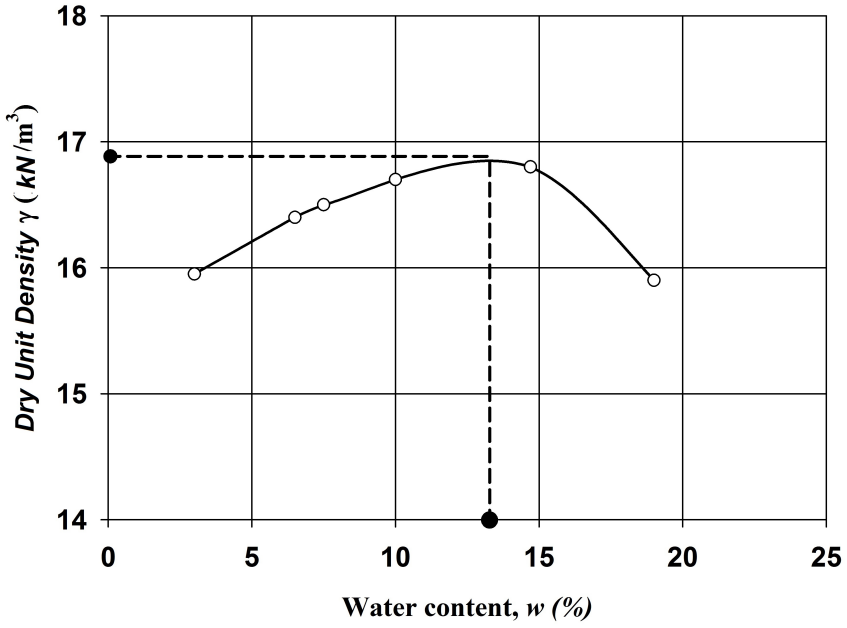

Figure A.1: Compaction test results of Unimin Silica Sand 7030

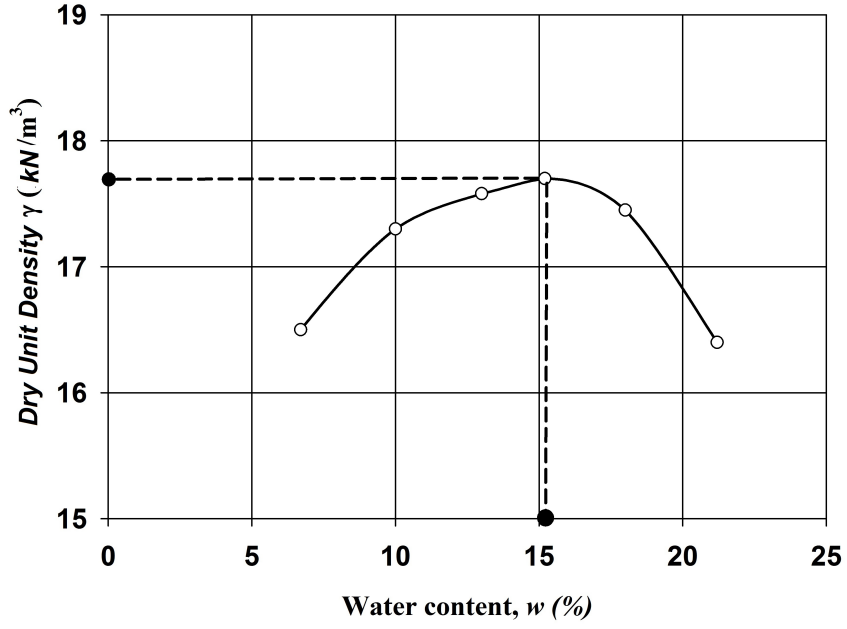

Figure A.2: Compaction test results of Industrial Sand

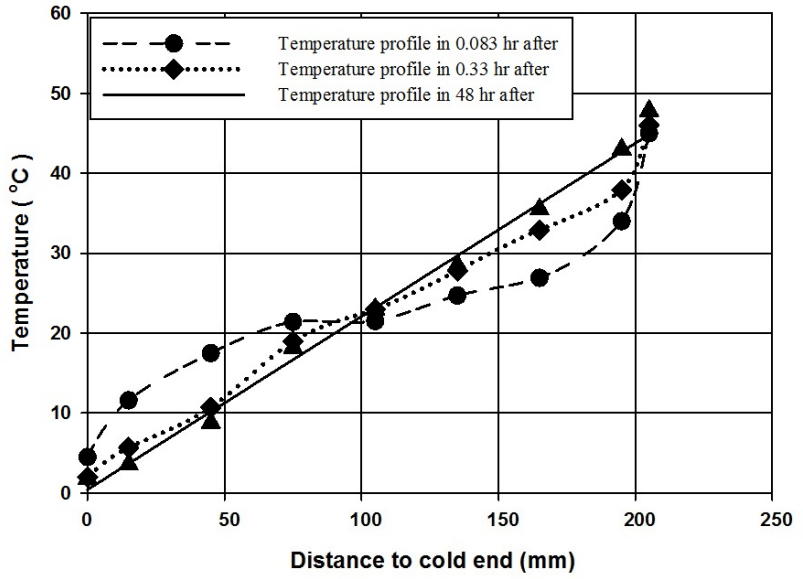

Figure A.3: Temperature distribution along soil specimen for Unimin Silica Sand 7030 at low initial water content

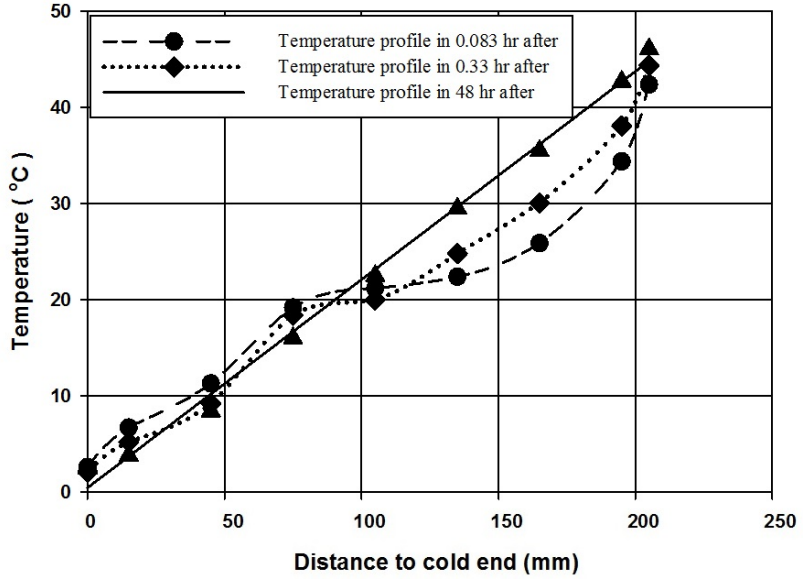

Figure A.4: Temperature distribution along soil specimen for Unimin Silica Sand 7030 at high initial water content

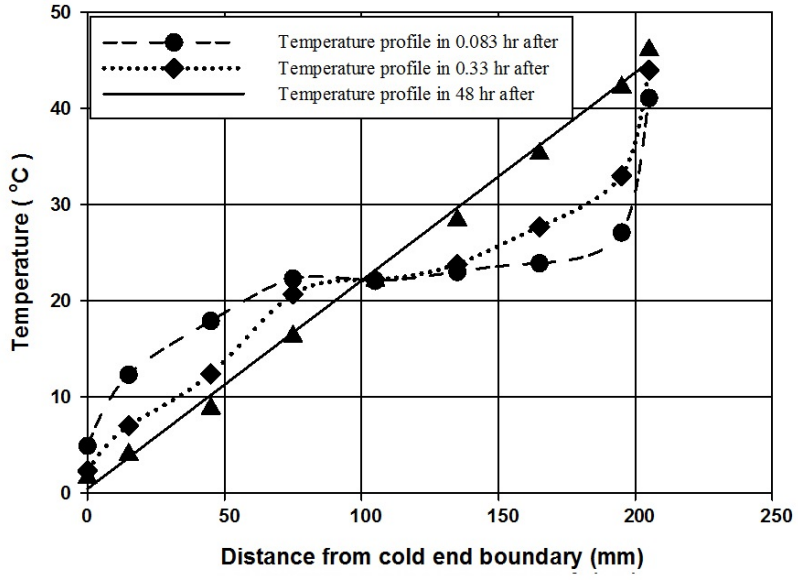

Figure A.5: Temperature distribution along soil specimen for Industrial Sand at low initial water content

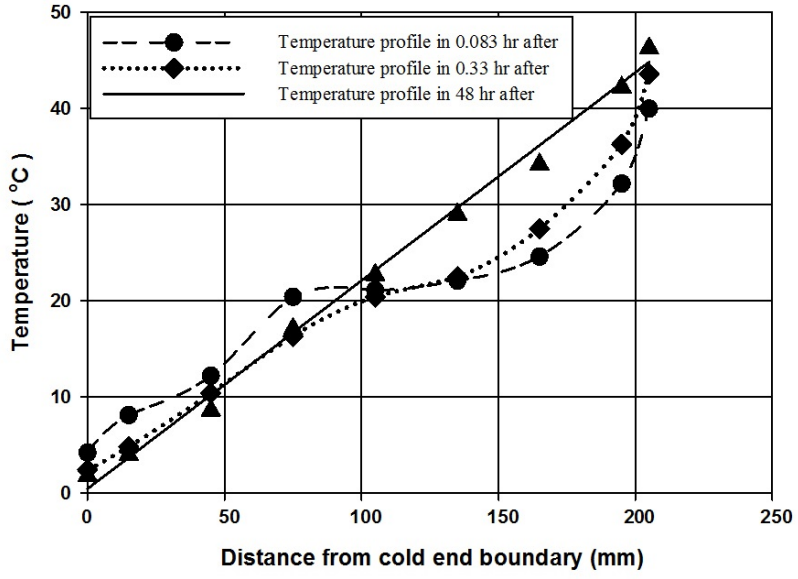

Figure A.6: Temperature distribution along soil specimen for Industrial Sand at intermediate water content

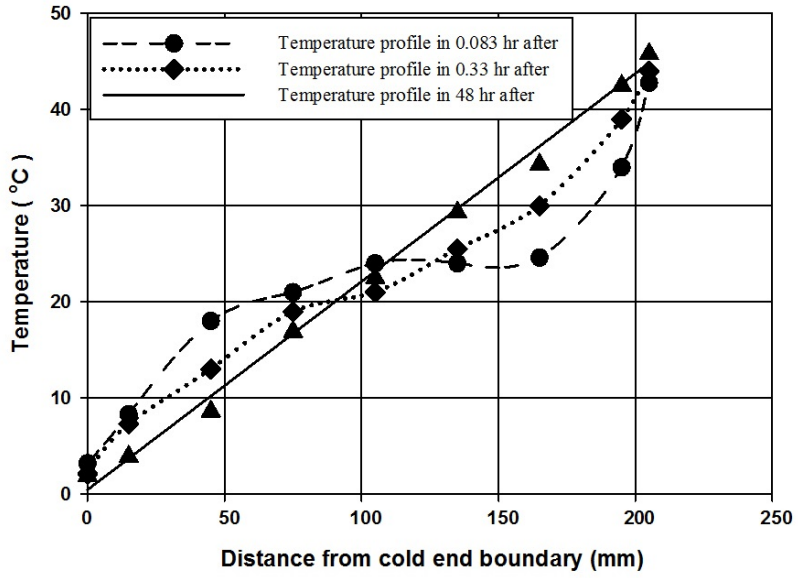

Figure A.7: Temperature distribution along soil specimen for Industrial Sand at high water content

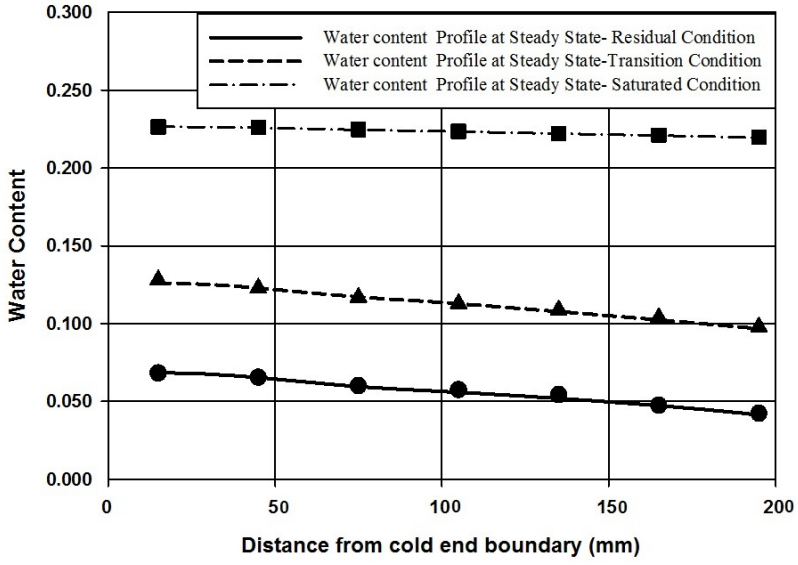

Figure A.8: Water content distribution along soil specimen for Unimin Silica Sand 7030 at each zone of SWCC at steady state

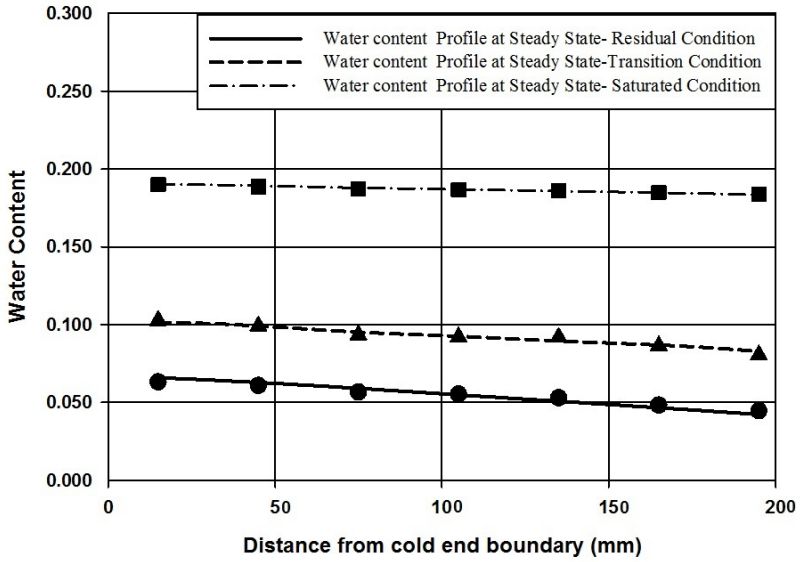

Figure A.9: Water content distribution along soil specimen for Industrial Sand at each zone of SWCC at steady state

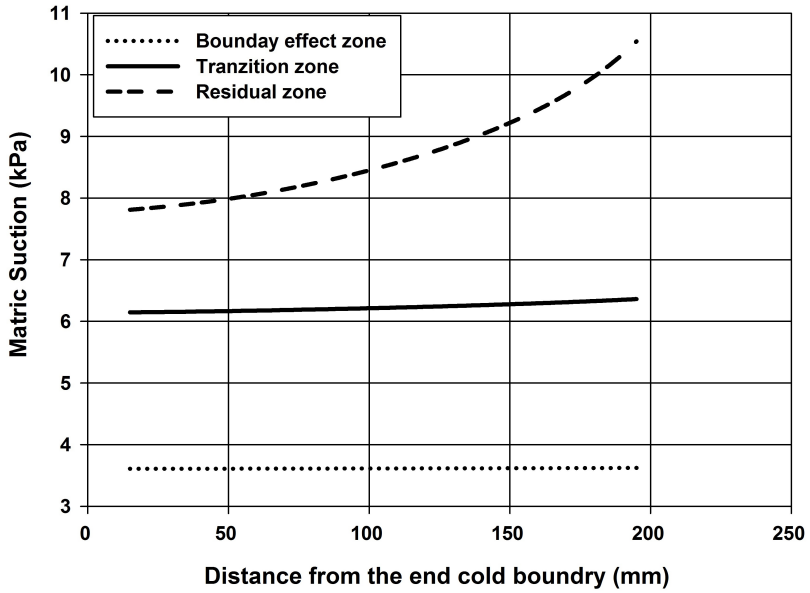

Figure A.10: Estimated suction profile at steady state at each zone of SWCC for Industrial Sand for m=1.6

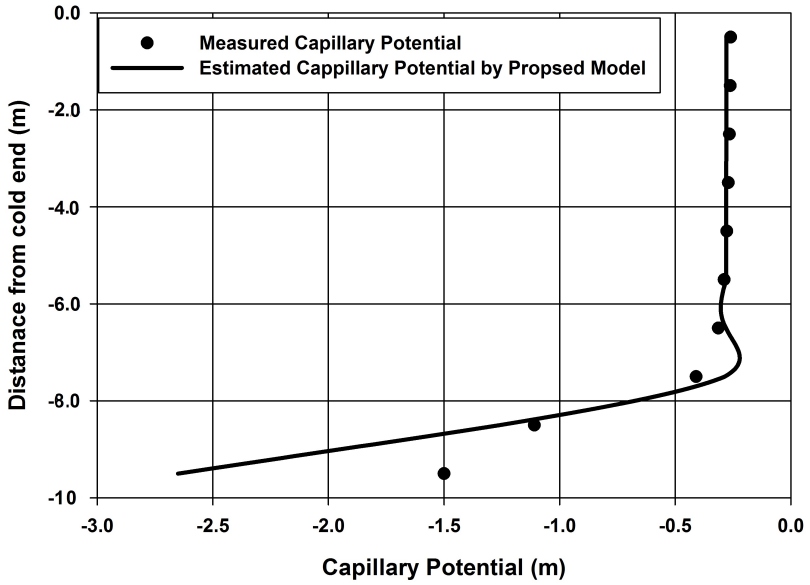

Figure A.11: Comparison between measured suction profile (Data from Derek 1997)and estimated suction profile at steady state

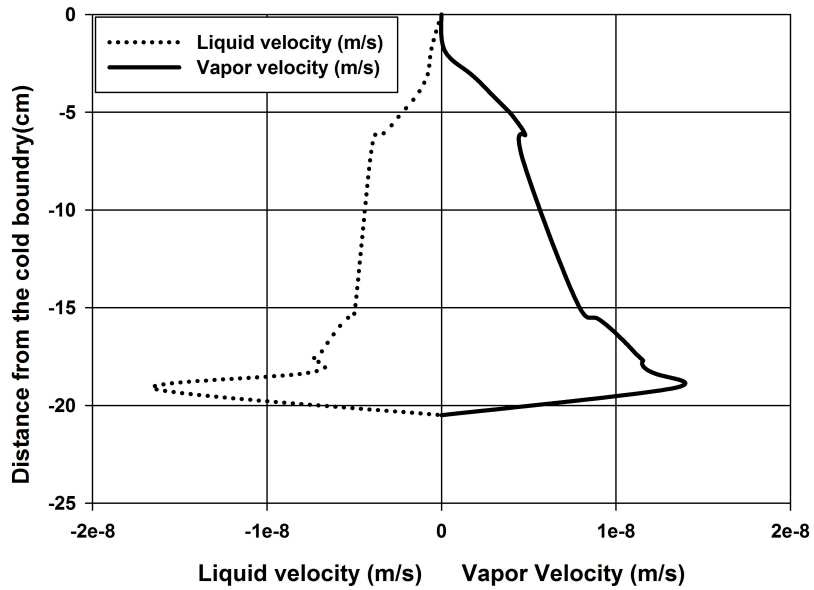

Figure A.12: Liquid and vapor velocity profiles of Unimin Silica Sand 7030 at m=1.5 for the residual zone at steady-state.

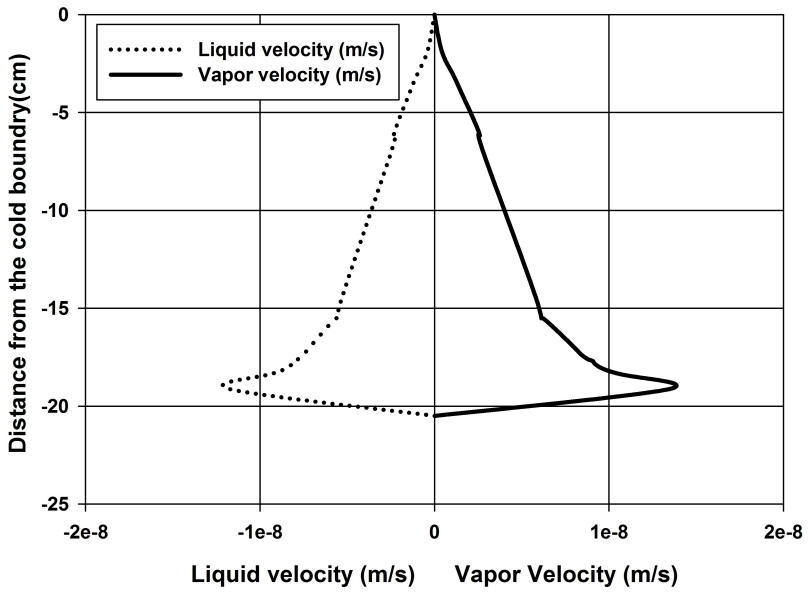

Figure A.13: Liquid and vapor velocity profiles of Unimin Silica Sand 7030 at m=1.5 for the saturated zone at steady-state.

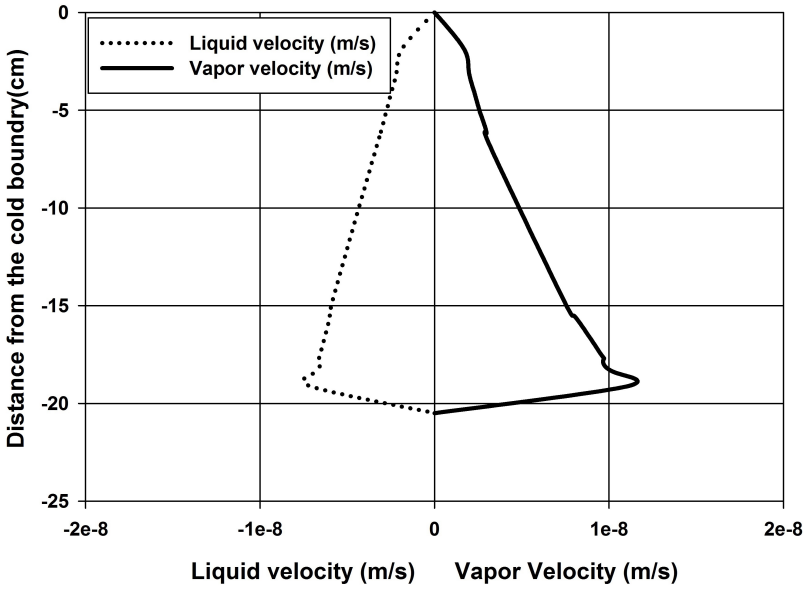

Figure A.14: Liquid and vapor velocity profiles of Industrial Sand at m=1.6 for the residual zone at steady-state.

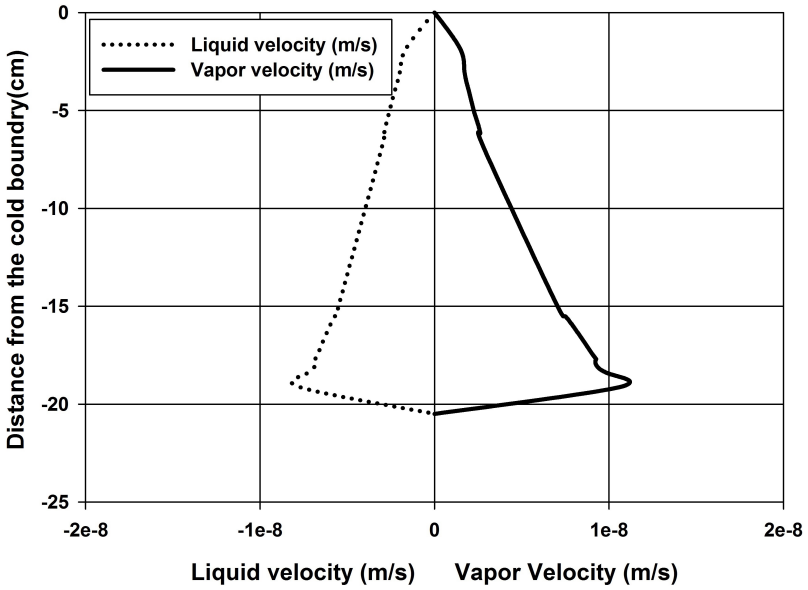

Figure A.15: Liquid and vapor velocity profiles of Unimin Silica Sand 7030 at m=1.6 for the transition zone at steady-state.

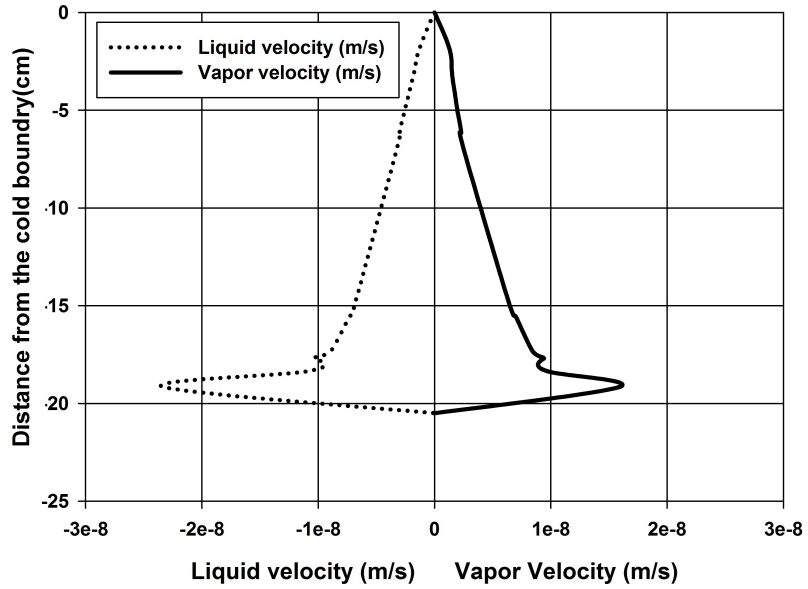

Figure A.16: Liquid and vapor velocity profiles of Industrial Sand at m=1.6 for the saturated zone at steady-state.

Appendix B

Photos of Study

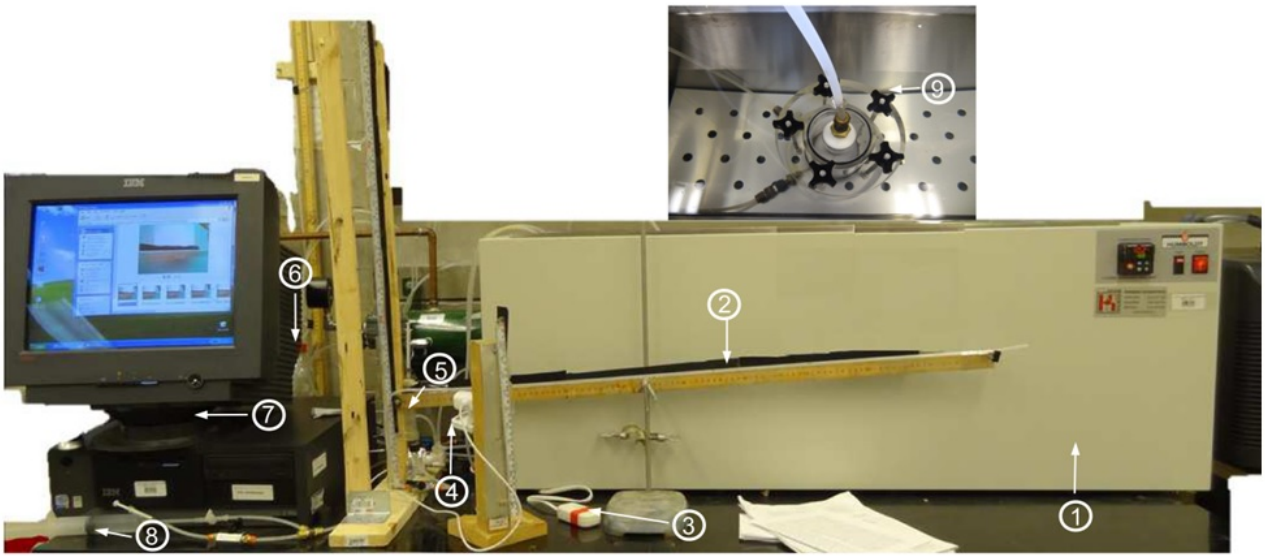

Figure B.1: Experimental setup for measuring SWCC at different temperatures

Figure B.2: Hydrometer water bath

Figure B.3: Designed pressure regulator

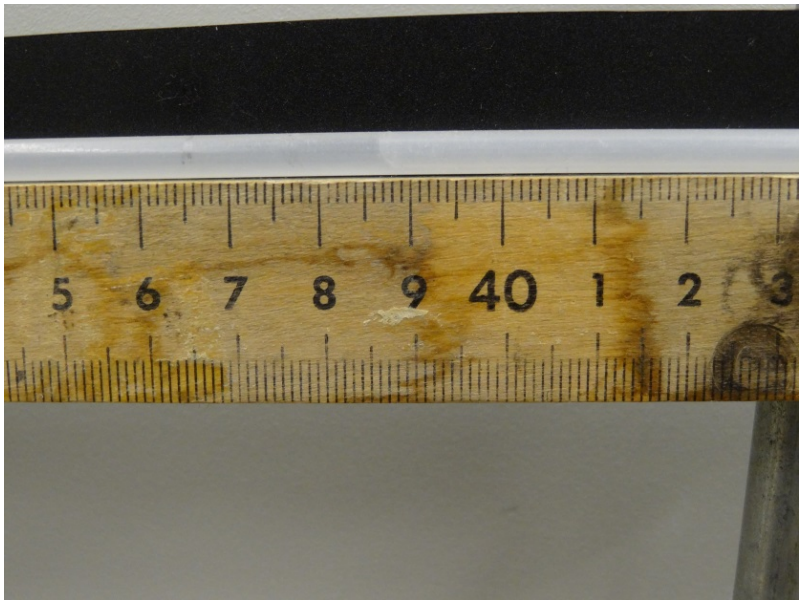

Figure B.4: Typical picture that was taken from the expelled level of water in plastic tube

Figure B.5: Soil sample at the end of the test at temperature 49 °C (a) Industrial Sand (b)Unimin Silica Sand 7030

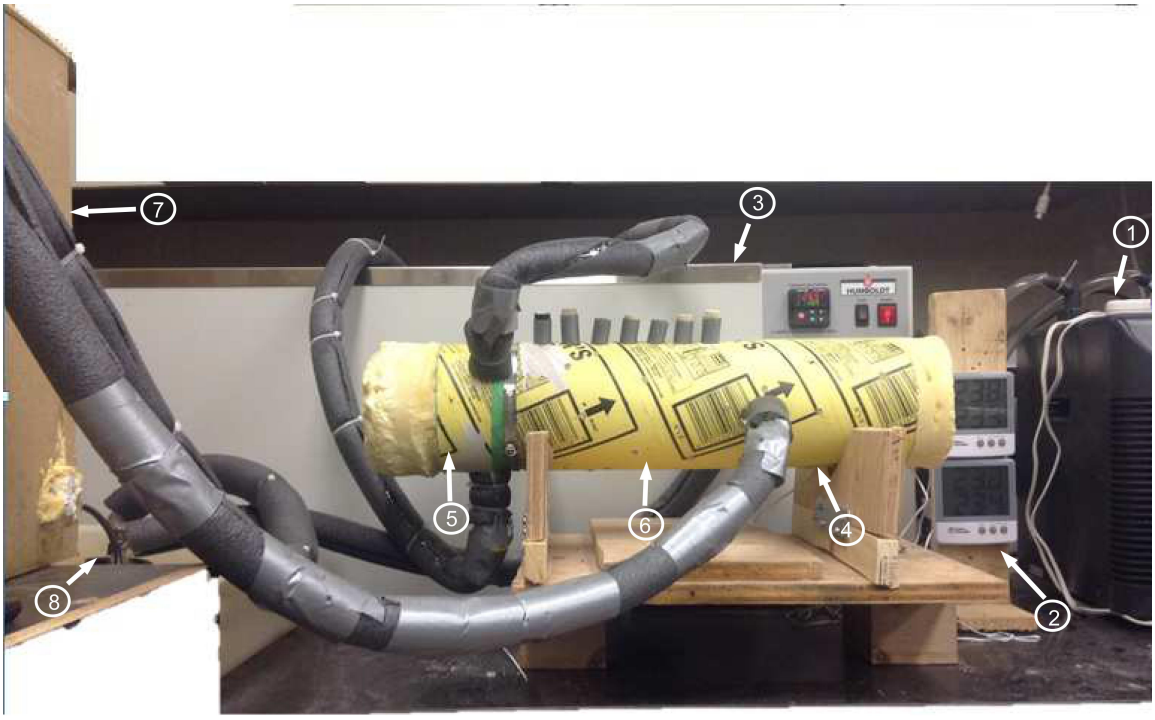

1-Dimmer 3-Thermo Bath 5- Aluminum Plat for colder par 7-Cooler box
2-Infrared temperature probe 4-Aluminum Plat for hotter part 6-Soil sample 8-Hydraulic pump

Figure B.6: Experimental setup for estimating SWCC of coarse-grained soils under temperature gradient

Figure B.7: Soil Column

Figure B.8: Soil samples in sealed plastic bags which are stored in humidity controlled box for 2 days

Figure B.9: Using aluminium tubes which is kept in ice water for measuring accurate reading of temperature

Figure B.10: Precise scale for measuring the water content of samples

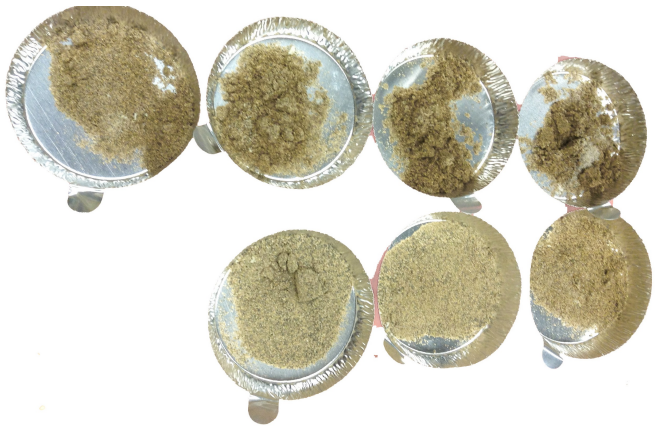

Figure B.11: Soil samples of different ports at the end of the test

Figure B.12: Hydraulic conductivity test